Kasyap Pradeep

Influence of artificially produced tinting colors on the corrosion resistance of AISI 304 stainless steel

MASTER'S THESIS

to achieve the university degree of

Master of Science

Master's degree programme: Production Science and Management

submitted to

Graz University of Technology

Supervisor

Assoc.Prof. Dipl.-Ing. Dr. techn. Norbert Enzinger

Institute of Materials Science, Joining and Forming
Graz University of Technology

Co-Supervisor
Dipl.-Ing. Dr. techn. Rudolf Vallant

Graz, July 2017

AFFIDAVIT

I declare that I have authored this thesis independently, that I have not used other than the declared sources/resources, and that I have explicitly indicated all material which has been quoted either literally or by content from the sources used. The text document uploaded to TUGRAZ online is identical to the present master ‘s thesis.

Date	Signature

Acknowledgements

Following a concentrated time of months, today is the day: making this note out of thanks is the finishing address my thesis. It has been a period of extraordinary learning for me in the scientific field, and additionally on an individual level. Composing this thesis has a huge impact on me. I would like to thank the people who have supported and helped me in such a great way all through this period.

I would first like to express my gratitude to my adviser Dr. Rudolf Vallant, for his awesome coordinated effort and wonderful support. Furthermore, I would especially thank Ms. Bernadette Gsellmann, Dipl.-Ing. BSc for sharing her amazing knowledge and expertise in this field. I thank the whole department of IMAT, TU Graz, for their excellent support.

I want to express our gratitude to Aperam Research in Isbergues (France) for providing the stainless-steel sheet materials and FELMI-ZFE institute for carrying out Energy-dispersive X-ray analysis / EDX and Raman spectroscopy for analyzing the oxide layers on the tinted samples.

Special thanks to Dr. Surya Deo Yadav, for introducing me to this marvelous world of scientific research and for supporting me all the time. Finally, I thank my parents, sister and friends for supporting me throughout all my studies.

Abstract

Stainless steel is supposed to be used more widely due to its high corrosion capability, in austenitic stainless steel AISI 304 is said to be the material which can withstand high corrosion resistance. The effect of simulated heat tint produced by a furnace in air at 600 and 1000° for 10 minutes are done on AISI 304 austenitic stainless steel. For evaluating the corrosion resistance on these tinted samples were analyzed using electro chemical corrosion techniques. Therefore, two different surface finishes 2B (skin passed) and 2R (bright annealed) were applied. The potentiostatic tests by linear polarization of the blank and tinted materials were performed in a 5% sodium chloride solution. It was found that the BTP for 2B at 600°C shows the similar values when considered the 2B at 1000°C. In the similar way 2R at 600°C is higher than for 1000°C. If compared to the blank materials the BTP is lower for the tinted specimens of 2B and the 2R surface finish, respectively.

After 1000°C tinting the 2R specimens showed a bit higher BTP than the ones of 2B, due to the rougher surface of the latter. After pickling off the tinting layers using a mixture of nitric acid (HNO_3) and hydrofluoric acid (HF) the BTP was even higher than for the blank material 2B, due to the more regular pickling surface. After pickling the 2R showed slightly higher BTP than the blank ones, as the latter showed some handling scratches. This means, that the tinting deterioration of the corrosion resistance could be fully restored.

The metallographic evaluation of the pits shows that 2B has more but shallow pits and 2R has less but deeper pits, formed mainly at the handling scratches. Thus, the less pits of 2R can be traced back to its smoother surface, having less imperfection nuclei for the pitting initiation (if it would have been scratch-free).

The heat tinted layers produced at the temperature of 1000°C was uniformly reddish-brown appearing and henceforth exhibited lower pitting potential and low corrosion resistance (against uniform and crevice corrosion, too) was observed on this samples in both the surface finishes namely 2B and 2R.

An estimate of the corrosion rate could not be determined due to the strong asymmetry of the anodic and cathodic sum current curves.

Kurzfassung

Die Auswirkung simulierter Anlauffarben auf rostbeständigem Stahl AISI 304 (1.4301) durch Ofenauslagerung für 10 Minuten bei 600 und 1000°C ohne Schutzgas wurde analysiert. Hierbei sind Proben mit zwei verschiedenen Oberflächenzuständen vorgelegen: 2B - kaltgewalzt, geglüht, gebeizt und kalt nachgewalzt (dressiert), sowie 2R - kaltgewalzt und in Wasserstoffatmosphäre blankgeglüht. Die Korrosionsbeständigkeit wurde in einem Potentiostaten in einer 5%igen NaCl-Lösung durch die Aufnahme von linearen Polarisationskurven - durch Bestimmung des Gleichgewichtspotentials (OCP) und des Durchbruchs- (BTP) bzw. Lochfraß Potenzials analysiert. Generell zeigt sich eine starke Reduktion der Korrosionsbeständigkeit durch die Anlauffarben, wobei der 2R Oberflächenzustand bessere Eigenschaften im Ausgangszustand und mit den Anlauffarben aufweist als 2B. Durch eine anschließende Beizbehandlung (Gemisch aus Salpeter- und Flusssäure) konnten die Anlauffarben wiederum vollständig entfernt und die Korrosionsbeständigkeit vollständig hergestellt werden. Durchgeführte Raman- und EDX-Analysen zeigen, dass an den Oberflächen der Anlauffarben kein Chrom-Oxid (Cr_2O_3) mehr vorliegt, sondern Hämatit (Fe_2O_3) - bei 2B mit Anteilen von Trevorit ($NiFe_2O_4$) und Magnetit (Fe_3O_4). Die durchgeführte metallographische Analyse der Lochfraß stellen zeigte prinzipiell relative große Streuungen in der Anzahl und der Dimension (Durchmesser und Tiefe). Neben Lochfraß ist auch Spaltkorrosion am Rand des Probenhalters und gleichmäßige Korrosion (an den Proben mit Anlauffarben) aufgetreten. Eine Abschätzung der Korrosionsrate konnte auf Grund der starken Asymmetrie der anodischen und kathodischen Summenstromkurve nicht ermittelt werden.

Abbreviations

2B	skin pass surface finish
2R	bright annealed surface finish
β_a, β_c	anodic and cathodic Tafel slopes [µA/mV]
BTP	Break through potential (pitting potential)
CCST	Critical Crevice Solution Theory
CE	Counter Electrode
E	Electrode potential (mV)
$E_{A/P}$	Active / passive potential (mV)
E_{corr}	Corrosion Potential (mV)
FEM	Field Emission Microscope
I	Current (µA)
i_{corr}	Anodic current density (µA/cm^2)
LOM	Light Optical Microscopy
OCP	Open circuit potential (mV)
RE	Reference Electrode
R_p	Polarizations Resistance
SCE	Saturated Calomel Electrode
SHE	Standard Hydrogen Electrode
T	Temperature (°C)
t	Time (h)
WE	Working Electrode

Table of Contents

List of figures

List of tables

1. Motivation and goal

Stainless steels have a considerable increase of utilizations in many industries including substitution for ordinary materials. In stainless steels, the austenitic stainless steel, especially 304 is frequently decided for its pitting and crevice corrosion resistance[1]. Be that as it may, there are a few issues enveloping the diminishment in welded joints corrosion resistance[2]. As depicted underneath, there are various parameters that detrimentally influence the corrosion resistance of welded 304 stainless steel. While a survey of these components is incorporated, to investigate each of these variables and their collaboration in detail is the main goal of this thesis[3]. It is the reason here to inspect the factors of heat tint scale which gives a huge impact on the corrosion resistance of stainless steel welds and discovering out the best possible solutions to remove the oxide layer by contemplating the factors into consideration[4]. In addition, the influence of the direct susceptibility to corrosion, heat tint can expand susceptibility to other corrosion mechanisms are clarified in the following parts of the thesis. Acknowledgment of heat tint scale is subject to the consistency of the utilization lead of the metal under particular working and service conditions. It is comprehended the more intense the heat tint as shown by progressively darker colors, the more conspicuous the loss in pitting corrosion resistance[1]. In light of this, there should to be an anticipated subjective pattern to the corrosion conduct of heat tinted welds presented to similar situations[5]. Tests were attempted to look at the pitting corrosion of heat tinted specimens which were artificially tinted by utilizing the oven and to show the predictability of corrosion performance by utilizing the electrochemical corrosion method[6].

The main questions appearing are the following: How strong does tinting deteriorate the corrosion resistance - Do parameters from the linear polarization tests vary from material to material - Can the corrosion characteristics be recovered after tinting by pickling - Can the oxide layer be characterized by EDX and Raman spectroscopy?

2. Stainless steels

Stainless steels have a chromium content ranging from 10-30% (see Figure 1). Chromium is the reason for oxidation and corrosion resistance in stainless steel [7]. At least one or more additional alloying elements might be utilized as a part of conjunction with chromium for most of the grades[8]. At the point when chromium is alloyed in small amounts (1 to 3 %), an unobtrusive increment in the corrosion resistance in apparent. In any case, as the measure of chromium approaches around 12%[9]. a dramatic change in corrosion resistance occurs; such a compound is for all intents and purposes impenetrable to rusting from any open air introduction to ordinary airs, for example, temperature, humidity, and rain variables. This does not really remain constant in saline or industrial environments. Thusly, a base necessity for a stainless steel contains no less than 11% chromium and that is fit for opposing assault from typical climatic presentation. It is basic that both the conditions are to be fulfilled for a steel to qualify as a stainless steel[10]. Numerous high alloyed iron-base alloys e.g. some tool steels, contain over 10.5% chromium, yet since of their high carbon content, they don't meet the base prerequisites for stainless steel[5][11].

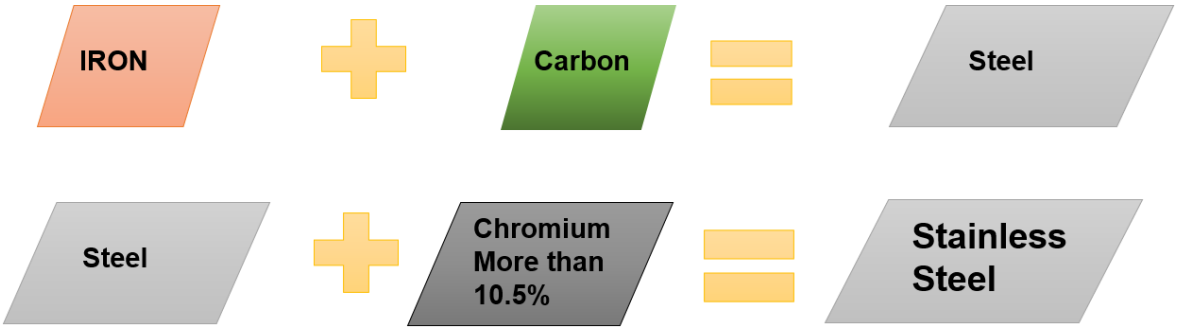

Figure 1 steel and stainless steel description

2.1 Stainless steel classification

Stainless steels can be classified into five main groups according to their microstructure [5][12]

- Austenitic
- Ferritic
- Martensitic
- Duplex (austenite/ferrite) and
- Precipitation-hardening alloy

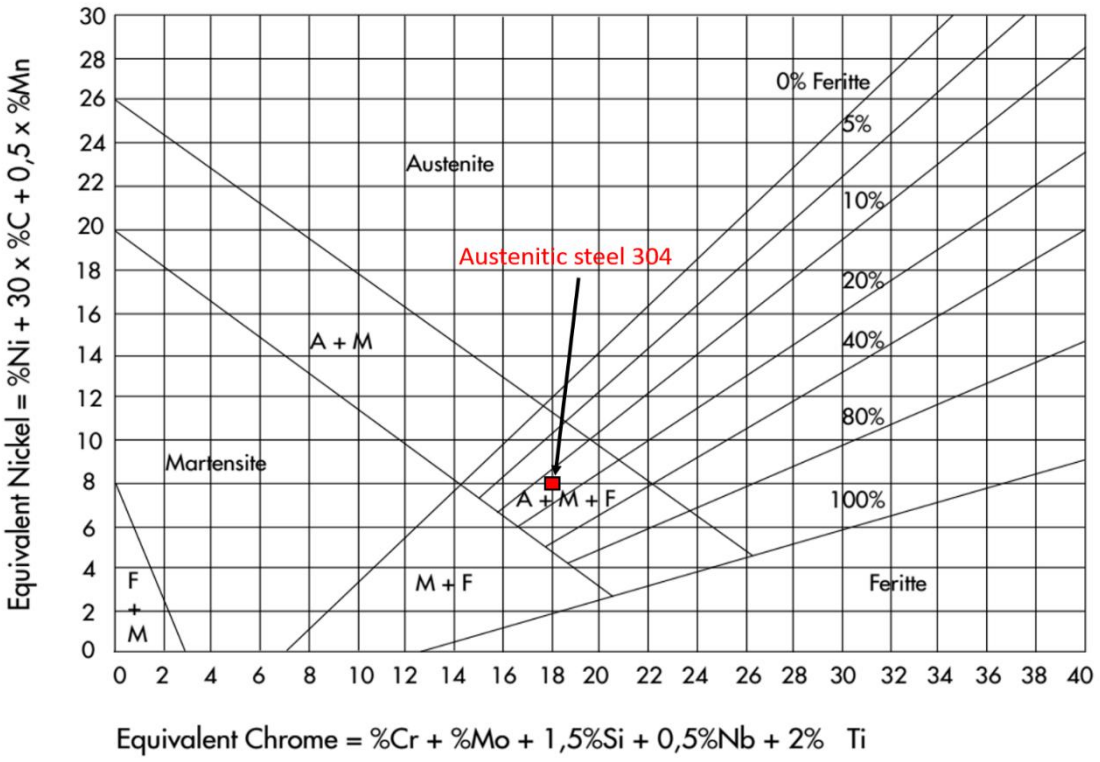

Figure 2 Schaeffler diagram (A-Austenite;M-Martensite;F-Ferrite) [13]

The Schaeffler diagram in Figure 2 represents the relationship between the composition (Cr- and Ni-equivalent) and the expected microstructural phases. One of the most important parameter that can explained through Schaeffler diagram is the chromium equivalent of a given alloy with respect to the percentage of ferrite formers Si, Mo and Cb beside Cr. The nickel equivalent can be calculated from the concentrations of austenite formers Ni, Mn and C[5].

In this research, the austenitic stainless-steel alloy 304 was used. Thus, this group, austenitic, of the stainless steels will be further described.

Austenitic stainless steels are the most widely used group of stainless steels. They are iron based alloys containing 16-30% chromium (Cr), 8-25% nickel (Ni) and less than 0.15% carbon (C). These alloys have face-centered cubic (fcc) lattice are nonmagnetic materials and cannot be hardened by heat treatment. Austenitic stainless steels seem to have fundamentally more prominent potential for aqueous corrosion resistance than the ferritic stainless steels. This is on the basis of the three most generally utilized austenite stabilizers, nickel, manganese and nitrogen all sum up to the inactivity[14].

The alloys of this group of stainless steel have an excellent resistance to general corrosion. However, in specific environments, they are highly susceptible to localized corrosion such as pitting, crevice corrosion. The 300 series of austenitic stainless steels are widely used and accounts for about 50% of all stainless steel production[15]. Type 304 stainless steel is the basic (18Cr, 10Ni) austenitic stainless steel.

2.2 Function of alloying elements

The properties of metals can be modified by adding alloying elements see Figure 3. In this way, the properties of stainless steel can be adapted so it can be used appropriately in specific environments. Below are brief information's about the benefits of each alloying element added to stainless steel[16].

Chromium: is the principle component that enhances the corrosion resistance of the alloy by framing the passive film on surface. Chromium gives resistance to oxidizing conditions and gives more resistance to localized corrosion attack [17]. Other elements in the alloy can impact the viability of chromium in forming or maintaining the surficial passive oxide layer.

Nickel: is added to balance out the austenitic structure of the stainless steel and improve the mechanical properties and fabrication qualities. Nickel likewise advances re-passivation if the passive layer is damaged.

Molybdenum: alongside chromium, molybdenum gives the biggest increase in corrosion resistance in stainless steel. Molybdenum, also increases hardenability by decreasing the risk of temper embrittlement. As the melting point of molybdenum carbide is very high it provides high temperature strength which is very useful in some tools[18].

Nitrogen is added to improve strength and corrosion resistance. It dissolves interstitially in steel and strengthens austenite in the same manner as carbon and it forms titanium and niobium which give more stability than chromium until carbon and nitrogen does not increase the tendency of sensitization. Nitrogen improves corrosion resistance and general pitting frequency with a slight ductility loss[19].

Carbon: it increases the strength of steel and is considered as a very strong austenitizer. In low carbon grades stainless steels, carbon is kept in 0.005% to 0.03% level to maintain desired properties and mechanical characteristics. Carbon in reaction with chromium forms chromium carbide precipitation typically at grain boundaries. This may negatively affect corrosion resistance by expelling a portion of the chromium from solid solution lattice in the alloy and, accordingly, decreasing the amount of chromium available to guarantee corrosion resistance [20].

Titanium and Niobium: are used to minimize the sensitization of stainless steel to reduce the possibility of inter-granular corrosion when the stainless steel in welded or heat treated. Titanium and niobium cooperate with carbon to shape carbides, departing the chromium in solution so a passive film can be formed.

Silicon: Silicon is added to steels as a deoxizer, as it expels disintegrated oxygen(O_2) from liquid steel in the process of steel refining. Oxygen(O_2) is undesirable segment in steel since it outlines oxide inclusions which can degrade toughness, fatigue, ductility resistance. It is additionally added to enhance electrical properties[21][22][23][24].

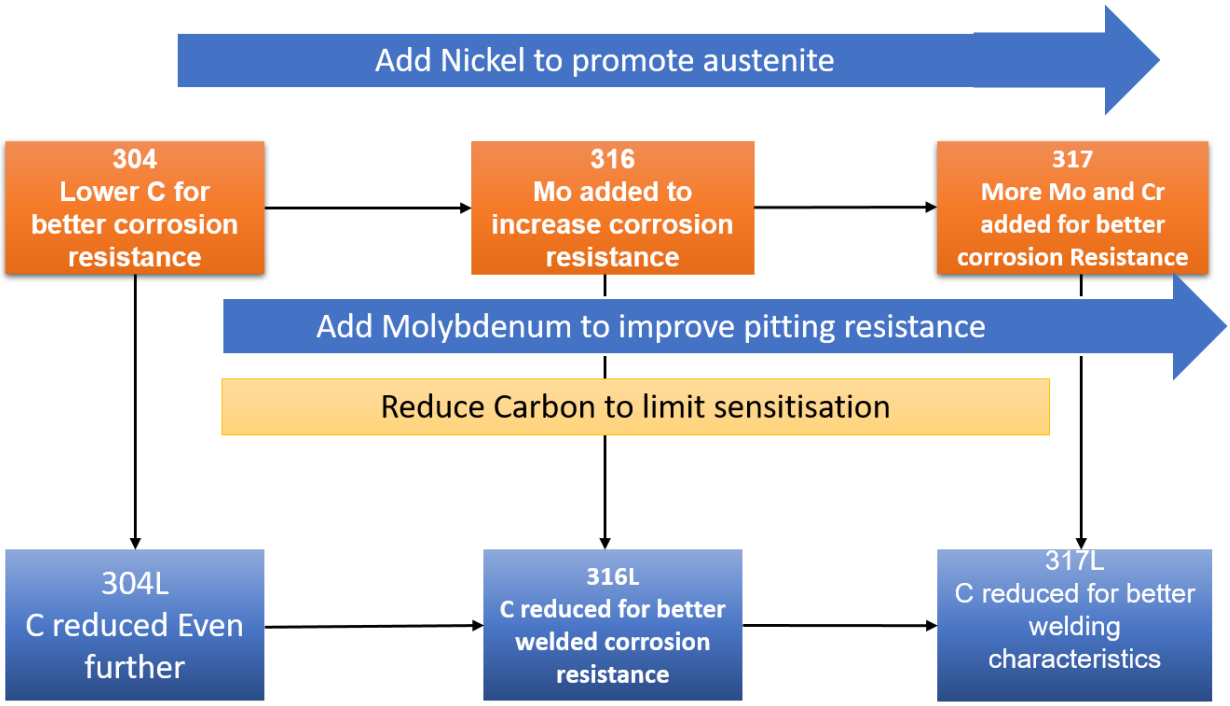

Figure 3 Function of alloying elements of austenitic stainless steel

Type 304 is known as the one of the most common grade of austenitic which is widely used for chemical processing equipment, beverage industries as it consists of 10% nickel and 18% chromium.

Type 316 when molybdenum added to the chrome and nickel for the type 304 for controlling pitting corrosion attack and as this grade consists of 11-14% of nickel and 16-18% chromium it can be mainly used for chemical processing, pulp and paper industry, for food and beverage processing.

Type 317 is a special grade of stainless steel which contains a higher percentage of molybdenum than 316 for higher corrosive environments and can be used in stacks that contain scrubbers[25].

2.3 Manufacturing of stainless steel

A review of the stainless steel making process for flat type products is given in the following section. The procedure can generally be separated into four stages. In the initial stage, a solid material with the required alloy composition is made. The second step is to create the desired plate and sheet thickness by rolling and annealing if required. The third step is to deliver the appropriate micro structure by heat-treatment. In the last fourth step the desired surface finish is accomplished[26].

2.3.1 Casting

The initial step of the procedure is to gather and liquefy the coveted measure of alloying components as shown in Figure 4. The crude materials are dissolved in an electric circular segment heater and from that point exchanged to the converter. Argon-oxygen decarburization (AOD) is the most widely recognized sort of converter. The reason for the AOD is predominantly to refine

the steel by reduction the carbon and Sulphur content, additionally in numerous stainless steels to include a specified concentration of nitrogen. Tests for composition analysis are taken from the melt and the composition can be adjusted by including all the more alloying components. The melt is then set into cast. Most of the steel is created by continuous casting for more economic issues. Ingot casting is utilized in most of the cases, particularly for small volumes or extremely requesting materials. Solidification of stainless steel is intricate from a microstructural perspective and depends basically on science and rate of cooling. Five diverse hardening modes are conceivable, in particular single stage austenitic, ferrite, eutectic, essential ferrite with second stage austenite and single stage ferrite. The level of small scale isolation and, thus, the level of large scale isolation rely on upon the cementing mode. Segregation can be seen even in the last item despite the fact that some level of homogenization happens during ensuing preparing steps[27].

Figure 4. Step 1.Manufacturing process of stainless steel the melt shop [28]

2.3.2 Reheating and hot rolling

The cast slab is heated to around 1250 ˝C before it proceeds to the hot rolling mill. Hot rolling is completed at high temperatures to enable recrystallization to happen and in this way softening which can be seen in Figure 5. Rolling process outcomes in development of surface texture, as further explained in following chapters. The texture is however fairly counteracted by repeated recrystallization cycles so cold distortion impacts the last surface. The microstructure after hot working comprises of a blend of recrystallized and in part twisted grains. Critical measures of intermetallic stages can likewise be found in the microstructure at this stage, contingent upon the creation and the temperature in the later phase of the hot working procedure. The material thickness is in the scope of 5 to 50 mm after hot rolling. Rolling at higher temperatures influences the microstructure as well as causes oxidation of the surface. The oxide is in the micrometer thickness and the plainly visible appearance is dark[29].

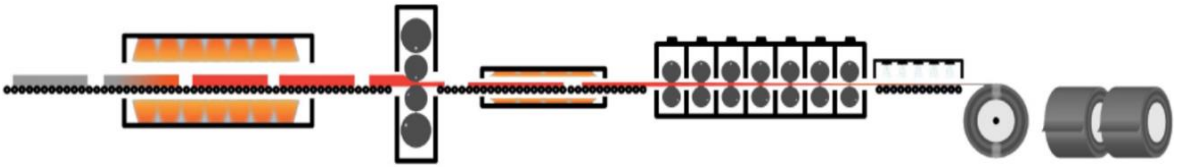

Figure 5 Step 2..Manufacturing process of stainless steel hot rolling mill[30]

2.3.3 Hot rolling and first annealing

The quality necessities for stainless steels are much higher for both mechanical and corrosion properties so the microstructure created after hot working is not agreeable. Along these lines, a different strengthening step is done after hot attempting to permit disintegration of auxiliary stages, static recrystallization and grain development. The general objective is to accomplish a blend of right stage adjust and grain size. The annealing temperature relies on upon the steel review yet is commonly 950 °C - 1150 °C for austenitic and duplex and 750°C - 850 °C for ferritic grades. The aggregate toughening time is of the request of minutes, contingent upon thickness. The toughening is regularly completed in oil or gas terminated heaters so further oxidation will happen in the strengthening step, yet the measure of oxide shaped is little contrasted with the sum framed in the hot moving stride[31] as shown in Figure 6.

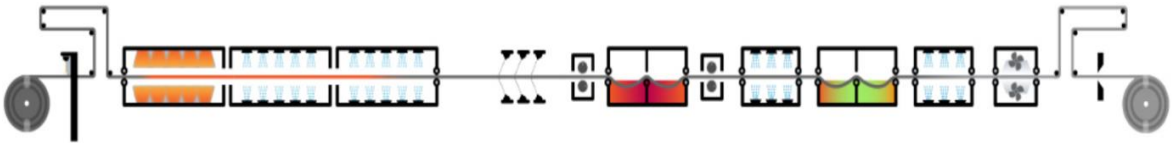

Figure 6 Step 3..Manufacturing process of stainless steel-first annealing and pickling[32]

2.3.4 Pickling hot rolled material

The subsequent stage is pickling, it serves to evacuate undesirable oxide shaped amid hot rolling and strengthening, and to expel the chromium depleted layer (CDL) under the oxide. Pickling regularly includes a progression of steps, a run of the mill arrangement for level items is mechanical descaling, neutral electrolytic pickling taken after by chemical pickling. A typical strategy for mechanical descaling is shot-impacting or shot blasting. The last stride in corrosive expects to evacuate the rest of the oxide and chromium-exhausted metal by oxidative dissolution. The most widely recognized pickling shower for stainless steels is a blend of nitric acid and hydrofluoric acid known as mixed acid. The steel may now be prepared for cutting and bundling. The surface complete created by this course (hot rolling, heat treatment, mechanical descaling and pickling) is called 1D and is genuinely dull so the material is not suited for applications with high stylish applications. For thinner items and items with high aesthetic necessities cold rolling is additionally utilized[29].

2.3.5 Cold rolling and annealing

Generally cold rolling begins at room temperature yet the temperature increments as the material thickness is reduced because of deformation heating. All things considered, the temperature is still quite low for recrystallization to happen not withstanding for expansive cold rolling decreases. The microstructural changes that happen during cold rolling are along these lines more radical contrasted with hot rolling. A related procedure relevant to the present work is hot rolling, which is completed at raised temperature yet underneath the temperature at which recrystallization happens. The microstructure in the process of rolling comprises of pancaked grains with high

dislocation density and perhaps at the same time it can also make form the deformation initiated marten site. The annealing procedure is similar to the hot rolled case with the distinction that the main impetus for recrystallization is significantly higher and that the annealing time is shorter on the grounds as the material thickness is reduced. Microstructural changes amid tempering can be considered in extraordinary detail utilizing dilatometry, a case of a mostly recrystallized austenitic steel is given in Figure 7. The tempering method oxidizes the base material however the subsequent oxide is just 300 nm on the grounds that no oxide is shaped amid the chilly moving stage. The oxide is additionally considerably denser and enhanced in chromium which exhausts the basic metal to a relative huge degree[33].

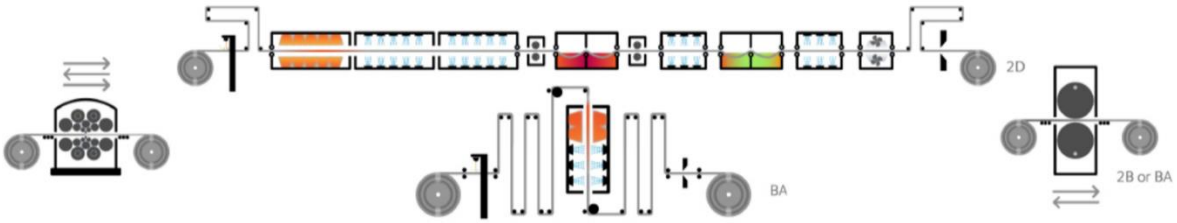

Figure 7 Manufacturing Process– Cold rolling and final annealing [34]

2.3.6 Pickling cold rolled material

Pickling cold rolled material is same like pickling hot rolled material. The chromium-depleted layer under the oxide must be completely evacuated with a specific end goal to achieve a corrosion resistance material. The surface quality of the pickled material is shiny and bright. The surface after cold rolling, annealing and pickling is signified 2D or 2E if a mechanical descaling stage has been incorporated, and is smoother than 1D. It is regular to slightly roll the steel between highly-polished rollers after pickling. This procedure is called skin passing and improves the surface quality further, this surface finish is called 2B and is the most widely recognized cold rolled finish.

2.4 Types of surface finish

Mill finishes (hot or cold rolled) which regularly experience pickling after the manufacturing procedure to evacuate the scale, are the essential supply condition for all stainless steel flat products. They are utilized all around for standard building and automobile parts according to the requesting necessities. The underneath specified surface finishes are most generally used to boost corrosion resistance.[35] (see *Figure 8*).

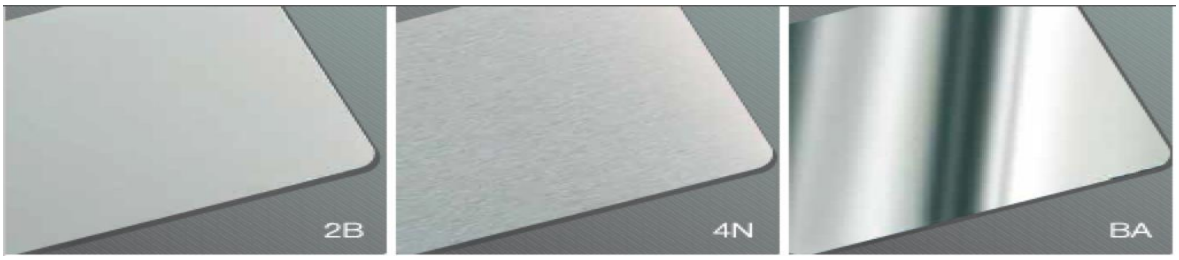

Figure 8 Types of different surface finishes[36]

2.4.1 Surface finish 2D

Process cold rolled, heat treated pickled.

It is a uniform, dull silver-grey finish that is connected to lower sheet thickness decreased by cold rolling. In the wake of rolling, the coil is heat treated to create a uniform microstructure (annealing) and to meet mechanical property prerequisites. Pickling or descaling is fundamental after heat treatment to expel the chromium depleted surface layer and reestablish corrosion resistance. Pickling can be the last stride underway of this finish, at the same time, when complete consistency or potentially evenness are crucial, there is a consequent last slight cold moving pass (skin pass) through dull rolls (not as smooth as 2B or 2R. A 2D finish is favored for deep drawing segments since it holds lubricants well. It is utilized as a substrate when a painted complete is sought in light of the fact that it gives fantastic paint adherence.

Applications are rail-car parts, chemical related equipment's, some parts of the furnaces.

2.4.2 Surface finish 2B

bright cold rolled, annealed, pickled, and skin-passed.

2B is a bright cold rolled finish usually delivered in an indistinguishable way from 2D (which has a lesser smoother finish compared to 2B), with the exception of that the last light cold rolled pass is finished utilizing polished rolls. This delivers a better reflective surface that looks like a shady mirror. Finish reflectivity can change from manufacturer-manufacturer and coil-coil with a few coils looking very mirror-like and others being genuinely dull as the final touch is given to 2B by tension levelling. 2B is a universally useful cold rolled finish ordinarily utilized for everything except outstandingly difficult deep drawing applications. It is more promptly cleaned to high shine than a no No.2D finish.

Applications are piping equipment's, cold storage equipment's, solar panels, washing machines, medical equipment's and wheel accessories.

2.4.3 Surface finish 4N

Process: polished with a 220-grit grinding belt.

It is portrayed by short, parallel cleaning lines, which broaden consistently along the length of the coil. It is acquired by mechanical cleaning a No. 3 complete (which is moderately reflective containing coarse parallel lines polished with a 40 micro inches' grit) with step by step finer abrasives. Contingent upon the necessities of the application, the last complete can be anyplace in the vicinity of 120 and 320 grit. Higher grit numbers create better polishing lines and more reflective finishes. The surface roughness is ordinarily Ra=25µm or less. This universally useful finish is generally utilized for restaurants and kitchen gear, customer facing facades and nourishment preparing and dairy hardware. On the off chance that a fabricator needs to mix in welds or do other restoring, the

subsequent cleaning lines are normally longer than on item cleaned by a maker or toll-polishing house.

Applications are furniture, tank trailers, crockery and kitchen appliances.

2.4.4 Surface finish 2R

Process: cold rolled and bright annealed.

It is delivered by heat-treating (annealing) in a controlled air furnace. It has a mirror like appearance however may have some shadiness and different blemishes. A complete that is assigned "BA" has just been bright annealed. A finish that is assigned 2BA has been bright annealed and afterwards gone between exceedingly polished rolls. A negligible measure of roll pressure (skin pass) is connected. The procedure enhances levelness and complete consistency however does not fundamentally diminish thickness. Bright annealed stainless is in some cases polished to accomplish a more mirror-like finish. It is regularly determined for applications where a profoundly reflective surface is sought[33].

Applications are medical implants, cooking equipment's, refrigerators, building equipment's.

2.5 Passivity of metals

About all metals are thermodynamically receptive in most indigenous habitats, e.g. moist air, contaminated or hot, and water when it is saline, acid or basic. Most metals rapidly build up an oxide film when presented to dry, immaculate and cool air. In case of moist air there is always a chance for formation of wet corrosion. This film would soon stop to thicken on the grounds that it frames a strong boundary between the metal and oxygen through which metal and oxide particles are hindered to penetrate. This is the least difficult type of passivation.

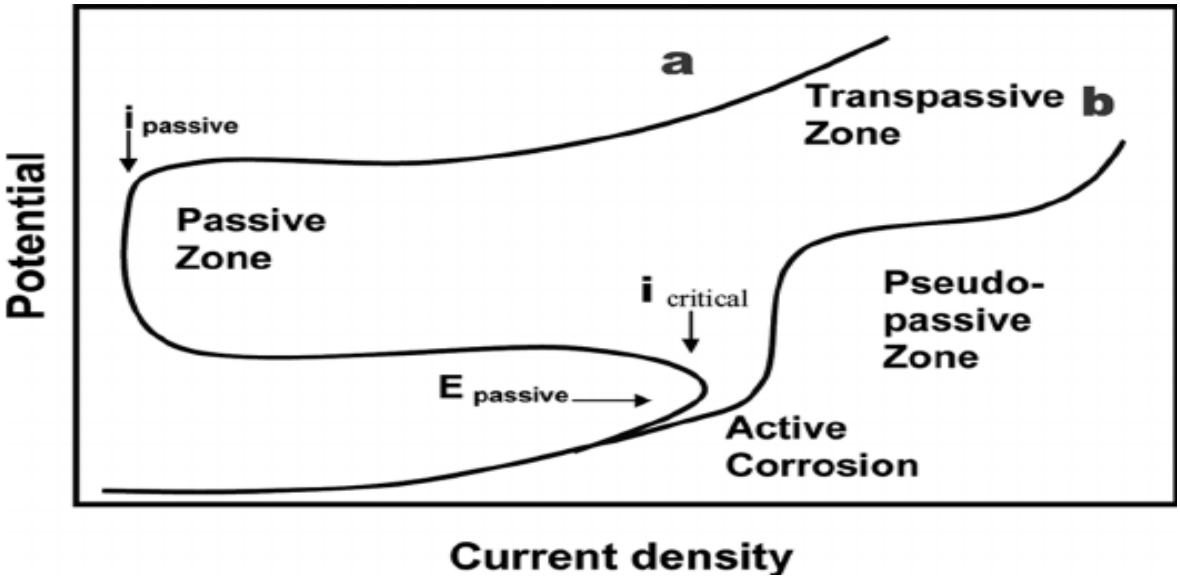

Figure 9 Anodic dissolution behavior of an active-passive metal [38]

The investigation of passivation is enormously done in the presence of fundamental anodic process by using an external cathode. In case of absence a general oxidizer can be equipped for giving cathodic response at the nominal load. By such means the anode electrode potential and current density related with different passivation phenomenon can be promptly measured. Accordingly, passivity is a strange behavior seen amid the corrosion of specific metal alloys, it is characterized basically as the "loss of substance reactivity under certain natural conditions". In the passive state, the corrosion of a metal is low. It is essential to take note of that amid the move from the active to passive area, a 10^3 to 10^6 reduction in corrosion rate is normally watched.

Figure 9 outlines schematically the run of the mill conducts of an active-passive metal. The metal at first shows the regular conduct like non-passivating metals. That is, as electrode potential is made more positive, the metal takes after Tafel behavior and dissolution rate increments exponentially. This is the active corrosion potential range. At more respectable possibilities, dissolution rate abatements to a little esteem and remains basically autonomous of potential over an impressive potential area, called passive zone. At long last, at exceptionally respectable possibilities, dissolution rate again increments with expanding potential in the trans-passive zone.

The position of the maximum anodic current density (ic) is one of the imperative qualities of active-passive behavior which can be characterized by the primary passive potential E_{pp}. This current is termed the critical anodic current density for passivity i_c which is followed by a passive potential range accompanied by exceedingly small passive current. Figure 9 illustrates the reduction in dissolution rate going with the active to passive transition. This reduction in dissolution rate simply over the primary passive potential is the after effect of film formation at this point. The trans-passive region where dissolution rate again increases with increasing potential, is apparently due to the destruction of the passive film at high positive potentials[39][40][41].

From the aforementioned points, passivity is defined in two ways which are still in force today**.**

1. A metal is passive in the event that it significantly opposes corrosion in a given environment coming about because of strong anodic polarization.

2. A metal is passive on the off chance that it considerably opposes corrosion in a given situation in spite of a strong thermodynamic tendency to respond.

By the definition stating that a metal is passive if, on expanding the electrode potential toward more noble values, the rate of anodic dissolution in a given environment under steady state conditions becomes out to be not as much as the rate at some less noble potential[42].

On the other hand, a metal is passive if, on expanding the concentration of an oxidizing agent in a gas phase, the rate of oxidation, without external current, is not as much as the rate at some lower concentration of the oxidizing agent. These alternative definitions are equal in some conditions where the electrochemical hypothesis of corrosion applies[42]. There are two ordinarily communicated perspectives with respect to the idea of the passive film.

The first principal holds that the passive film (definition one or two) is dependably a diffusion-barrier layer of reaction products, for instance, metal oxide or other compound which isolates metal from its condition and which backs off the rate of response[43]. This is now and then alluded to as the oxide-film hypothesis[44].

The second holds that metals that are passive by definition one, are secured by a chemisorbed film, for instance, of oxygen[42][45]. Such a layer dislodges the ordinarily adsorbed water particles and backs off the rate of anodic dissolution including hydration of metal ions [46].

2.6 Passivation and Re-passivation

Passivation is another method that can make the metal more resistant against corrosion. Since passivation is a major topic in this master thesis, it will be explained more thoroughly in the next section.

Pickling usually means removing the relatively heavy, dark oxide films caused by annealing or high temperature thermal stress relief conducted in oxidizing atmosphere. In this work pickling had achieved good improvement in corrosion resistance (pitting potential). This was observed when pickling was carried out at room temperature. The most ordinarily utilized bath for evacuating oxide scale is a mixture of nitric acid of 10-15wt.% adding 0.5-3wt% hydrofluoric acid. On the other hand, pickling paste might be utilized. As these acids are exceedingly harmful, proper wellbeing precautionary measures must be taken. The method that was used for the pickling was using the chemicals namely nitric acid and hydrogen fluoride with the rest concentration of water [47]. The composition of chemicals that's used for the experimental procedure was explained in the further chapters.

2.7 Tinting colors

Heat-tint alludes to an oxide layer that creates close by heat treatment or the welds in stainless steel manufacturing process[48]. This process is the aftereffect of deficient gas protecting of welds enabling O2 to get to the surface of the metal causing heat tinting roots of the welds[49], see Figure 10.

This chromium oxide layer, which is not to be mistaken for the normally happening ultra-thin 2nm layer which gives stainless-steel its corrosion resistance, is formed as a thicker scale with an Amalgamation of nickel, iron and also different oxides (for example Cr2O3 Chromia)[50][51]. It is comprehended that this colored metal oxide film in different situations influence the corrosion

resistance of welded stainless steel joints[46]. It is the environment at the service that decides the severity of this effect. In benefit corrosion effect on heat tinted weld roots is likely to happen in fluid situations. Any level of heat-tint might be not permissible if the oxide can bargain benefit cleanliness[1][4][52].

In the process of heating, the normal straight-forward detached layer develops in thickness as chromium diffuses out of the base material matrix heat tint hues running from a pale straw to a dull-blue oxide scale[53][54]. The blue heat tint oxides are most prone to localized corrosion attack [4]. The heat tint scale consists of a heterogeneous oxide comprising of the metallic components of the stainless-steel [55]. The characteristics of the oxide-surface rely on upon the accompanying:

- Temperature and time of heat exposure
- Expanded limit at higher temperature-limits takes into account expanded dissemination of chromium.
- Composition and properties of the environment in contact with the hot metal surface.
- an inert gas or anode covering is utilized to expel or counteract O2 from interacting with the surface of the metal.
- Chemical arrangement of the base metal underneath the heat tint oxide.
- Physical state of the surface (staining) before heat tinting.

The heat tint scale is a weak obstruction to corrosive media (for example electrolyte) because of irregularities and chromium depletion inside the oxide. This absence of a rational passive oxide film on the weld can bring about confined corrosion at welded areas in few forceful situations[1]. possible corrosion mechanisms include pitting corrosion, Crevice corrosion, and in raw water or waste water atmospheres.

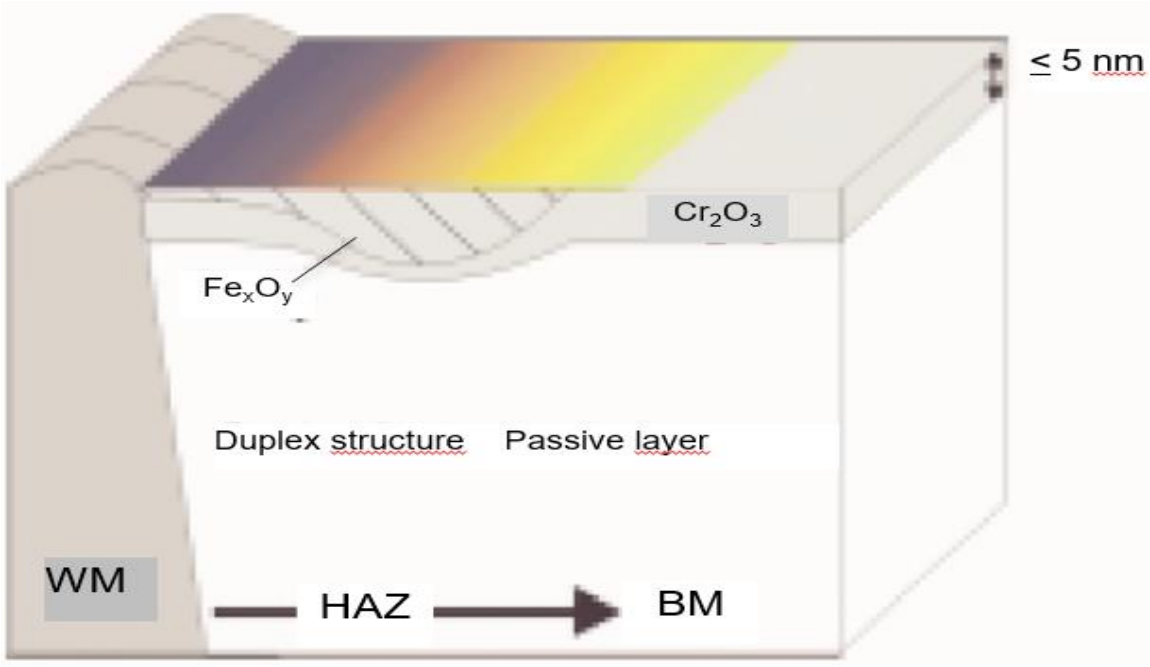

Figure 10 distribution of tinting colors at TIG weld seam (temperature gradient) [56].

In the process of heat tint development, chromium diffuses from the base metal into the heat affected zone (HAZ) as chromium is oxidized stronger than iron in the steel[57]. The diffusion zone depth reaches out the extent that the heat will enable the diffusion to happen[58]. This diffusion of chromium into the scale leaves a thin layer with reduced chromium content just underneath the heat tint scale, compare Figure 10[59][60]. As chromium is in responsible of giving stainless steel its corrosion resistance, this area would now have reduced resistance to localized corrosion especially within the sight of oxidizing acid solutions[61]. Corrosion that would not happen somewhere else can start in the depleted areas unless the heat tint and the subsequent thin depleted area are anticipated or potentially evacuated[62].

2.7.1 Heat Tinting acceptance

There is perpetual open deliberation as to satisfactory levels of heat tint on stainless steel welds[4][1]. Two noteworthy themes of verbal confrontation that test the stainless steel and client ventures are a tradable graphical outline that delineates distinctive levels of oxidation and a comprehension and concession to satisfactory levels of oxidation for various conditions [63]. The more extreme the service condition is, the lower the resilience for the nearness of heat tint.

Welding of 304 stainless steel requires purging by an inert gas both earlier and during welding, to displace the residual oxygen of the air[64]. Since, in field establishments, 100% powerful inert gas purging is hard to accomplish because of nearby conditions around the weld, there are fluctuating levels of oxidation that happen[65]. Consumable water frameworks, for instance, are normally set in benefit in the as welded condition and grinding, pickling or different methods for expelling heat tint are either not satisfactory or not plausible[66][1]. Subsequently, the training is to inspect finished welds and decide whether the level of oxidation is underneath a worthy farthest point. In the case when oxidation is excessively extreme, the weld is removed and newly welded[1]. The inquiry is, how can one analyze heat tint severity and how severe is heat tint[4][33]. Inward investigation of the root of butt welds in piping is troublesome and the understanding of the outcomes is subjective[67].

2.7.2 Heat-tinted Surfaces Repairing

In a few applications including nearby stainless steel pipe welding, removing all heat tint oxides after welding is exceptionally hard to do, even subsequent to utilizing proper gas cleansing[68]. During conclusion of stainless steel pipes by welding heat tints are in some cases identified during review in regions that are difficult to get to, for example, inside circumferential butt welds on smaller diameter pipes[4][69]. These areas are impossible to access by mechanical methods for chemical cleaning requires huge volumes of acid solutions for be transported to work areas and the transfer can be troublesome as some regulations can be prohibitive on such chemicals[4][70]. Cleaning of outside pipe butt weld surfaces to reestablish the corrosion resistance can be completed without any difficulty. Be that as it may, evacuation of undesirable heat

tints on weld root surfaces can be troublesome, tedious and costly, especially at remote employment destinations.

The corrosion resistance of regions that have been heat tinted can be reestablished by methods for mechanical and additionally chemical cleaning[4][1][2]. As specified above there is a thin layer beneath the heat tinted region that has a low content of chromium. To keep the onset of corrosion of this surface it must be evacuated [1]. This should be possible mechanically by grinding, brushing, blasting or it can be evacuated synthetically by a procedure known as pickling. Grinding is a typical practice for the removal of imperfections, for example, shallow surface imprints, weld spatters. In the event that dishonorably cleaned, a surface can turn out to be more susceptible to corrosion than the first heat tinted surface. Grinding or brushing operations can spread and imbed the heat tint oxide at first glance, or uncover the Cr-depleted layer without totally removing it[39]. A case of poor cleaning is the setting of a stainless steel weldment caused by stainless steel wire brushing. For this situation, it is trusted that a stainless steel brush of various organization was utilized to clean the welds, leaving stores of sub-par material or the expulsion of the exhausted surface layer was deficient [71]. The two primary constituents of stainless steel pickling items are hydrofluoric and nitric and acids. In that capacity, mind must be practiced in the utilization of pickling operators both from a natural viewpoint and metallurgical perspective. On the off chance that corrosive contact times with the stainless steel and in addition the last flushing methods are not legitimately controlled, corrosion can be started in the treated zones. It is critical that all hints of pickling items, pickle deposits and tainting are totally washed from the surface of the steel parts to accomplish a completely corrosion safe and stain free surface[4].

3 Corrosion of Stainless Steels

When corrosion is discussed, most people think about the corrosion appearing on a material that is not resistant in the environment. This corrosion appears as rust on the surface of the material, like it is for unprotected unalloyed steel. However, if the material is soluble in the environment, the metal can be dissolved in the solution as ions. The latter is an electrochemical process where the metal is dissolved to form a more stable formation [60]. The corrosion process includes both an anionic and a cathodic reaction which is occurring on the surface of the metal. These reactions are two half-cell reactions, one oxidation and one reduction. During a corrosion process, both a charge- and a mass transfer occur on the metal surfaces. For corrosion to occur there has to be metallic contact between the anodic and cathodic sites and there has to be an electrolyte present as well. The cathodic reaction is a reduction, where the oxidation number of the oxygen is decreased and electrons are consumed. The anodic reaction is the oxidation. Here is a loss of metal due to that the metal oxidizes and dissolves into the solution as ions. Since the two reactions are coupled, if one of them is changed, so is the other [8].

3.1 Corrosion Resistance

The passive chromium-rich oxide formed on stainless steel surfaces is the reason behind the stainless steel resistance to staining, i.e. to rust and corrosion [72], which is not found in ordinary carbon steels. The oxide can readily form in oxidizing atmospheres and has the ability to selfheal (At the point when actuated by oxygen inside the air or water then it is this layer which repairs gently scratched or any damage to the surface), i.e. if the surface is scratched new oxide will form on the unprotected metal and once again protect the underlying steel from corrosion. A prerequisite for the self-healing is of course that oxygen is present and that the environment is not too aggressive. The structure of the oxide layer has been described as similar to chromite (Cr_2O_3), and the thickness of the oxide layer is about 1-2 nm. Even the minimum amount of chromium (~11%) is sufficient to form the passive layer on the surface, but the stability of the passive film increases with increasing the Cr content up to 17%. The alloying by chromium and the passive surface layer formed implies that all stainless steels, are practically resistant to general corrosion under normal conditions. The stainless steels are however sensitive to some localized attacks like e.g. pitting, crevice or intergranular corrosion. To withstand these types of stainless steels attacks, especially in reducing atmospheres, additional alloying is required, but may not be sufficient. One way to indicate the stainless steel corrosion resistance in reducing atmospheres and towards localized attack is the Pitting Resistance Equivalent (PRE). The most common empirical formula therefor is –

$$PRE = Cr\% + 3.3Mo\% + 16N\%.$$

The PRE can indicate how well the stainless steel can withstand pitting during use in chloride atmospheres, in seawater and comparable others. By way

of example for the use in seawater a PRE in excess of 40 is recommended. In comparison, the investigated 304 stainless steel has just a PRE = 17,5 – 20,8 depending on its concrete chemical analysis.

3.2 Types of corrosion

There are eight types of corrosion; uniform, crevice, pitting, stress-corrosion cracking, galvanic, intergranular, dealloying and erosion.

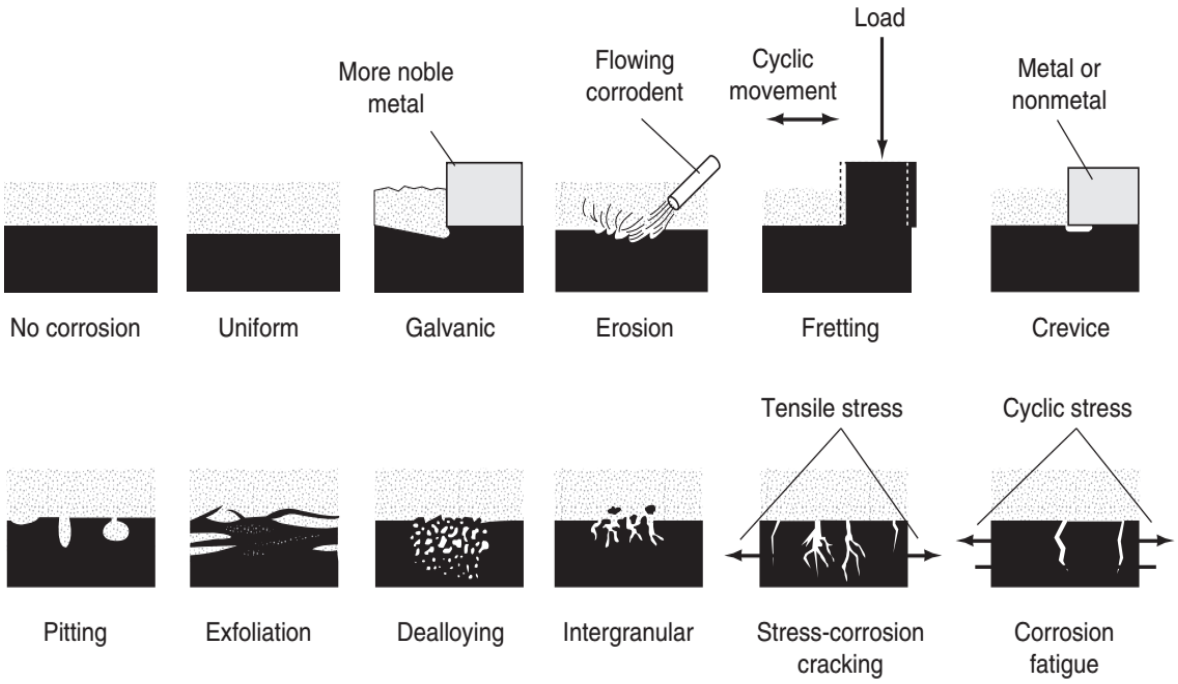

Figure 11 Different types of corrosion

In Figure 11 these eight types are schematically shown. Three of them form a group called localized corrosion. These are crevice, pitting and stress-corrosion cracking. In all the localized corrosion types, the metal is attacked in certain positions, where some of the other types forms a uniform corrosion that spreads over the entire metal surface.

General corrosion	corrosion that spreads equally over the surface of a material.
Uniform corrosion	The corrosion attack that is distributed uniformly on the surface of the metals, and sometimes it is referred as the corrosion that proceeds at the same rate over the surface of the metal[73]
Pitting corrosion	Localized corrosion that is confined to a little area, appearing as pits.
Crevice corrosion	A type of localized corrosion and happens under an indistinguishable condition from pitting. In general,

	corrosion attack begins more effortlessly in a tight crevice than on an un-shielded surface.
Erosion corrosion	a conjoint activity including a destructive streaming of solid particles which quickened loss of material.
Cavitation corrosion	advancement and fast fall of cavities, often vapor bubbles.
Galvanic corrosion	corrosion of a metal because of contact with a more noble metal in a destructive electrolyte.
Fatigue corrosion	Material cracks caused by rehashed worries in a destructive domain.
Stress corrosion	Corrosion caused due to parallel event of cracking when connected at a present tensile stress

Table 1 Types of corrosion [74]

3.3 Pitting corrosion

Pitting corrosion is characterized as is described by assaults at little discrete spots on the steel surface which appears as pits. Pitting is a destructive effect and it happens for the most part on metal surfaces which owe their corrosion resistance to passivity. The significant outcome of pitting is the breakdown of passivity, as can be seen in Figure 12, that is, pitting, as a rule, happens when there is breakdown of surface films when exposed to pitting condition.

Pitting corrosion is affected by a wide range of parameters, metal composition including environment, temperature, potential and surface condition. Critical ecological parameters which includes pH, aggressive ion concentration and inhibitor concentration. Other phenomenological parts of localized corrosion incorporate the stochastic idea of the procedures and the phases of limited assault including metastable attack, stable development, passive film breakdown and maybe eventual growth.

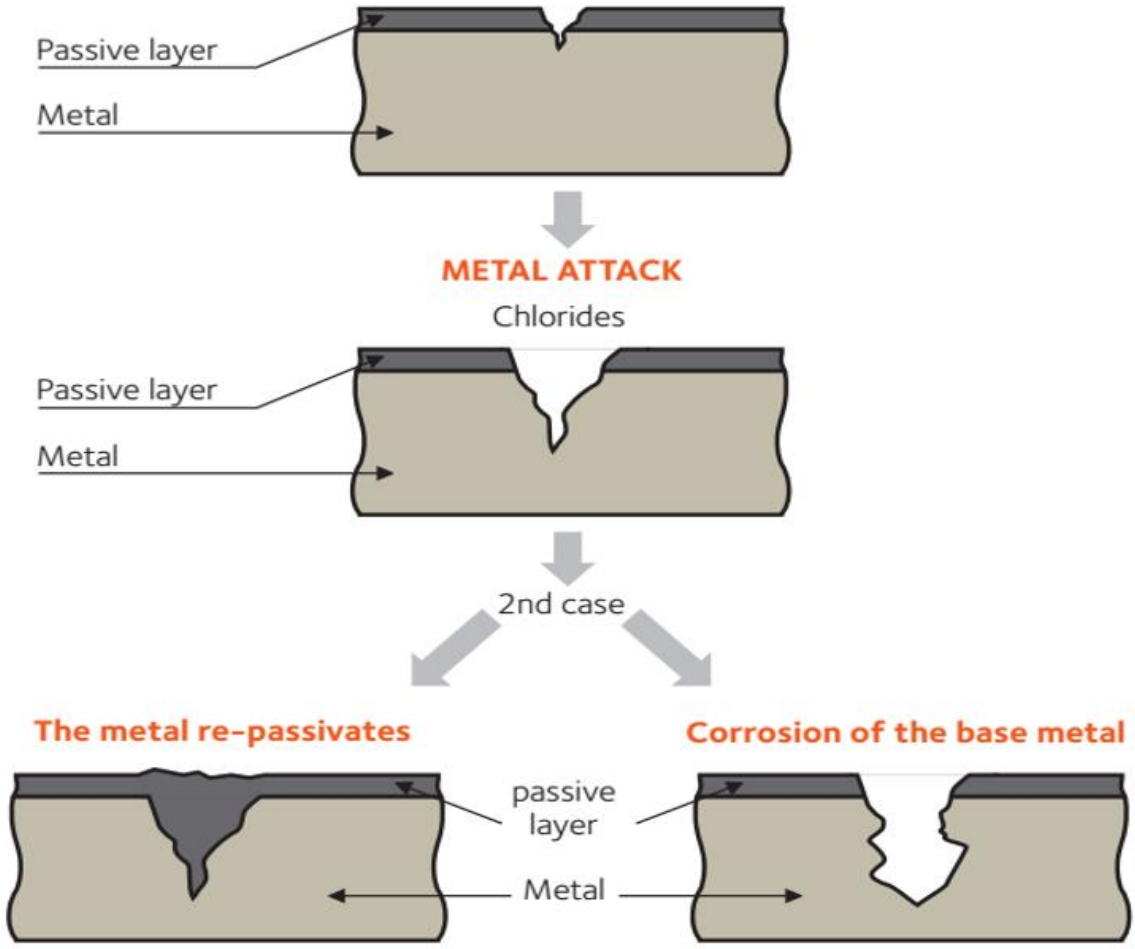

Figure 12 Pitting corrosion mechanism [75]

Pitting can be considered to comprise of different stages: passive film breakdown, metastable setting, pit development, and pit smothering or passing. Any of these stages might be thought to be the most basic. For example, once the passive film separates and a pit starts, there is a probability that a steady pit will develop. Then again, pits will not start in the event that they cannot develop in any event for a brief span. The passive state is required for pitting to happen; however, a few analysts trust that details of the passive film creation and structure assume a minor part in the pitting procedure. This view is bolstered by the way that numerous perceptions of setting propensity can be completely represented by development contemplations. Moreover, pit development is basic in down to earth uses of disappointment forecast. At last, the metastable pitting stage might be believed to be the most essential, on the grounds that exclusive pits that survive this stage end up noticeably stable developing pits. Investigations of metastable pits can hence give knowledge into key parts of setting, on the grounds that both start and soundness are entering figures metastable pitting [76].

3.3.1 Passive film breakdown and pit initiation

Passive film breakdown and the points of interest of pit initiation as shown in Figure 13 involve the minimum comprehended part of the pitting phenomenon. Breakdown is an uncommon event that happens to a great degree quickly on a

little scale, which cannot be observed with the help of direct observation. The passive film is frequently drawn schematically as a basic layer covering the metal and blocking access of the environment to the metal. In reality it is much more complicated as it completely depends on alloy composition, atmosphere, potential, and exposure related data, this film can have a scope of thickness, structure, organization, and stability. Regular latent films are very thin and support a to a great degree high electric field (on the request of 106 to 107 V/cm). The passage of a finite passive current density is confirmation of constant response of the metal, to bring about film thickening, dissolution into environment, or sometimes there may be combination of both the conditions. The perspective of the passive film similar to a dynamic structure, as opposed to static, is critical to the proposed mechanisms of passive film breakdown and pit initiation [52].

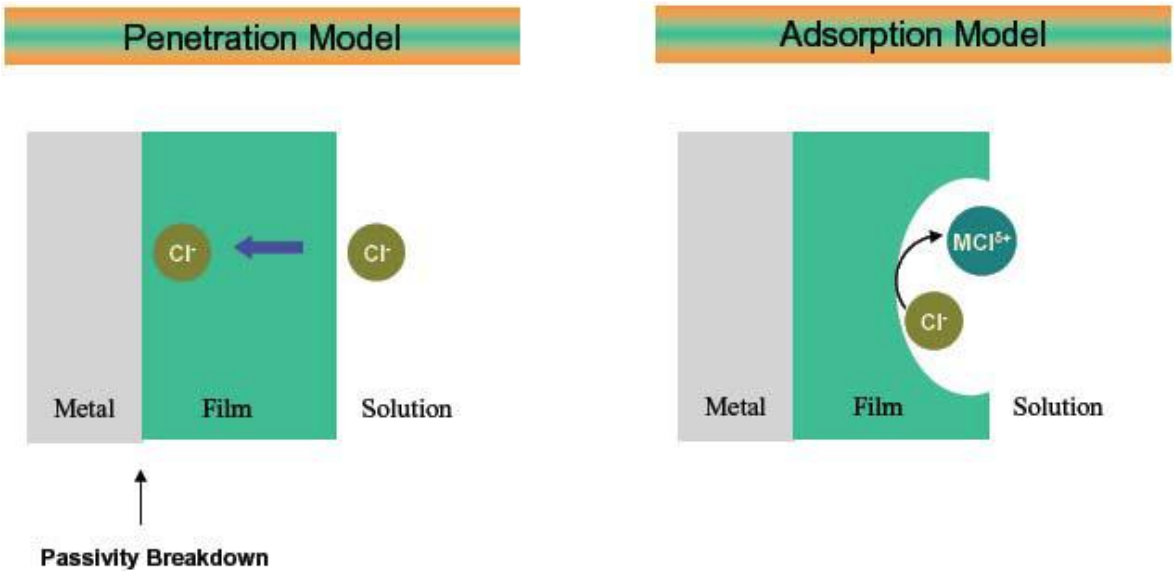

Figure 13 passivity breakdown by chloride ions-[77]

Speculations on breakdown of passive film and start of the pit have been arranged into three principle steps that emphasis on film breaking, latent film infiltration, or adsorption. Similarly, with such circumstances, distinctive components or blends of these instruments might be legitimate for various metal-condition frameworks.

Similarly, as with most such circumstances, distinctive components or blends of these instruments might be legitimate for various metal-condition frameworks. These mechanism of chloride ions have been considered as far as pure metal systems. However, pits in real alloys arc regularly connected with inclusions or second-stage particles, and these variables should likewise be reconsidered.

3.3.2 Pitting corrosion propagation mechanism

The pitting corrosion mechanism of stainless steel can be isolated into three consecutives ventures as takes after: start, metastable spread and stable engendering. The start step is a local breakdown of the passivating oxide layer

by aggressive ions. The corrosion procedure would then be able to proceed in the unprotected metal uncovered by the start step. The corrosion rate is increased by the way that a much more aggressive environment is created by the corrosion reaction (so called the metal dissolution in the pit and the formation of hydrogen-ions (pH decrease) itself. In any case, at the prior phases of pit proliferation, when the pits are still little, the pits can re-passivate suddenly. This stage is regularly alluded to as metastable pit development. The phase of stable proceeding of pitting is achieved when unconstrained re-passivation is never again conceivable henceforth pitting corrosion happens.

3.3.2.1 Susceptibility to pitting

There are different ways of estimating the alloy's susceptibility to pitting, amongst which, are listed below

- by determining the alloy PRE-number
- by determining the characteristics, the pitting potential of the alloy
- by determining the critical pitting temperature of the alloy
- by measuring the weight loss, counting the number of pits per unit area.
- by determining the least amount of aggressive ions propagating the pitting.

The PRE-number method has already been discussed in the introduction. The remaining methods will be discussed in detail in the following sections[78].

3.3.3 Characterization of pitting potentials

Different electrochemical polarization techniques are used to determine the characteristics of the pitting potentials of an alloy. The basis of electrochemical corrosion testing is derived from the potential theory which isolates the oxidation and reduction reactions of corrosion and hypothesizes that the total rates of all oxidation responses parallel the total rates of all reduction reactions on the corroding surface.

The protection potential is obtained at the point where the reverse scan polarization curve intersects the forward scan else, if the reverse polarization scan does not intersect the forward scan, then the protection potential is estimated using a threshold current density. Potentiostatic polarization potential is favorable when more information (such as localized initiation time, stability and propagation) is needed as opposed to cyclic potentio-dynamic polarization. When pitting potential is used, a critical aspect of pitting resistance is the magnitude of the difference between the critical pitting potential (E_{pit}) and the corrosion potential (E_{corr}), Generally, pitting should not occur in situations where E_{corr} remains negative to E_{pit}.

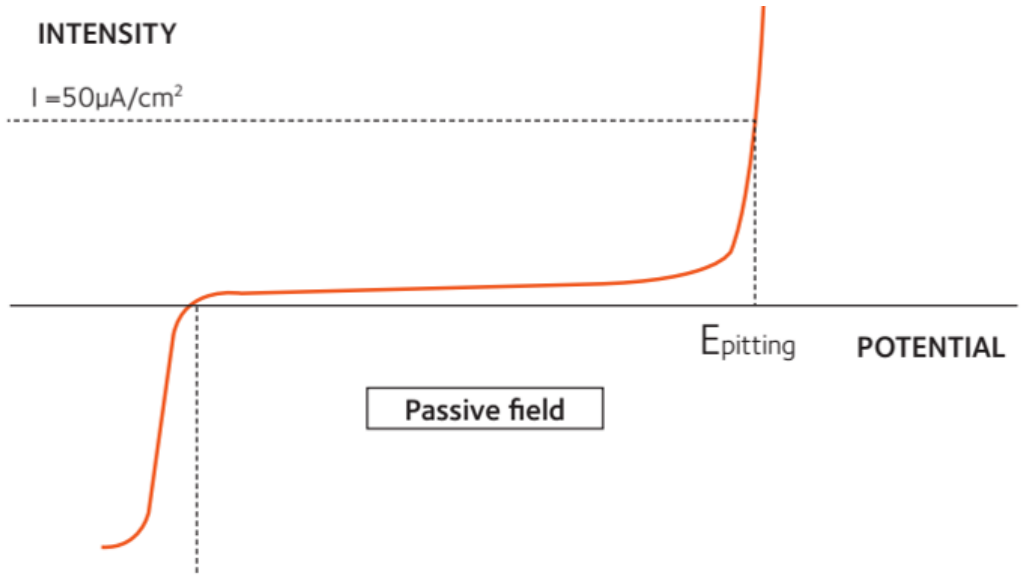

Figure 14 Schematic showing the passivity of pitting corrosion[79]

3.3.4 Critical pitting temperature

A potentiostatic polarization where a single potential step is applied (typically to 700mV vs SHE (standard Hydrogen Electrode) according to ASTM G150 [80] result in obtaining the critical pitting temperature of the alloy. The Critical Pitting Temperature (CPT) defines the lowest potential - independent temperature, below which pitting does not occur.

3.3.5 Other methods to evaluate the pitting corrosion

Pitting corrosion can also be estimated by measuring the number of pits per unit area, weight loss, and if possible, the size and depth of pits formed in the standard solution and, by determining the lowest concentration of aggressive ions causing the pitting.

3.3.6 Factors affecting pitting corrosion

Both external and internal factors affect pitting corrosion. Hence, combat pitting corrosion in stainless steels is targeted at addressing these factors by either decreasing the corrosiveness of the environment (external factors) or increasing the pitting corrosion resistance of the materials (internal factors). Decreasing the corrosiveness of the environment is not always practical in some applications. Here often corrosion inhibitors are applied, especially for closed circuits. A significant number of studies have been developed focusing on increasing the pitting corrosion resistance of stainless steel alloys. However, understanding of the environment is important in order to develop a solution to any corrosion problem. Hence, efforts to combat pitting corrosion in stainless steels includes evaluating the effect of both external (environment composition, temperature, electrode potential) and internal parameters (alloy composition, heat treatment, microstructure and surface preparation) among others. The following paragraphs will discuss these factors affecting pitting corrosion in detail[61][81].

3.3.7 Effects of external factors on pitting corrosion

These are mostly environmental factors which affect pitting corrosion of stainless steels. They include temperature, pH and, availability of aggressive ions and their concentration as well as the oxygen content in the electrolyte. These factors are discussed in detail in the following sections.

3.3.8 Effect of pH

The most available literature indicates that pitting corrosion is much less dependent on pH values. However, in their recent studies, found that corrosion test results for stainless steel tested at pH 1.0, 7.4 and 9.0 indicated both general and pitting corrosion resistance are negatively affected by a decrease in pH. They also found that although the general and pitting corrosion resistance of the stainless steel severely deteriorated by exposure to low pH solution, re-passivation of the stainless steel was possible. However, re-passivation of the stainless steel at a pH of 7.4 and 9.0 was not observed. They concluded that re-passivation may have been possible at low pH because the samples in this group were polarized to low potentials. It is further found that increase in the pH from 7.4 to 9.0 did not affect the corrosion resistance of the stainless steel. This suggests that there is a pH threshold above which general and pitting corrosion resistance of stainless steel is less dependent on pH. In other researches, it was found that low pH and stagnancy provided most favorable conditions for pit growth. Under conditions of 4-5 ppm dissolved oxygen and 25° C, observed that pits grew between 450 and 325 microns at pH 4 under static and dynamic conditions, when 304 stainless steel specimens were immersed in 300 ppm chloride solutions for 4 months. At higher pH (7 and 10), and the same conditions, the depth rarely exceeded 70 microns [82] .

3.4 Crevice corrosion

Crevice corrosion is a type of localized corrosion and it may rise when there is existence of narrow opening or gap between metal and metal/non-metal components as shown in Figure 15. Non-metallic components that can cause crevice corrosion are rubber, glass, wood, plastic and even living organism (bacteria). Crevice corrosion can also occur where unintentional crevices exist, for instance cracks, metallurgical defects and others. Crevice corrosion for the most part happens where nearby gradients of oxygen focus exist. At the point when there is a crevice, oxygen inside the crevice electrolyte is reduced or consumed where the rest of the metal surface has prepared access to oxygen. All things considered metal surface becomes cathodic with respect to crevice area. The bigger the proportion amongst cathode and anode area will give addition of corrosion rate. Crevice corrosion mechanism is same like mechanism of pitting corrosion. Crevice corrosion of steel in the surrounding of chloride ions in the arrangement is represented in the Figure 15.

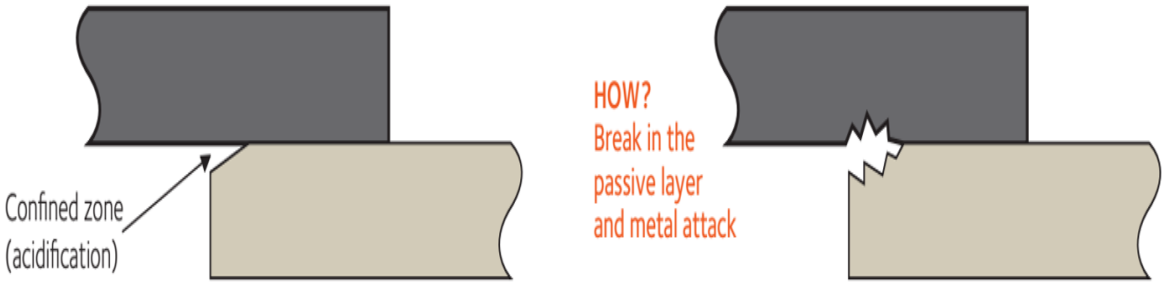

Figure 15 Crevice corrosion mechanism [79]

Crevice corrosion usually happens in austenitic stainless steel and additionally different composites of stainless steel that build up a hindrance or passivation layer, and for this reaction to happen, three conditions must exist. Initially, the metal must be electrically associated with the outer metal outside the crevice. Besides, the arrangement in the crevice must be stagnant and give an ionic way to the metal outside of the crevice. Thirdly, the outside metal surface must be passive.

At the point when these conditions are met, differential air circulation cells might be set up where the oxygen in the crevice gets drained, making the crevice turn into the anodic site for metal dissolution reaction. Metal ions hydrolysis happens inside the crevice, and chloride ion relocation into the crevice brings about acidic chloride conditions inside the crevice. At this point, the crevice solution causes the loss of strength and the quick breakdown of the protective layer in the crevice [74].

3.4.1 Theories Governing Crevice Corrosion

Basic crevice corrosion theories have been proposed are Critical Crevice Solution theory and IR drop theory. Both frameworks tried to give a clear idea to the begin and spread of crevice corrosion of passive metals in contact with an electrolyte. In any case, of the two proposed frameworks, IR voltage drop component gets more thought as the choice instrument especially for active/passive metal composites. The reason behind its unpopularity is that it gives an understanding to corrosion process in both chloride-containing and chloride free conditions not in any manner like the Critical Crevice Solution Theory (CCST).

The principal hypothesis to address the onset of crevice corrosion was the solidification mechanism or the CCST. It was created by It recommends that the adjustment in the electrolytes chemical composition and the arrangement of a crevice with high concentrations of hydrogen and chloride ions are in charge of the breakdown of the passive films on the metal surfaces.

The CCST considers the impact of crevice geometry (i.e. the width and depth of the crevice gap) on mass transport of dissolved ions into and out of the crevice prompting the improvement of a basic crevice arrangement. In light of the

adjustments in localized science inside the crevice, the de-passivation of the passive film on the alloy will happen. At the point when a low pH and a high chloride ions concentration focus in the crevice arrangement causes damaging of the passive film, the arrangement is said to have achieved a basic state and subsequently dynamic fissure formation will start as seen by high rates of corrosion proceeding in the crevice. This system of localized corrosion depends on hydrolysis of metal particles (called acidification) and the mass transport of disintegrated ions i.e. chlorides all through the crevice, however totally excludes the electrode potential E, and its appropriation, E_x, inside the localized cell. Be that as it may, it considers the current produced in the crevice because of the mass transport of ions all through the crevice. Hence, a system was proposed to represent the potential dissemination inside the crevice amid the onset of crevice corrosion.

The IR drop theory was created by Pickering [83]. As indicated by this Mechanism, crevice corrosion movement comes about because of an IR voltage drop in the crevice solution which makes a localized electrode potential on the crevice wall inside the active peak region of the polarization curve. Along these lines, crevice corrosion would suddenly begin when the potential difference between the crevice mouth and the interior was sufficiently enough to make anodic areas end up noticeably active. This potential difference is known as the IR drop in the solution where I is considered as the ionic current streaming out of the crevice or pit, and R is the resistance of the crevice/pit electrolyte[84][85].

3.4.2 Factors Affecting Crevice Corrosion

There are a few elements that are in charge of crevice corrosion start in stainless steel compounds. Such factors incorporate mass and crevice arrangement, oxygen content, pH, chloride concentration and temperature. Moreover, alloy composition, mass transport all through a crevice, metal disintegration and passive film attributes are variables that additionally can impact the crevice corrosion severeness Geometrical angles, for example, the outside to inside crevice area proportion, width and depth of the crevice are likewise known to add to this phenomenon.

3.4.2.1 pH and Temperature Effects

During the corrosion procedure, increment in temperature enhance the response energy of metal disintegration and reduction reactions causing the breakdown of the passive region. Fundamentally, an increase in temperature causes an expansion in the conductivity of electrolytes consequently prompting a relating increment in the rate of electrochemical reaction and anodic current.

Be that as it may, Lee (1981) [86] examined the impact of temperature on crevice corrosion start and produces in 5 distinctive crevice samples of AISI 304 and 316 stainless steels drenched in normally circulated air through seawater for 28 days at 10, 25 and 50°C. Visual perception of start times and gravimetrically decided spread rates were found and the corrosion currents were ascertained. It

was recognized that more corrosion was seen at 25°C than at 10 or 50°C following 28 days of introduction. The higher corrosion rates at 25°C can be ascribed to enhancing in the reaction kinetics of the disintegration and diminishment responses, and additionally to an expansion in mass transport of species into the crevice. In any case, at a higher temperature of 50°C, oxygen dissolvability is reduced, along these lines diminishing the outside cathodic response rate, which thusly brings down the rate of corrosion. The molybdenum–free type 304 stainless steel tests showed faster corrosion start than type 316 alloys.

3.4.2.2 Effects of Crevice Geometry

Crevice geometry is another imperative crevice corrosion weakness. The nearness of adequately tight crevice supports the setting up of the differential air circulation depressions and the differential grouping of protons (H^+ ions). The nucleation and spread of this effect is related with the creation and improvement of restricted arrangements inside the crevice distinctive to the general solution. Oldfield and Sutton (1978) demonstrated that crevice corrosion start time in seawater expanded as the crevice depth measurement expanded from 0.1μm to 1μm. Besides, in a comparative report suggested that for a crevice depth of 0.1cm, a hole of under 0.01μm may be required for start of crevice corrosion of type 304 stainless steel in normal waters with 1000mg/l chloride concentration.

Past examinations likewise demonstrated that crevice corrosion start time is explicit subjected to the width/depth ratio of the crevice geometry. An expansion in crevice gap width therefore builds the season of start. A wider crevice diminishes the chloride particle movement in the crevice of AISI 304 stainless steel consequently expanding the corrosion start time. In view of these perceptions, it was clarified that narrower crevice gap would be fundamental for crevice corrosion to reduce the chloride concentration because of oxygen diffusion limitations[87].

4. Experimental Methods

The model of the experimental procedure is done with the following steps:

Sample preparation

a) Finding the shape and size of the sample for tinting process and for the potentiostatic corrosion tests by trying different shapes and sizes for creating artificial oxide layers on the specimens
    - For dilatometer, rectangular specimens of size 10 mm*6 mm were used for a time of 180 secs.
    - For the furnace, the cylindrical specimens of diameter 12 mm were used.

b) Choosing the right method for the cutting of the samples.
c) Finding the external supplier for the cutting of the samples.
d) Getting the sample in the desired size.
e) Tinting parameters
    a) Finding the right parameters for the tinting process with trial and error basis method with a lot number of samples tests and different tinting time (from 2 to 20 minutes) with a set of temperatures (from 200°C to 1100°C to figure out the required (different colors at least two) artificial oxide layers.
    b) Tests were conducted from minimum to maximum temperatures to get the desired output on the samples.
f) Pickling solution
    a) Literature search for getting the proper composition of the pickling solution[88].
    b) Pickling tests at the proper composition of the chemicals (HNo_3 (Nitric acid) +HF (Hydrogen Fluoride) + water (H_2O)) at room temperature.
g) Potentiostatic tests
    a) Electrolyte solution composition for the tests from 3 different concentrations (1%, 3.5% and 5%NaCl).
    b) Finding the input parameters by conducting a wide number of sample tests using trial and error basis.
        - for i-interrupt (such as current range with various values of current, set potential) as shown in Figure 16.

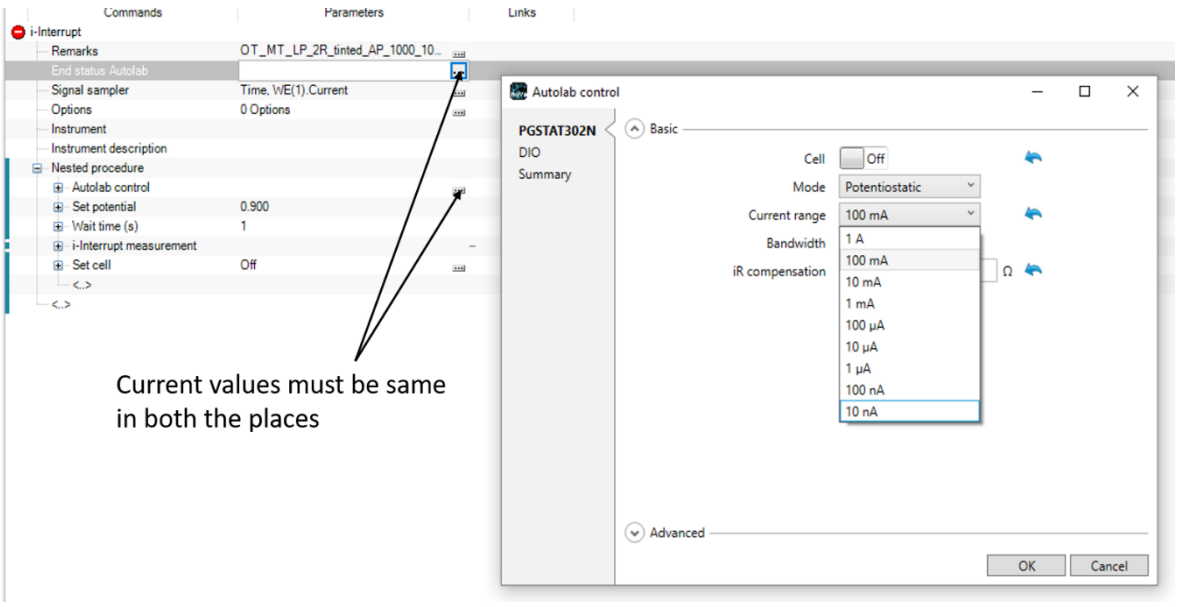

Figure 16 i-interrupt current range

- for positive feedback increment (current range (considered same as the i-interrupt), iR compensation), repetition n times, increment parameter (which can be set from 10 to 200, but tried for 100 and 200 repetitions with an increment parameter of 1 and 0.1) as shown in the Figure 17.

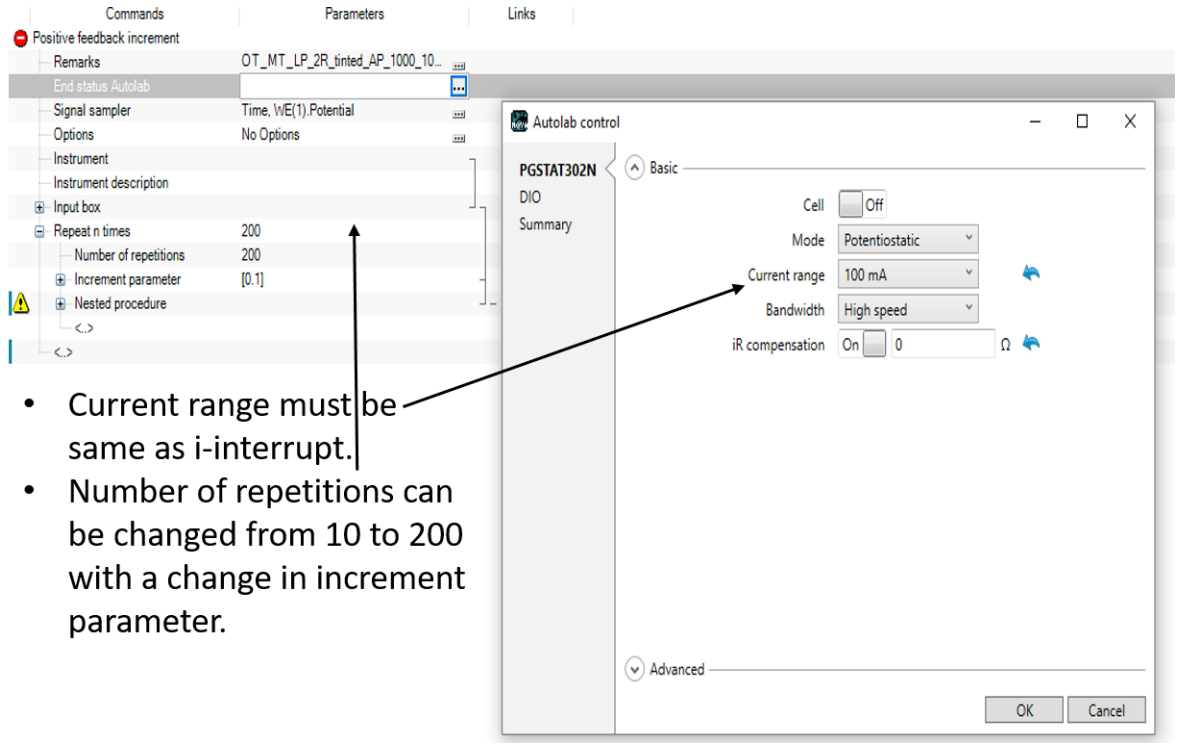

Figure 17 Positive feedback increment values (current range and number of increments).

- for test I vs E (current range, iR compensation)

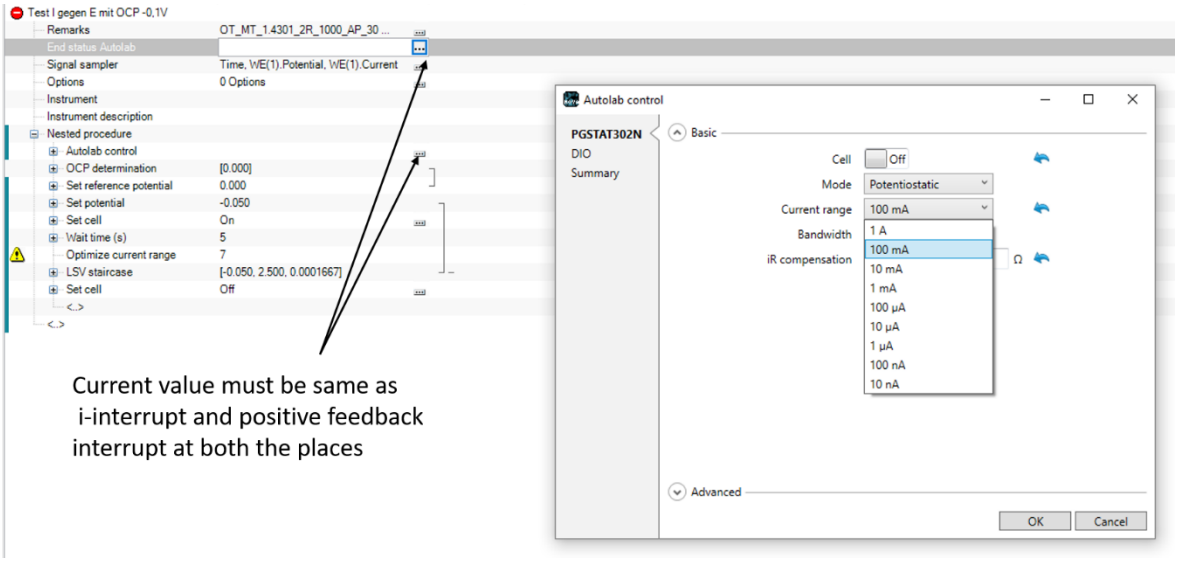

Figure 18 I vs E current range.

- for test I vs E (iR compensation)

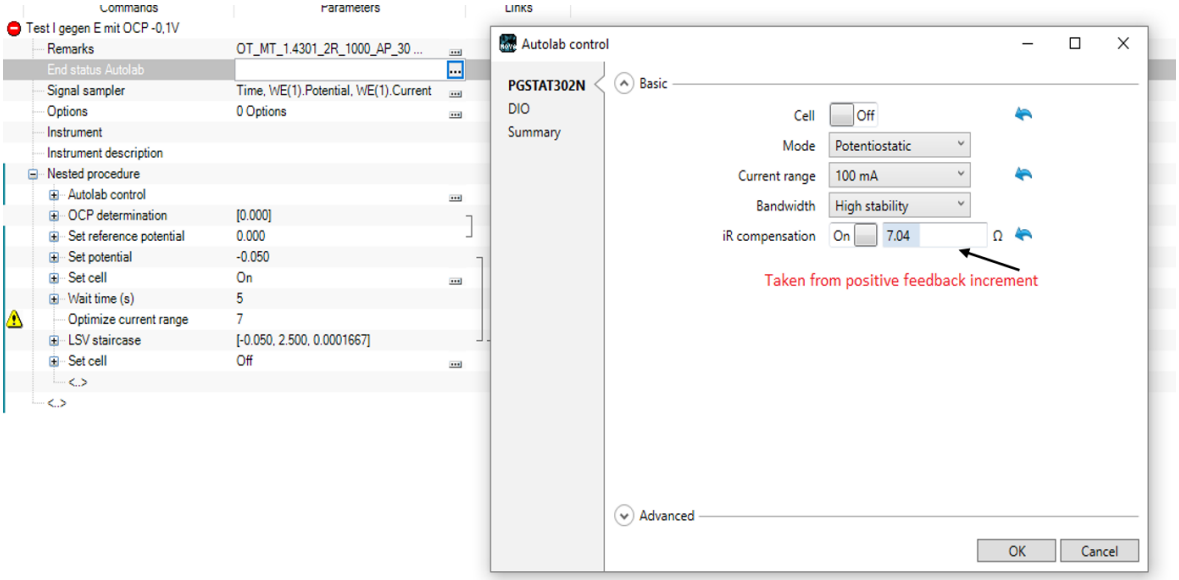

Figure 19 iR compensation for test I vs E with OCP -0.1.

- OCP determination (maximum time))

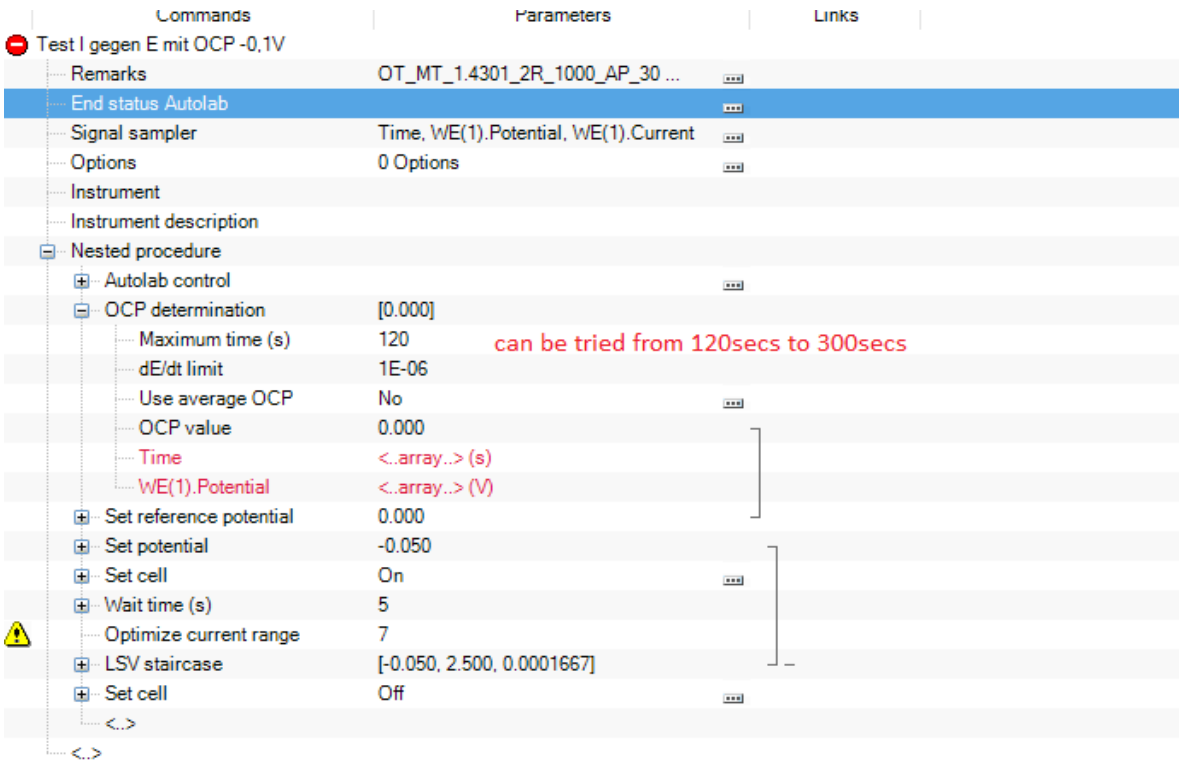

Figure 20 Test I vs E OCP time Determination.

- LSV staircase (step potential and scan rate)

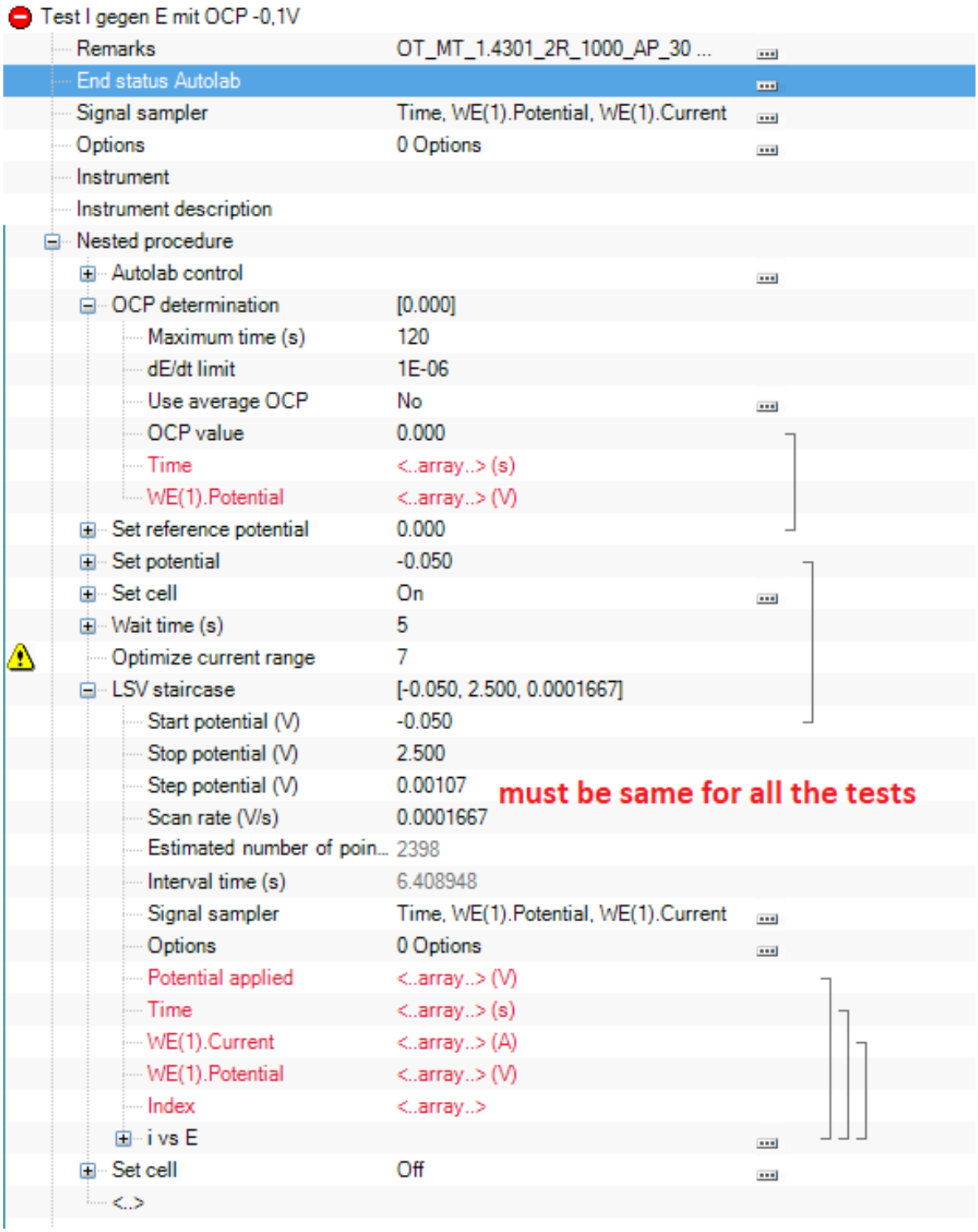

Figure 21 I vs E LSV Staircase step potential and scan rate.

c) Finding the right procedure of -I vs E linear polarization tests from the set of available tests by using various set of parameters.
d) Standardizing the procedure for the next tests

h) Measurements

a) Collecting the required data such as OCP and BTP.
b) Taking the required values for further calculations
c) Converting the values into graphs (OCP, BTP, BTP-OCP) for the comparison

i) Metallography
a) Sample cutting for the cross-section evaluation
b) Warm embedding
c) Grinding and polishing
d) LOM evaluation
e) Measuring the depth and width of the pits

j) EBST and Raman spectroscopy FELMI
a) Cr-Oxide layer evaluation

4.1 Sample Specification

The AISI 304 stainless steel sheets were received in the size of an A4 format (625cm$^{2)}$ with two different surface conditions, namely 2B (skin pass) and 2R bright annealed) and in two different thicknesses: 1,6mm for the 2B and 2.0mm for 2R. The 2R which tends to have a brighter and smoother surface finish came with some scratches probably from handling and transport. After trying many different shapes for the artificial tinting process finally we choose to make the specimen in the cylindrical shape due to the specimen holder capability and the 1cm2 area for measuring the corrosion. Then the cylindrical specimens of 12 mm diameter as shown in Figure 22 (also see appendix A (1) Figure 47) are manufactured by water jet cutting taken out form two DIN A4 format sheets (625cm^2) which was done at the CECON company in Krottendorf.

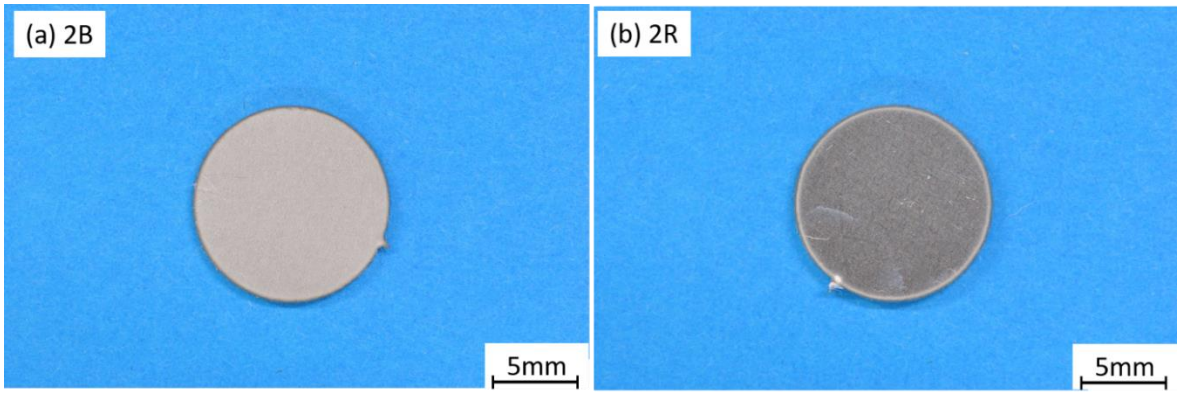

Figure 22 Samples after cutting from the sheets (blank)

The labeling of the samples is categorized into 5 different types:

1. Blank of 2B (skin passed) and 2R (bright annealed) - taken from the water jet cutting.
2. 2B_600°C and 2B_1000°C– where the specimens were tinted at 600°C and 1000°C each for 10 minutes in the oven.
3. 2R_600°C and 2R_1000°C – where the specimens were tinted at 600°C and at 1000°C each for 10 minutes in the oven.

4. 2B_600°C_AP and 2B_1000°C_AP – where the specimens were tinted at 600°C and 1000°C each for 10 minutes in the oven and then were pickled to remove the artificially formed oxide layer.
5. 2R_600°C_AP and 2R_1000°C_AP – where the specimens were tinted at 600°C and 1000°C each for 10 minutes in the oven and then were pickled to remove the artificially formed oxide layer.

Sample no.	Surface finish	Sample no.	Surface finish	Tinted/blank	Tinting Temper-ature and time
1	2B	5	2R	Blank	-
2	2B	6	2R	Blank	-
3	2B	7	2R	Blank	-
4	2B	8	2R	Blank	-
5	2B	9	2R	Blank	_-
11	2B	10	2R	Tinted	1000°C,10 mn
12	2B	11	2R	Tinted	1000°C, 10 min
13	2B	12	2R	Tinted	1000°C,10 min
14	2B	13	2R	Tinted	1000°C,10 min
15	2B	14	2R	Tinted	1000°C,10 min
6	2B	16	2R	Tinted	600°C,10 min
7	2B	17	2R	Tinted	600°C,10 min
8	2B	18	2R	Tinted	600°C,10 min
9	2B	19	2R	Tinted	600°C,10 min
10	2B	20	2R	Tinted	600°C,10 min
16	2B	21	2R	tinted+AP	600°C,10 min
17	2B	22	2R	tinted+AP	600°C,10 min
18	2B	23	2R	tinted+AP	600°C,10 min
19	2B	24	2R	tinted+AP	600°C,10 min
20	2B	25	2R	tinted+AP	600°C,10 min
21	2B	26	2R	tinted+AP	1000°C,10min
22	2B	27	2R	tinted+AP	1000°C,10min
23	2B	28	2R	tinted+AP	1000°C,10min
24	2B	29	2R	tinted+AP	1000°C,10min
25	2B	30	2R	tinted+AP	1000°C,10min

Table 2 List of specimens

All the above-mentioned samples were taken in a batch of five samples each to carry out the potentiostatic corrosion tests and evaluate the results. The samples that were used in the experimental procedure were listed in Table 2 with the type and the sample numbers in detail.

4.2 Heat Treatment of the samples - Tinting

Initially the dilatometer was used for producing the artificial tinting layers and as the measuring area and the sample placement into the potentiostat was one main problem, the oven was chosen as an option with cylindrical samples with a measuring area for the potentiostatic corrosion tests.

The artificial tinting was produced at IMAT TU Graz laboratory by using an oven Nabertherm p330 which is one of the high-performance laboratory furnaces

which are available with temperature limits of 1400°C to 1600°C.the main advantage in these kind of furnaces is that a temperature of 1400°C can be easily reached in 40 minutes based upon the conditions of operation, see Figure 23.

Figure 23 Nabertherm p330 furnace[89]

Figure 24 shows the display of the furnace control: Keyboard block, Program LED, Display and Over temperature limit controller (optional).

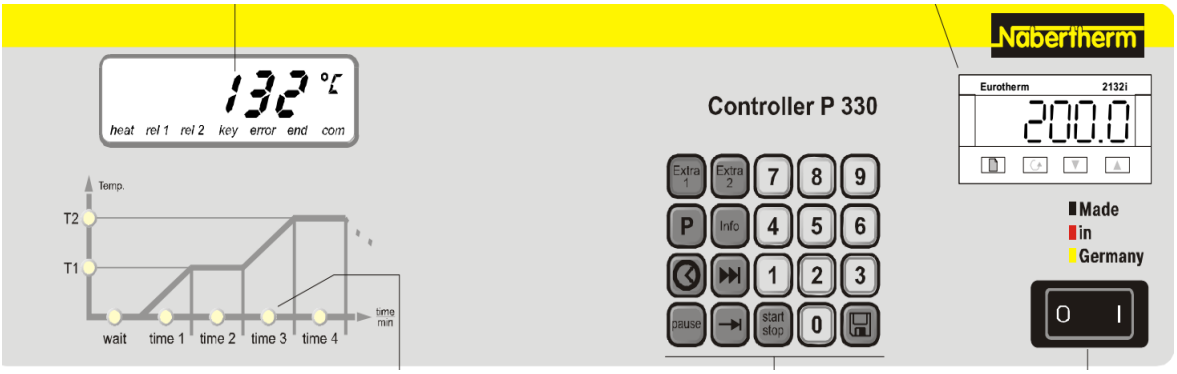

Figure 24 Nabertherm control panel[89]

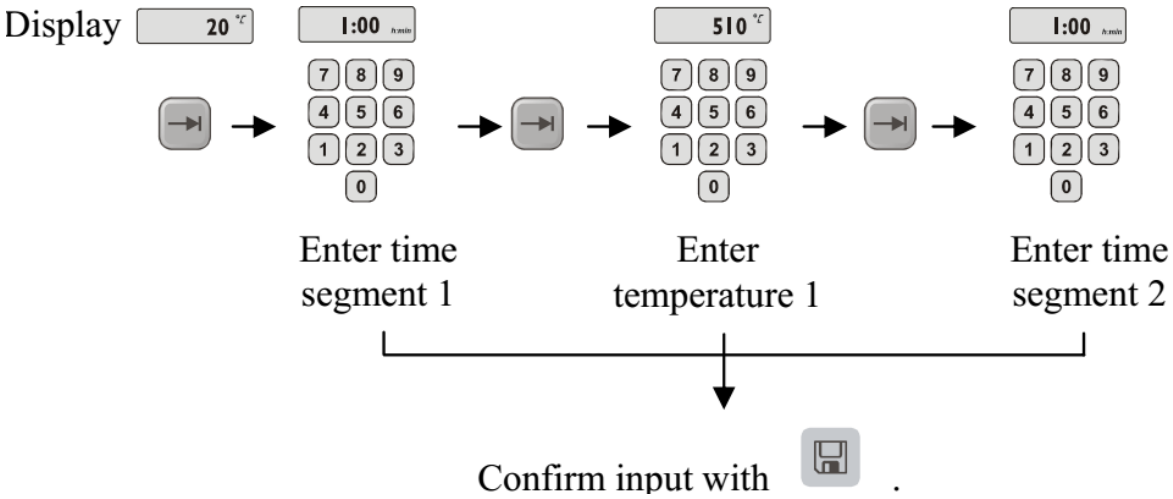

Figure 25 keyboard of Nabertherm p330 furnace[89] *and parameter input*

The procedure is as follows: Start the program and repeat the mentioned steps in Figure 25 in order to enter a different temperature and time. The time temperature curve is shown in the Figure 26 for the two different temperatures namely 600°C and 1000°C applied with a constant heating rate of 10°C / minute was chosen for both temperatures where the samples were held in the furnace for 10 minutes. All the samples (for example 2B and 2R 600°C) were done individually in batches (5 specimens each) to get a more constant oxide layers. Therefore, the procedure was as follows:

- 60 minutes for gradual heating to attain the required temperature.
- 60 minutes of holding time to maintain the required temperature in the oven in which last 10 minutes was used to produce artificial tinting for the samples and
- 60 minutes for the gradual cooling.

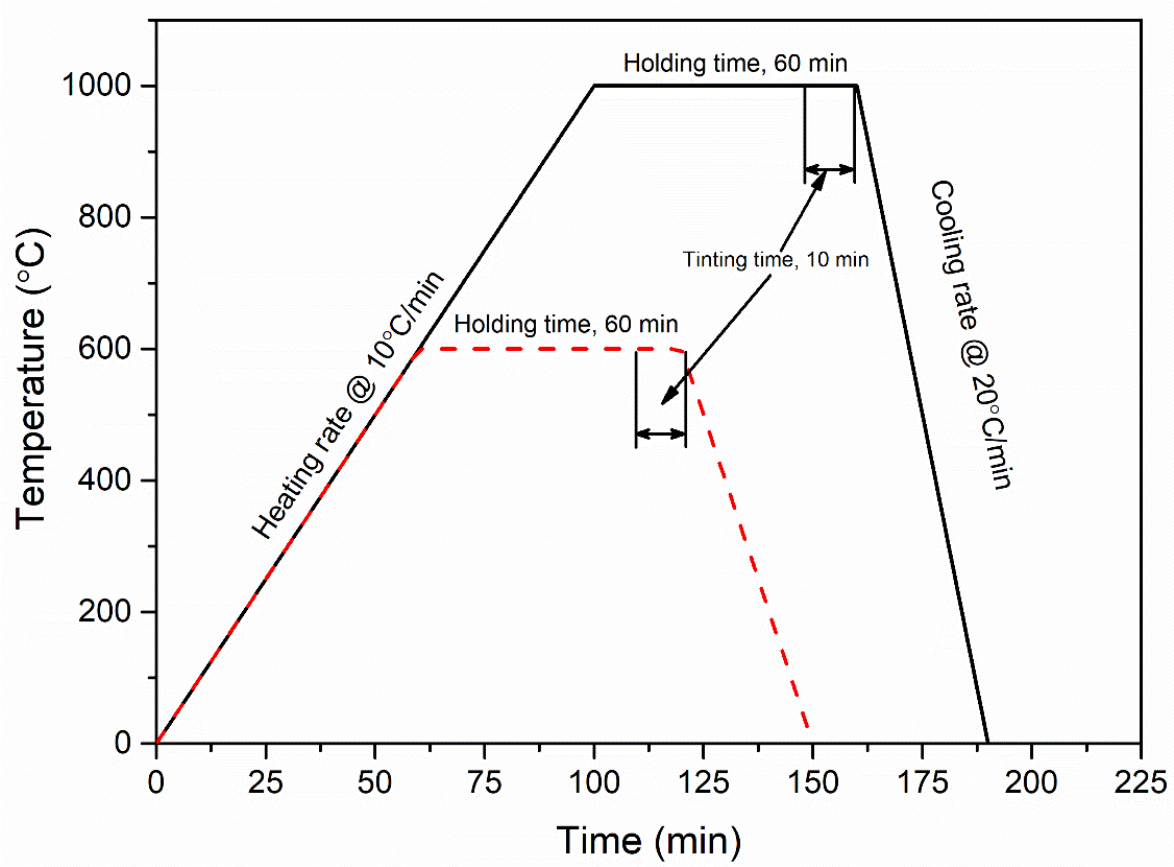

Figure 26 time-temperature curve for tinting the samples

During this process, the oxide layer which is a mixture of nickel, iron and other oxides was formed which looks similar to the layers that is formed alongside of the heat-affected-zone (HAZ) during welding. The chromium which is playing a key role in the stainless steel for its better corrosion resistance tends to diffuse outward from the base material and leave a thin chromium reduced layer which consists of a very low percentage of chromium is formed beneath the heat tint scale[90]. So for regaining the corrosion resistance the chromium oxide layer must be removed by using several methods mentioned above. The samples after the tinting process can be seen in Figure 27.

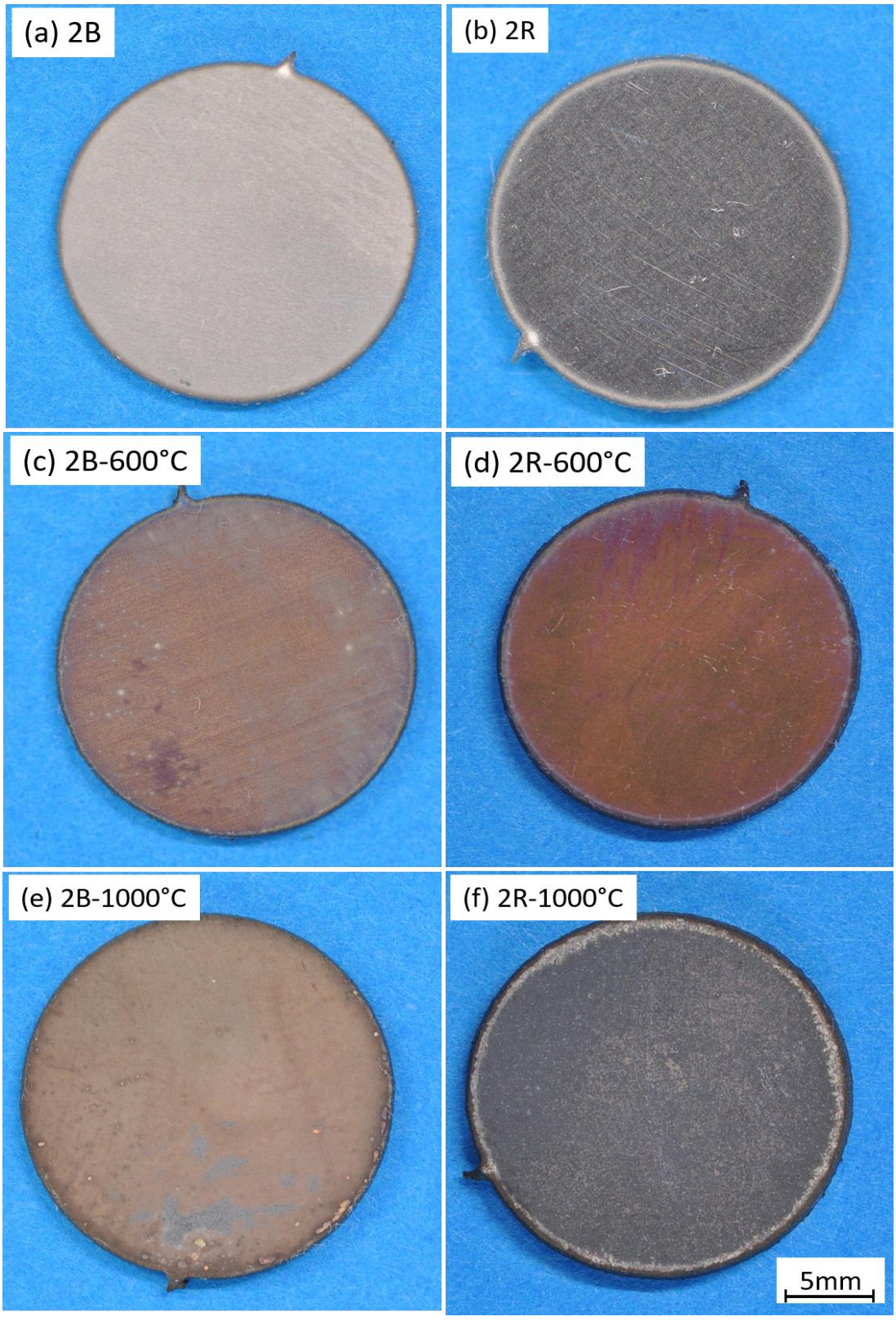

Figure 27 blank and tinted samples at 600 and 1000°C / 10min

4.2.1 Factors Affecting Tinting Colors

The following factors are considered as the important ones for the formation of different tinting colors

Oxygen level: When the surface seems to be rough then it oxidizes faster so therefore darker colors can be formed on the samples. So in this case the 2B has a thicker oxide layer when compared with 2R as the surface roughness of 2B is higher than 2R.

Steel chromium content: The delay of the formation of the colors is directly proportional on the material resistance to the oxidation.

Surface condition: As mentioned above same like oxygen level, surface condition shows the same results likewise if the surface is rough it oxidizes faster, causing darker colors.

Surface contaminants: the parameters such as coatings, lubricants, rust and finger prints can affect the heat tint, but they do not change the extension of HAZ[91].

4.2.2 Effects during this process

Heating that is caused by the welding or cutting procedure and consequent quick cooling outcome in both chemical and metallurgical changes. Oxidation is one of the most observable and quick change, and it is likewise in charge of the bright hued bands. A light surface nitriding additionally can happen, bringing about an expanded hardness and diminished weldability of the metal [92].

Another regular impact is corrosion, derived from stainless steel's delicate nature. Extreme heat causes the precipitation of chromium carbides around the grain boundaries. In these regions, chromium content drops less than 10.5 percent, and steel loses its capacity to frame a passive film and gives up its capacity to be stainless. The outcome is the alleged inter granular consumption. In outrageous cases, metal will turn dark[70].

High temperature likewise can initiate hydrogen embrittlement. Gas diffuses through the metal and makes a high pressure inside the cross section, diminishing its elasticity and toughness. On the off chance that the hydrogen gas is not evacuated, it can cause unconstrained breaking even few hours in the wake of heating. From a metallurgical perspective, heat creates confined solidifying. In a few conditions, austenitic stainless steel can transform into martensitic, expanding its hardness and in addition its fragility. In different cases, heated metal can wind up noticeably weaker[93].

4.3 Pickling

Even though there are many possible ways available for removing the chromium oxide layer on stainless steels which is formed during the heat tinting such as grinding, heat treatment and abrasive blasting they are not much preferable as they gradually found to be detrimental to the resistance for the pitting corrosion. In many cases pickling is considered as one of the most efficient and most widely used in most of the cases as its consists of an aqueous solution of nitric and hydrofluoric acid (HNO_3+HF). By using this pickling agent it can be

observed that the surface condition of the material can be improved by reformation of the chromium oxide layer and removal ot the chromium depleted region. Due to the presence of nitric acid chromium content can be increased in the material which leads to the improvement of overall surface quality to certain extent by reducing the defects. In the process the nitric acid is accompanied with the formation of hexavalent chromium (Cr^{6+}) which increase the corrosion resistance of stainless steel and with the presence of chlorides and fluorides chromium always tends to increase the corrosion resistance and there is always a chance of sigma phase formation [94].

1) Role of HNO_3
    - H^+ ions generator
    - Powerful Oxidizing agent
    - Helps for giving the brightness for the pickled product.
2) Role of HF
    - Complexing Agent for FE^{3+}, Cr^{3+}, Ni^{2+}
    - H^+ supplier.

During this process two conditions must be kept in mind

1) This process must be carried out under an expert's guidance as both the acids used for the pickling are dangerous and mishandling of the solution can cause a rapid attack on the human skin.
2) Care must be taken as the surface condition plays an important role in the formation of localized corrosion.

The concentration of the pickling solution was taken according to the ASTM Standard A380/A380M [88] .65 % of Nitric acid with addition of 40% Hydrogen fluoride with a mixture of water makes a pickling solution.as mentioned below and the samples were immersed for 10 minutes in the pickling solution.

The procedure was conducted as per the standards with the following steps

1. Wear the personal protective equipment like glasses, gloves, apron before starting the test as the pickling solution consists of harmful acids.
2. Stir the solution thoroughly such that the elements are completely mixed.
3. Place the samples inside the solution with the help of the crucible tongs.
4. Wait for 10minutes.
5. Remove the samples using the crucible tongs.

6. Rinse them with ethanol.
7. Clean the samples with distilled water.
8. Use soft material to clean the water.
9. Repeat the steps 1-8 for all the samples.

As shown in the Figure 28 it can be seen that the samples regained the same surface condition as the blank material and can be noticed by visualization with the human eye.

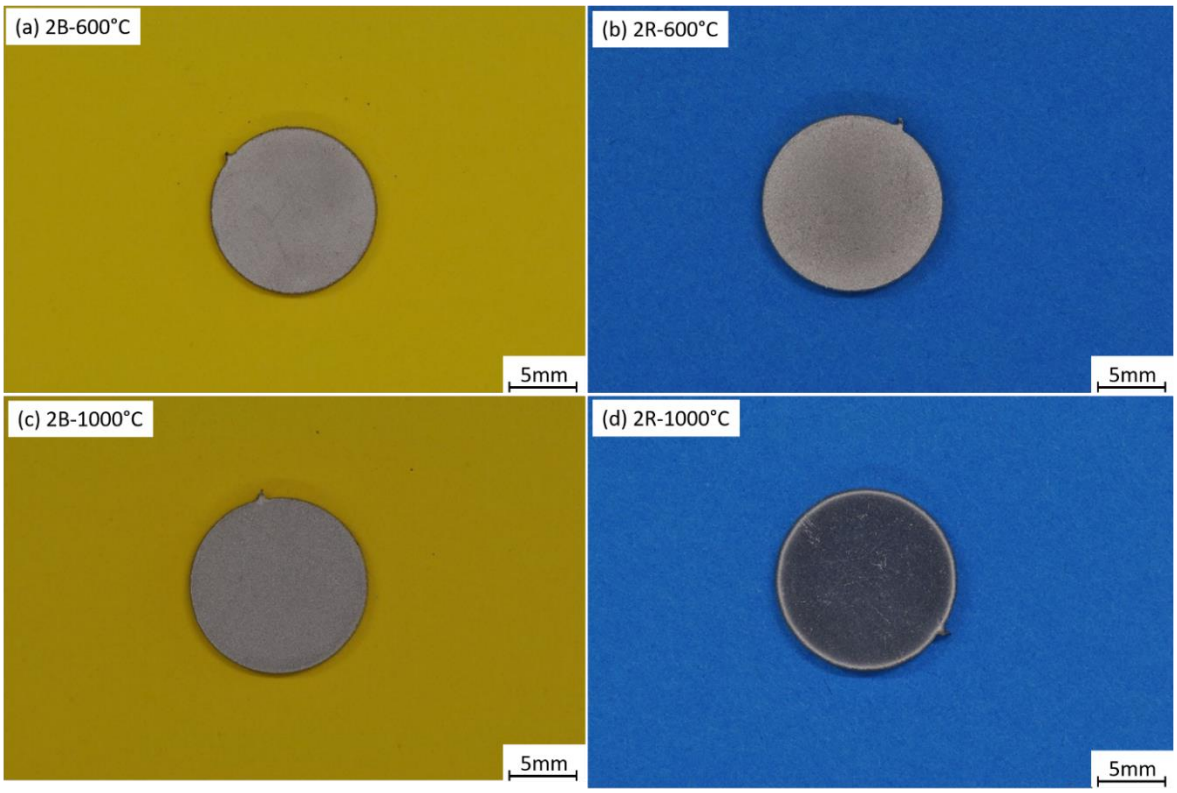

Figure 28 Samples after pickling

4.4 Potentiostatic tests

4.4.1 Electrolyte Preparation and pH control

5% Standard Sodium chloride solutions were prepared using analytical grade NaCl salt. The prepared concentrations (5% NaCl in 1 liter of water) and pH values ranged from 6 to 9, respectively. The pH and temperature of the electrolyte was measured before and after the tests using a digital pH meter (ORION, model: 420 A). The solution was replaced after each sample just before the test in order to have the same boundary conditions.

The preparation of the solution can be made in the following steps

1. Measure the weight of the NaCl powder of 50g.
2. 1 liter of water in to the container and stir well until all the NaCl was completely dissolved into the water.
3. Measure the pH and Temperature and note down the values.

4. Pour the solution into the 1-liter corrosion cell slowly by avoiding the water bubbles.

4.4.2 Potentiostat

The potentiostat is defined as the electronic instrument that measures and controls the voltage difference between a working electrode and a reference electrode which in other words says the current flow can be measured between the working electrode and reference electrode.

The potentiostatic tests were conducted at TU Graz IMAT corrosion lab by using the PGSTAT128N, a low noise, low current and fast potentiostat which has a capability of measuring maximum 800mA and compliance voltage of 12V. The software that is used for connecting the data from the laptop to the potentiostat is nova 1.9 version, see Figure 29.

Figure 29 Potentiosat – Galvanostat PGSTAT 128N [95]

The mechanism of the potentiostat can be explained by potential (E) or voltage (V), where potential is the driving force for the redox equation and it can be always measured against a reference electrode. The positive voltage is said to be oxidation and negative voltage is reduction. Generally, the reduction and oxidation reactions happen at 0 Volts.

In the same way, the current (A) which can be expressed as current density is the electrode flow gives result to form a redox reaction which measures the rate of reaction (electron/ second), If the current is zero then the redox reactions may occur and it is not possible for corrosion to happen.

.

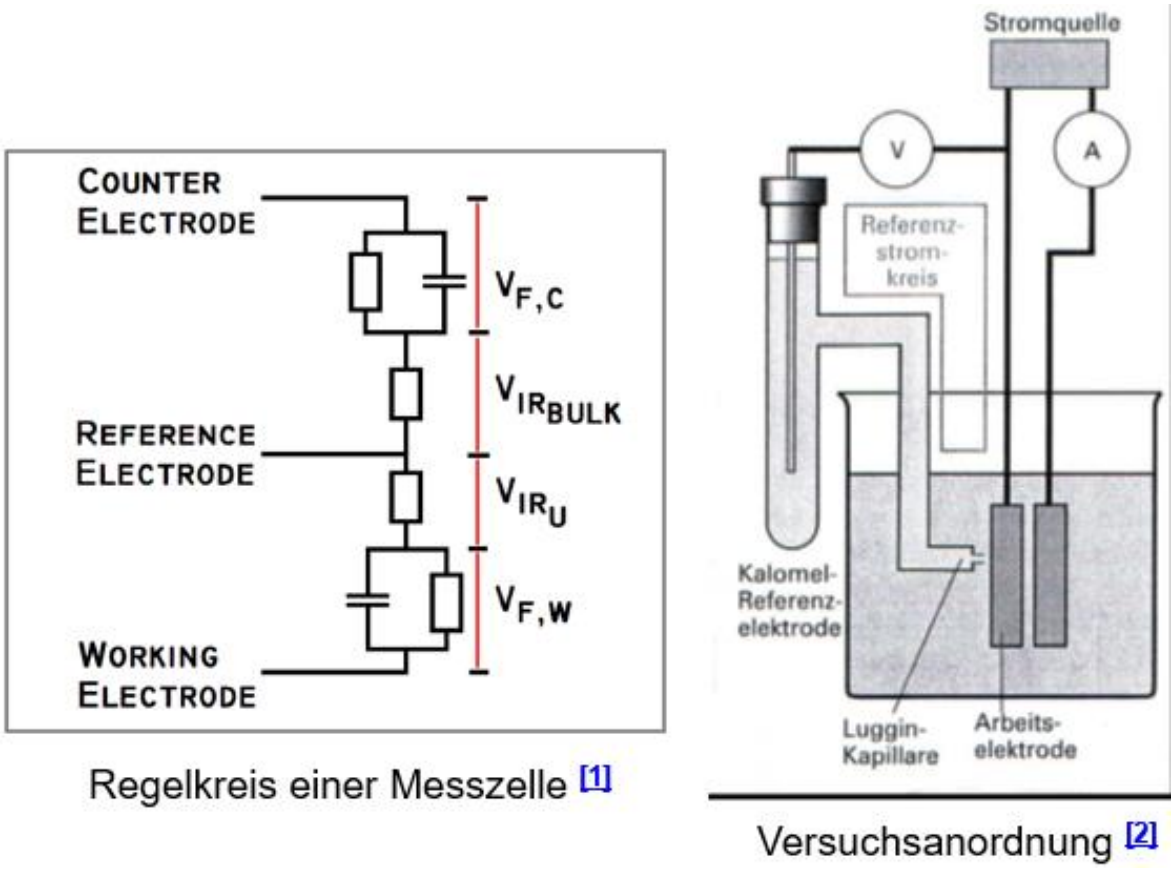

Figure 30 Control circuit and experimental arrangement for potentiostatic measurements[95]

4.4.3 Corrosion Cell

The corrosion cell used for the experiments is called three electrodes cell which has a capacity of 1litre electrolyte and was designed according to the ASTM standards (G5, G59, G61)[96],[97],[98]. There is an inlet and outlet available for the water or other cold or hot liquids as shown in Figure 31.

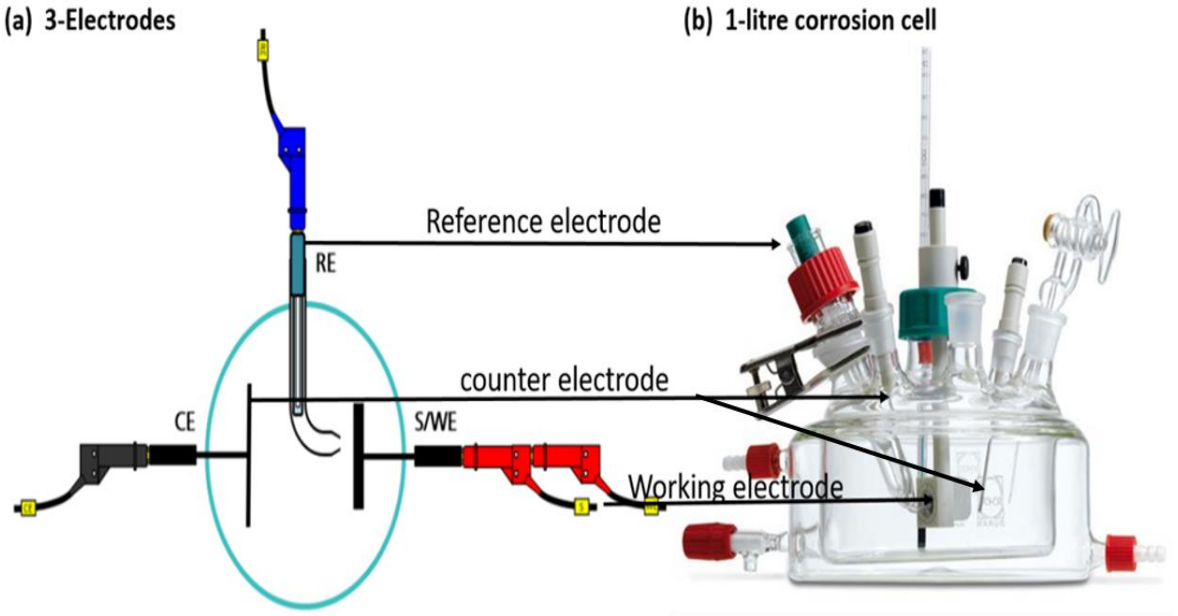

Figure 31 3 Electrode and 1-liter corrosion cell [99]

It consists of three electrodes that are immersed in the solution as follows:

- The reference electrode is made of Ag/AgCl which is filled with 3 M KCl solution. Before starting the experiment make sure that the electrode contains enough solution during the measurement. The electrode is connected to the blue banana plug of the cell cable. The electrode should be placed inside the capillary. The Luggin capillary is fitted with a spherical ball joint which allows positioning of the capillary tip with respect to the sample holder. Please make sure that when mounting the sample holder, the position of the Luggin capillary is such that the tip of the capillary is located directly in front of the sample holder. The purpose of the reference electrode is to provide a stable and reproducible voltage to the working electrode. The standard reference electrode potential is 210 mV ± 5 mV with respect to the Standard Hydrogen Electrode (SHE) as shown in Figure 32.

Figure 32 Ag/AgCl reference electrode, Metrohm socket B[100]

- The counter electrode which is made of stainless steel 316 of 2mm diameter can be inserted in the supplied electrode holders mainly used to measure the corrosion current in the electrolyte, as shown in Figure 31. The role of the counter electrode is to supply the current that is required for the working electrode without limiting the measured response of the cell[101].

- The working electrode is the tested sample itself which can be used with the help of a sample holder to mount the small flat metal sample on which corrosion analysis needs to be performed. The sample can be mounted and unmounted by removing and locking ring by hand. A plastic seal is used to limit the exposed surface of the sample to 1cm^{2}The sample holder can be placed in the corrosion cell in such a way that the distance between the sample and the luggin capillary is minimized. Connection is made by connecting the working electrode cable of the auto lab to sample holder. For the tests AISI 304 stainless steel, samples were cut from sheets that had a diameter of 12.5 mm with thickness of 1.5 mm for 2B and 2mm for 2R. The exposed surface area was 1cm^2. The test procedure for all the samples is a potential scan from -0.2V vs the open circuit potential to +0.1

V vs the open circuit potential with a sweep rate of 1mV/s in a 5%NaCl electrolyte solution at room temperature.

4.4.4 Electrochemical Measurements

4.4.4.1 Open Circuit Potential Measurements OCP

The OCP is determined as the free corrosion potential (E_{corr}) is a good indication of the metal tendency to corrode in a certain solution. The sample's potential was measured against the Standard Hydrogen Electrode (SHE) for duration of 300 seconds. Having a relatively fixed (not drifting) potential is an indication that the sample has stabilized in the solution. The following parameters are found under a certain test duration time of 60 seconds for stabilization of the OCP.

- The sample period: this parameter determines the measuring rate per second. The applied sample period was 1 second.
- The potential stability: When measuring the open circuit potential (OCP), if the drifting rate falls below the stability this will result in terminating the experiment polarization rate in mV. The stability was set to be zero mV.
- The sample surface area immersed in the solution of 5% NaCl was $1cm^2$.
- Conditioning: that is applying constant potential to the metal for a certain period to hold the metal surface in a certain state; i.e. producing or removing an oxide film. The conditioning potential is always expressed versus the reference electrode potential.
- IR Compensation: A high cell resistance will result in a voltage (IR) drop; fortunately, the Metrohm PGSTAT 128N is capable of compensating for this drop by turning on IR compensation. This option was not used in all experiments, as the 5% NaCl solutions used are highly conductive.

4.4.4.2 Linear Polarization Resistance and Tafel slopes

The three-electrode setup was used to perform linear polarization tests where CE means counter electrode (AISI 316L), WE mean working electrode (sample) and RE means reference electrode (SHE). The role of the potentiostat is to provide the desired polarization of the sample (WE) by controlling the electric current flow through CE. This way the driving force available for cathodic/anodic reaction on the sample surface can be indirectly controlled. As soon as the sample is immersed in the solution, the potential between WE and RE starts to settle. This potential is called as Open circuit potential (OCP). The linear polarization resistance is the slope of E-I relationship at the OCP (i.e. at zero current) and it provides a method of estimating the instantaneous corrosion rate.

The corrosion test is based on linear polarization of the WE. The difference between the reference electrode and working electrode is always controlled by

the potentiostat. The polarization ŋ is defined as the over potential E minus the E_0 (OCP): ŋ= E-E_0

The polarization limits are usually several hundred mV around the OCP. In this work, the measurements were performed in the potential range from -150 mV to 200 mV with respect to OCP with a constant scan rate of 1 $mV.s^{-1}$. The electric current density (i) for the desired polarization is recorded with potential (E) and the results are plotted as log (i) vs. E. From the experimental data corrosion potential (E_{corr}), corrosion current density (i_{corr}) and polarization resistance (R_p) could be acquired.

For every sample, the linear polarization test was applied around 105min to 135min for different samples with different conditions.

The test parameters are:

- Initial E: is the starting point for potential sweep; initial E was -0.02 V vs. OCP
- Final E: is the ending point for potential sweep; final E was +0.02 V vs. OCP
- Scan Rate: it was 0.1667 mV/s
- The OCP Determination is taken as 300 seconds.
- β_a and β_c are the anodic and cathodic Tafel slopes in [µA/mV]. As shown in Figure 33. The default values for these parameters were accepted; however, the corrosion current density i_{corr} was calculated directly form the OCP.

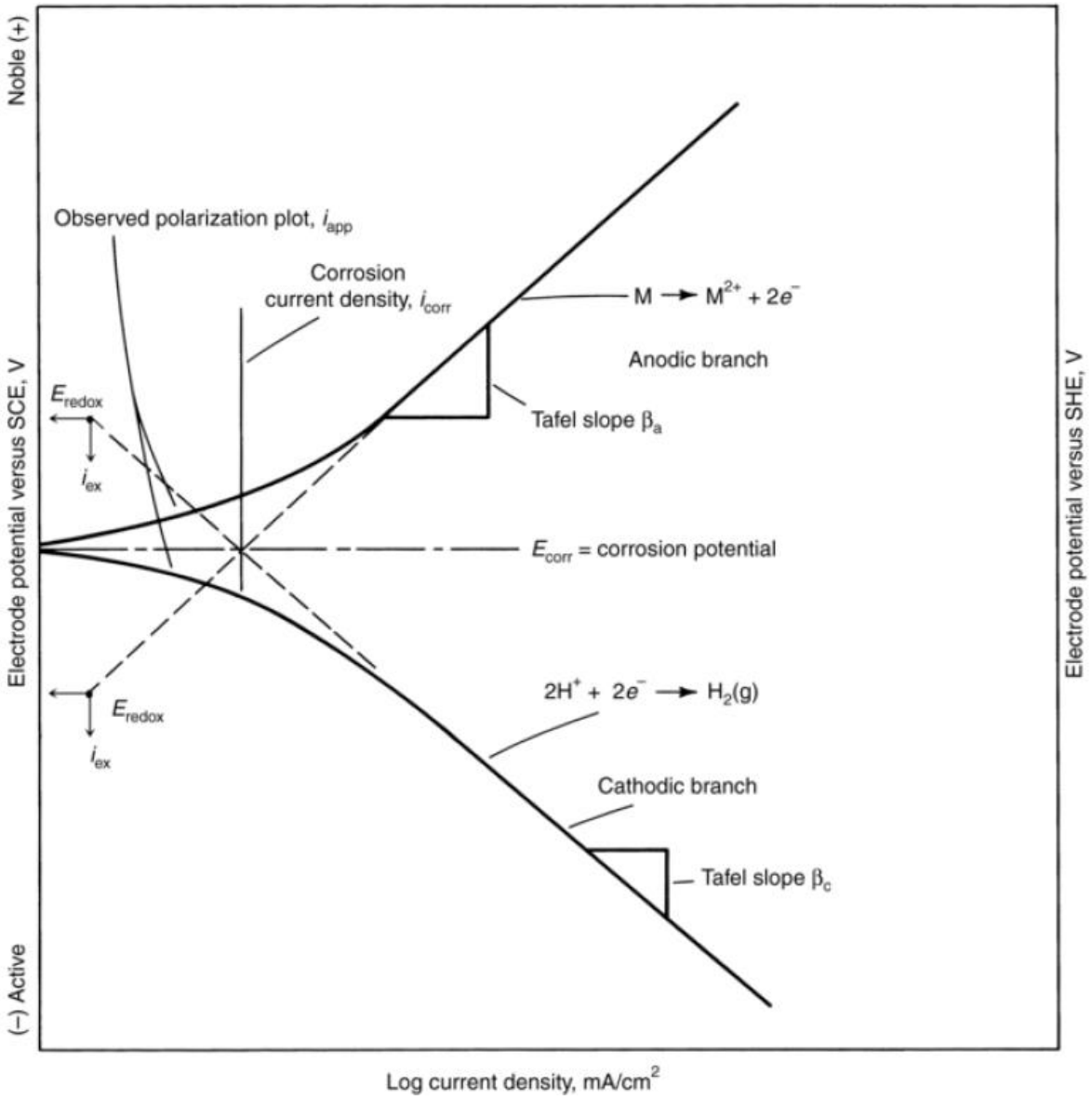

Figure 33 Tafel slopes for a single charge-transfer-controlled cathodic reaction and charge-controlled anodic reaction. βc and βa are Tafel slopes (Ref. C. Wagner, W. Traud, Z. Electrochem., Vol 44, 1938, p 391)

The linear polarization test was used for calculating the corrosion current but the Tafel slope was around zero on the anodic side. This means that the anodic reaction was influenced by the diffusion controlled oxygen corrosion reaction ($O_2+2H_2O+4e^-$ -> $4OH^-$), beside the visible H_2-gas formation during the experiment, see Figure 34 and Figure 35.This means that the evaluation of the corrosion rate using the Tafel slopes could not be applied. Therefore, the curves were converted into linear type for the evaluations.

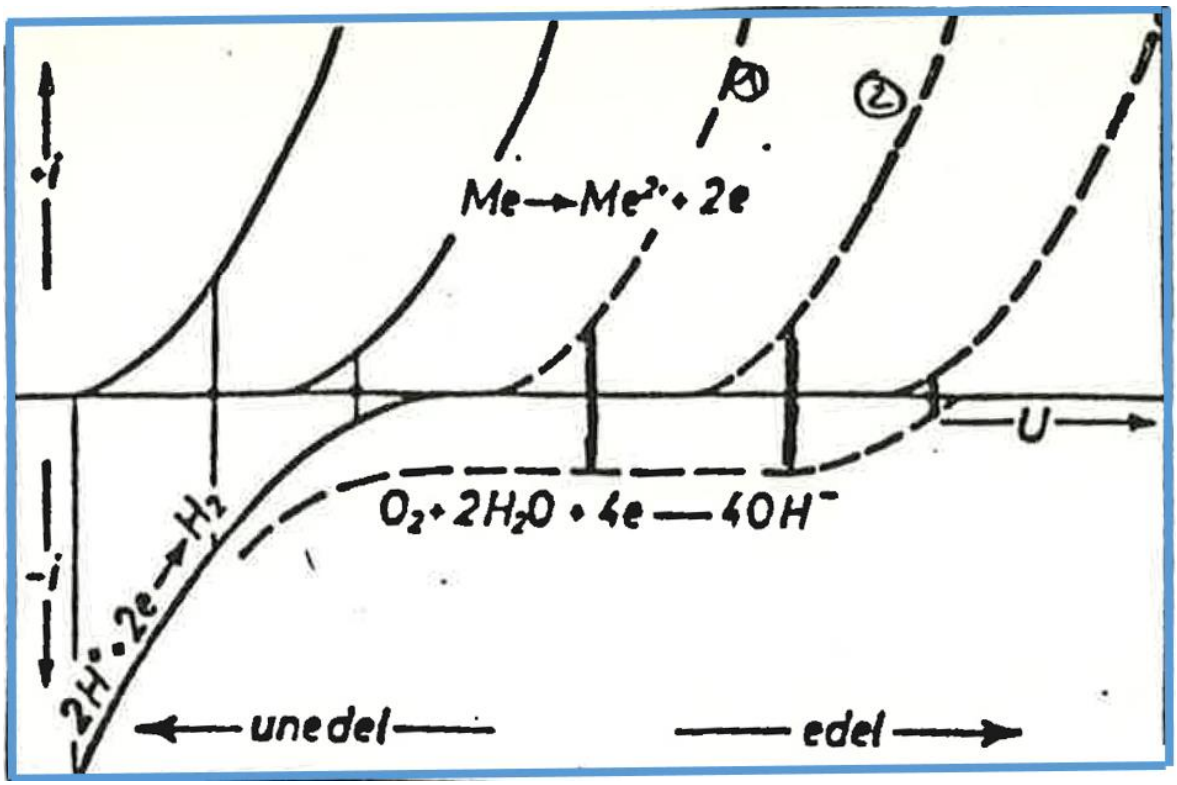

Figure 34 Anodic current characteristics for hydrogen gas formation and oxygen consumption (Ref. H. Zitter, Korrosionskunde, MU Leoben 1987)

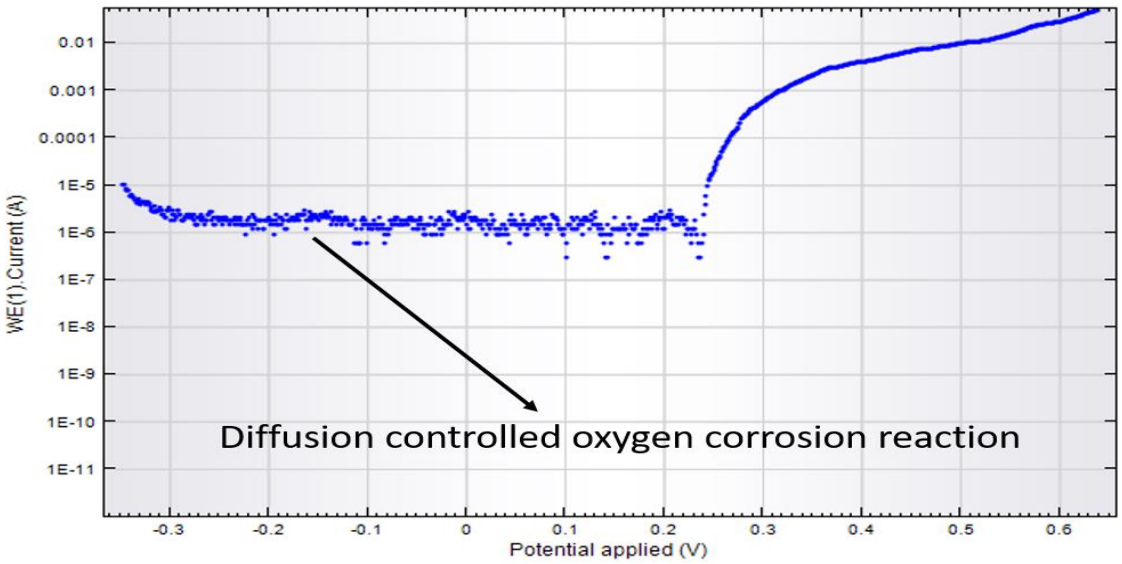

Figure 35 Measured current (log scale) vs. potential curve.

4.4.4.3 Finding the Procedure and parameters for the potentiostatic tests

1) The preconditioning of the working electrode involves the following consecutive steps

- Setting the PGSTAT 128N to potentiostatic mode and selecting the initial current range
- Setting the potential to the preconditioning value, 0 V
- Switching the cell „On “and waiting for 5 seconds and it can be defined by seeing Ru exponential which should be in Ω always. If it comes in

kΩ/mΩ then it's always better to change the electrolyte solution and start the experiment from beginning.

- Finding the most suitable current range (by trial and error basis as shown in chapter4 point number 4)
- Set the current range in i-interrupt to the required range according to the procedure.

For this procedure, the nova 1.9 software control command was set in the 100 mA current range.

2) Then depending on the resistance fluctuation we calculate the IR compensation for the linear polarization IR corrective procedure by using positive feedback increment option by setting the current range same as in i-interrupt.

For example, as shown in Figure 36,there is a change in in the wave from 91st to 92nd repetition so

Then we calculate 9.1*0.8=7.28

So the IR compensation will be 7.28Ω.

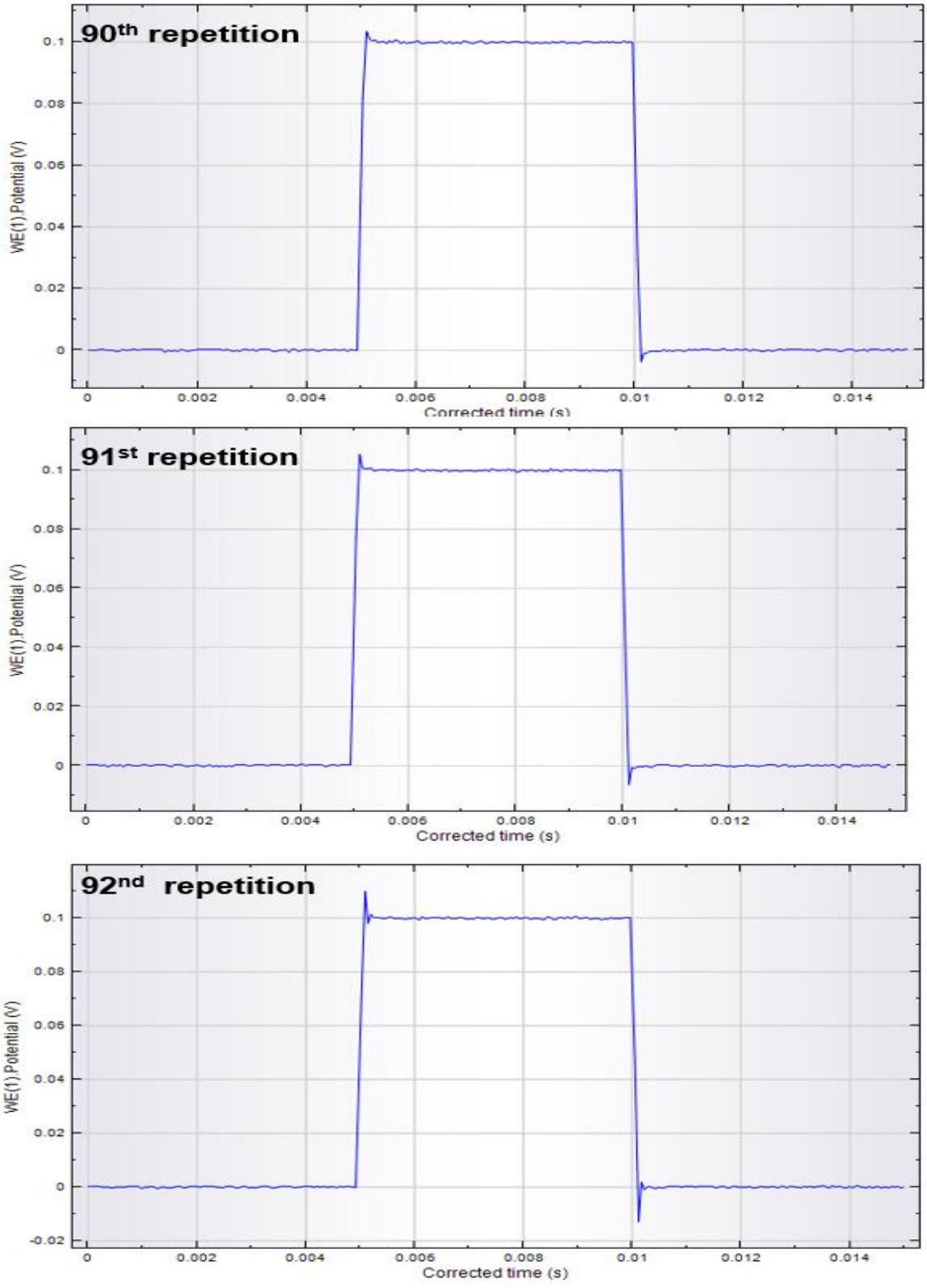

Figure 36 Finding the parameter in n-number of repetitions for calculation of iR compensation for Linear polarization method.

Set the same parameters in linear polarization IR corrective, run the procedure and see the curves in the test.

4) Choose I vs E option in the standard procedure and set the same parameters and see the start and stop potential values depending on the linear polarization results (if the test stopped before the desired current range).

5) Repeat the same procedure for all the specimens.

After conducting a lot of sample tests, the parameters were taken as stated below

I-interrupt

- Current Range:100 mA
- Band width: High stability
- iR compensation: off

Positive Feedback increment

- Current Range: 100 mA
- Number of repetitions: 200
- Increment parameter: 0.1

Linear Polarization IR Korrektur (correction)

- Current Range:100 mA
- iR compensation taken from Positive Feedback increment in Ω as shown above
- OCP determination
    - Maximum time: 300 s
    - Set Potential: -0.250 mV
- LSV staircase
    - Start Potential: -0.250 mV, Stop potential:1.700 mV
    - Step Potential:0.00107 mV, Scan rate: 0.0001667 mV/s

.4.4.4 Measurements

All the data are transferred from nova 1.9 to the excel® and origin® in order to generate calculations such as OCP, BTP and BTP- OCP. They were plotted to evaluate and compare the test results for all the samples.

4.5 Metallography

To quantify the corrosion attack, additionally light optical microscopy (LOM) using a Zeiss Axio Observer Z2m® is performed on cross sections of the specimens. Therefor one of five specimens per investigated condition is

analyzed, i.e. cutted, embedded with Struers MultiFast® black resin, grinded with SiC and polished with diamond paste down to a surface roughness of 1 µm. For that, the depth and the diameter of the appeared pits can be seen in Figure 37were measured and the mean value calculated.

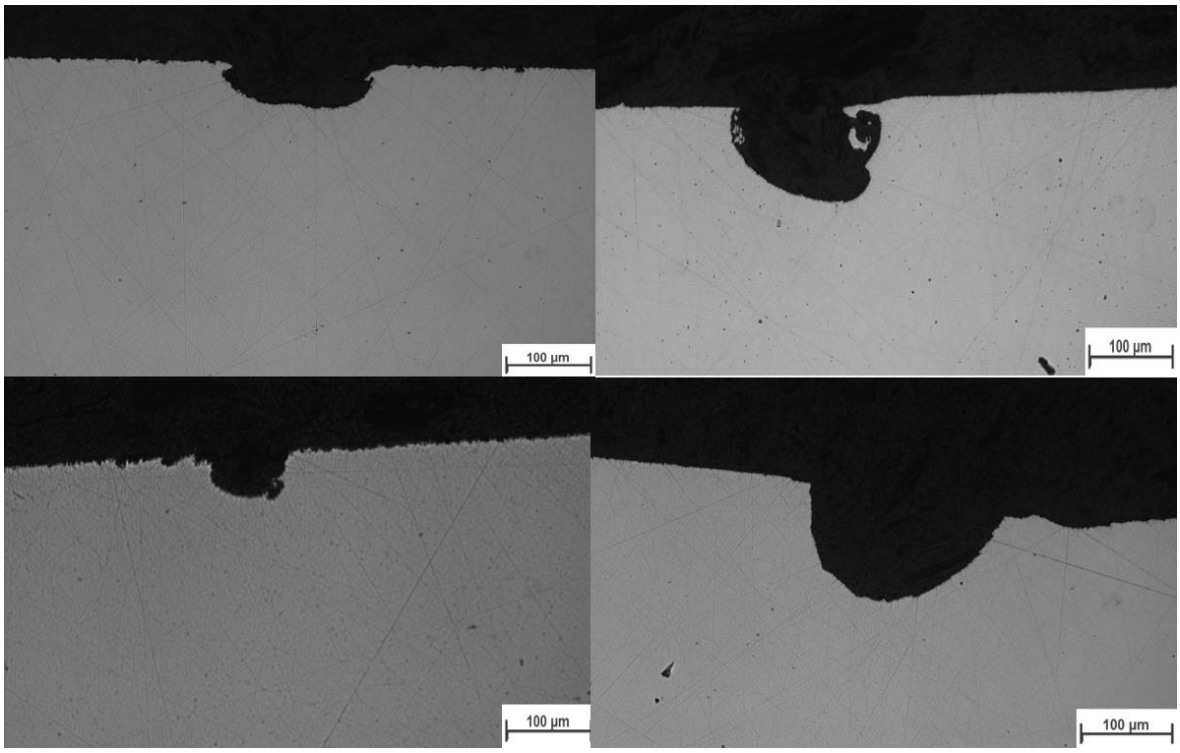

Figure 37 Metallography evaluation of the pits.

4.6 Energy-dispersive X-ray analysis / EDS

Energy Dispersive X-ray spectroscopy (EDS, EDX, EDXS or XEDS), once in a while called energy dispersive X-ray analysis(EDXA) or energy dispersive X-ray microanalysis (EDXMA), is a scientific system utilized for the essential examination for instance. It depends on an association of some source of X-ray excitation and a sample e. Its portrayal abilities are expected in huge part to the basic rule that every element has an extraordinary nuclear structure permitting an interesting arrangement of peaks on its electromagnetic emission spectrum (which is the primary guideline of spectroscopy)[102].

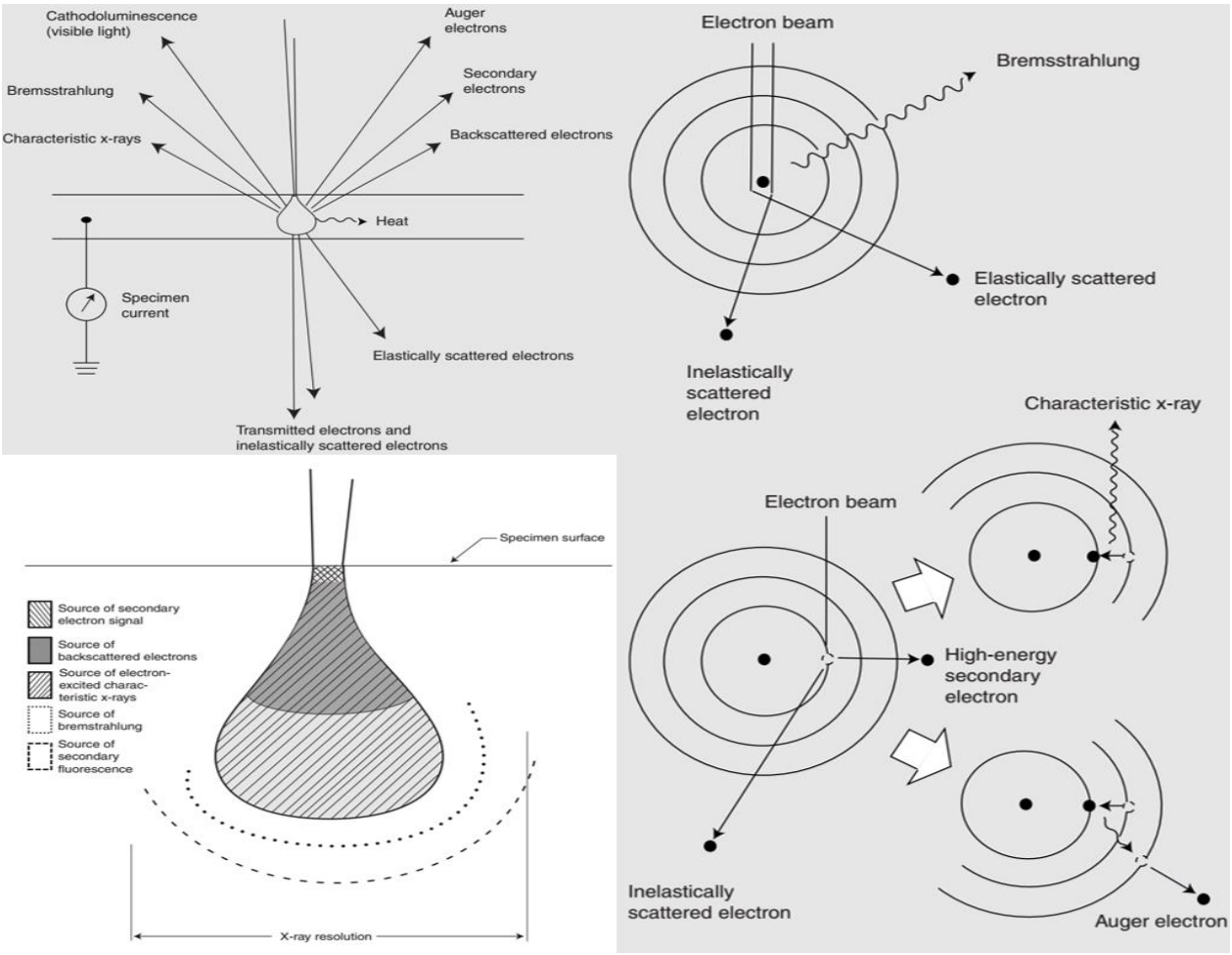

Figure 38 top left showing principle results of an electron beam interaction within a specimen, right top and bottom showing different signals that can be detected in an electron column, bottom left shows volumes of electron specimen interactions [103]

To empower the emission of X-beams from a sample, a high-energy light emission particle, for example, electrons or protons (see PIXIE), or a light emission x-rays, is engaged into the specimen being contemplated. At rest, an atom inside the sample contains ground state (or unexcited) electrons in discrete energy levels or electron shells bound to the nucleus. The incident beam may energize an electron in an internal shell, shooting it from the shell while making an electron gap where the electron was. An electron from an external, higher-energy shell at that point fills the hole, and the change in energy between the higher-energy shell and the lower energy shell might be discharged as a X-ray. The number and energy of the X-rays emitted from a sample can be measured by a energy-dispersive spectrometer[104]. As the energies of the X-beams are normal for the difference in energy between the two shells and of the nuclear structure of the emitting element, EDS permits the essential composition of the sample to be measured.[105]

4.7 Raman spectroscopy

4.7.1 Raman effect

Raman effect is a nondestructive spectroscopic technique which is used to find the molecular properties (such as vibration, rotational and other low

frequency modes) on a metal surface layer by using a scattered light resulting from photon-molecule collisions.

The mechanism of the measurement is as follows: At the point when monochromatic radiation is occurrence upon sample then this light will communicate with the sample in some form (absorbed or scattered in some way, might be reflected). It is the scattering of the radiation that happens which gives the information about molecular structure. The vast majority of the radiation typically uses a coherent source for example laser in many cases, the radiation in this cases are elastically scattered which is also called as Rayleigh scatter.

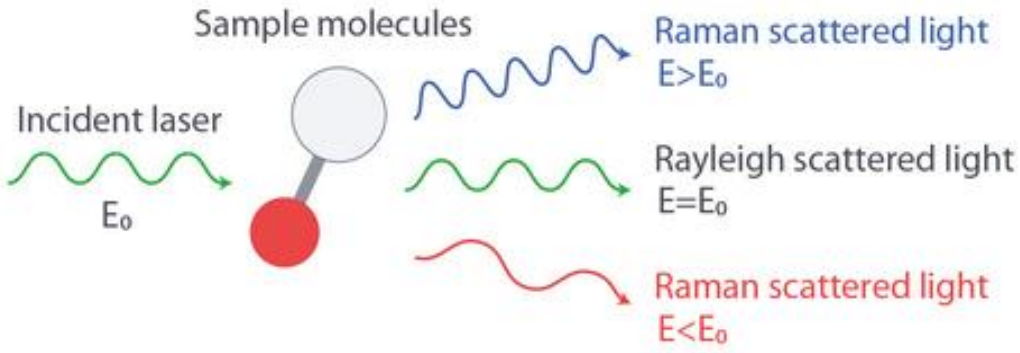

Figure 39 Scattering of light by molecules [106].

4.7.2 Analyzing the oxide layers on tinted samples

The properties of iron-oxide layers formed at different temperatures 600°C and 1000°C during the artificially tinting process were studied using the Raman effect. Using the surface spectroscopy, the structures and composites of the heat tinted oxides were explored. The outcomes show blue and red oxides to have a double layered structure with chromium-depleted layer and iron-rich external layer and an internal layer with less iron and more chromium. In the base material a chromium depleted layer was found under the heat tinted oxide on an induction heated sample.

5. Results

5.1 Tinting

Artificial oxide layers were produced, which represent the tinting colors after welding in the heat affected zone (HAZ). The appeared tinting colors are brown with blue shimmer at 600°C and blue-grey with brown shimmer at 1000°C. According to literature the thickness of these layers should be 75 to 100 nm for the former and 125 to 175 nm for the latter.

5.2 Corrosion Tests using the Linear Polarization method

5.2.1 Temperature and pH during testing

During the linear polarization tests at 25°C the pH value increased from 6.57±0.35 to 9.60±0.35 for 2B and from 6.31±0.99 to 9.87±0.23 for 2R specimens due to the oxygen consumption and the hydrogen gas bubble formation at the counter electrode. Therefor a similar increase in pH value occurred for both surface conditions 2B and 2R. The test duration time varied between 2h 15min to 2h 45 min. (See Appendix A Table 4 and Table 5).

5.2.2 Measured values

Linear polarization curves show similar behavior for 2B (skin passed) and 2R (bright annealed), tinted at 600°C and 1000°C. A significant shift of the curves to lower break through potentials (BTP) is observed for all tinted specimens, compared to the blank ones. This negative shift is higher for 2B specimens if compared to 2R, as seen in

Figure 40. The occurring kink in the 2R 1000°C curve, i.e. the intermediate current reduction, is probably due to the observed formation and the following sudden detachment of an adherent and insulating layer of gas bubbles. But there is a better shift of the curves to higher potentials can be observed after the pickling is done. From these it can be said that the samples exhibit a better corrosive resistance than the blank materials.

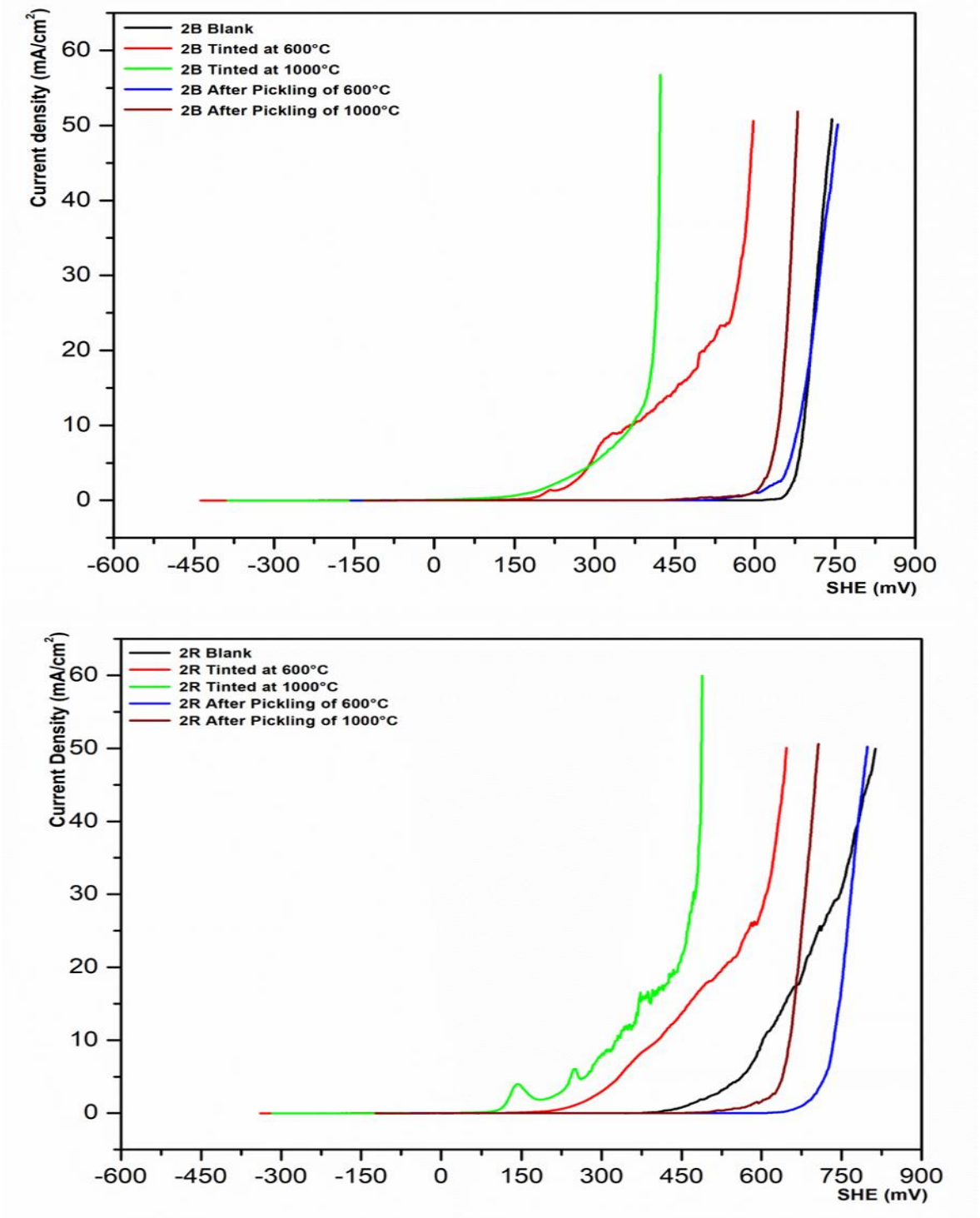

Figure 40 Curves of 2B and 2R from the Potentiostatic tests

As per the present comprehension of the pitting corrosion process from Figure 40 (also see appendix A Figure 52 and Figure 53) represent a critical threshold value, where meta stable pit nuclei inside the passive state of the stainless steel might be changed into stable developing/growing pits when the passive formation breaks down. For this situation, the steady pit is achieved when initiating conditions are established inside the pit, for example, high chloride concentration (salt film development) which is important to keep up the pits over a broadened time. The higher the chloride concentration, the lower the potential

at which pitting happens. The values of pitting corrosion at any given Cl− particle concentration rely on the chemical composition of the sample.

5.2.3 Pitting appearance on specimen surface after testing

After the linear polarization tests the samples exhibit clearly visible pitting and crevice corrosion (at the specimens edges) as shown in the stereomicroscopic images Figure 41 and it can be noticed that the blank of 2B has a higher number of pits but less deep in all the cases - namely blank, tinted at 600°C and 1000°C - when compared to the blank of 2R Figure 41 which have less number of pits but deeper.

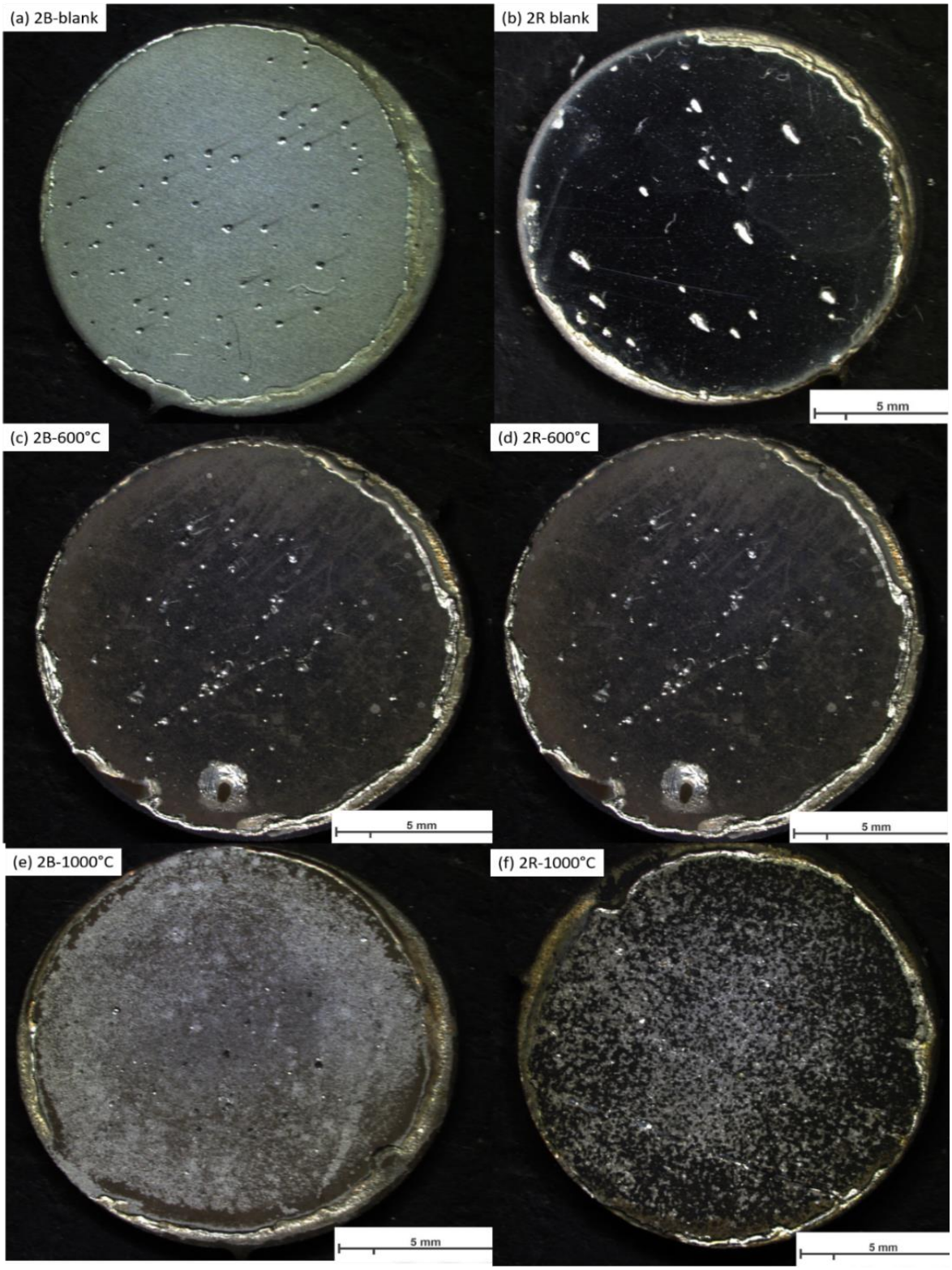

Figure 41 Pitting and crevice corrosion formed on the samples from the Potentiostatic tests

5.2.4 Open Circuit Potential (OCP)

The OCP was evaluated for all the samples individually and the results were compared based upon the surface type finish, see Figure 42.

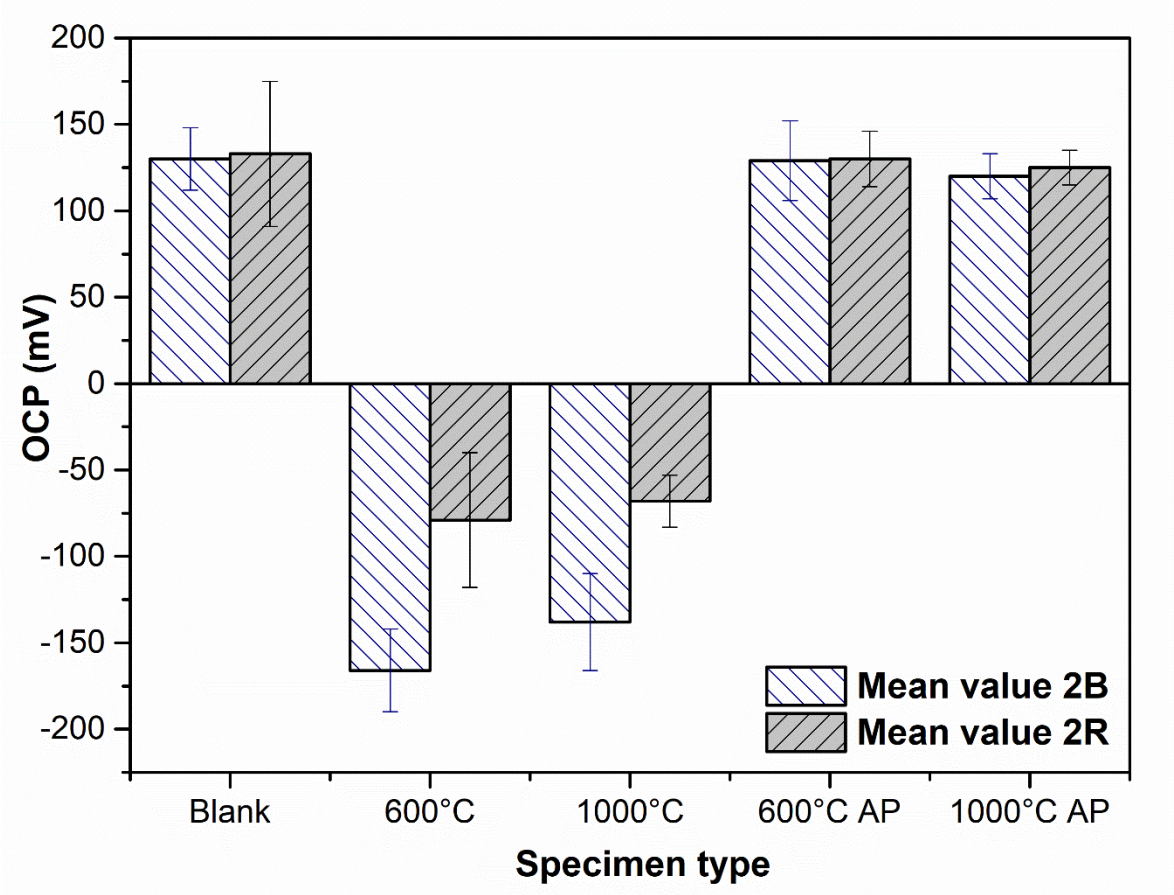

Figure 42 OCP of all the samples: Blank, tinted 10 min at 600 and 1000°C in air and after pickling (AP) / mean value and standard deviation of each 5 tested specimens

The Open Circuit Potential (OCP) is an important parameter that gives a clear image of the behavior of the specimen in the corrosion medium. The more positive the value of the OCP, the higher the corrosion resistance. For the tests that were performed the OCP was positive for the blank samples with 2B and for 2R, therefore, 2R shows a slightly higher corrosion resistance in this medium. Comparing the values for tinted samples at 600°C for 2B and for 2R, similar findings as for the blank specimens could be detected, whereas 2R shows a more positive potential and therefore higher corrosion resistance. For tinting at 1000°C the OCP values were found for 2B distinctively lower than for 2R. Comparing the values of the samples after the pickling the OCP values are found to be much better than the blank sheets and both 2B and 2R have nearly the same OCP. All the average OCP values with the standard deviation are shown in Figure 42. An overall higher deviation for the values of 2R are found in comparison with 2B, which could be caused by the difference in the surface finish (2R has smoother surface finish and has more scratches during transportation when compared to 2B) of the received specimens. Nevertheless, 2R shows a higher corrosion resistance according to the determination of the OCP values. From Figure 42 it can be seen that the tinting can be fully recovered by using the proper pickling method.

5.2.5 Break Through Potential BTP

Another indication for the corrosion behavior of the stainless steel sheet material is the Break Trough Potential (BTP), which is defined as the potential where the rise of current is high within a small in potential increase. The mean values and the standard deviation of each 5 tested samples for the BTP are shown in Figure 43.

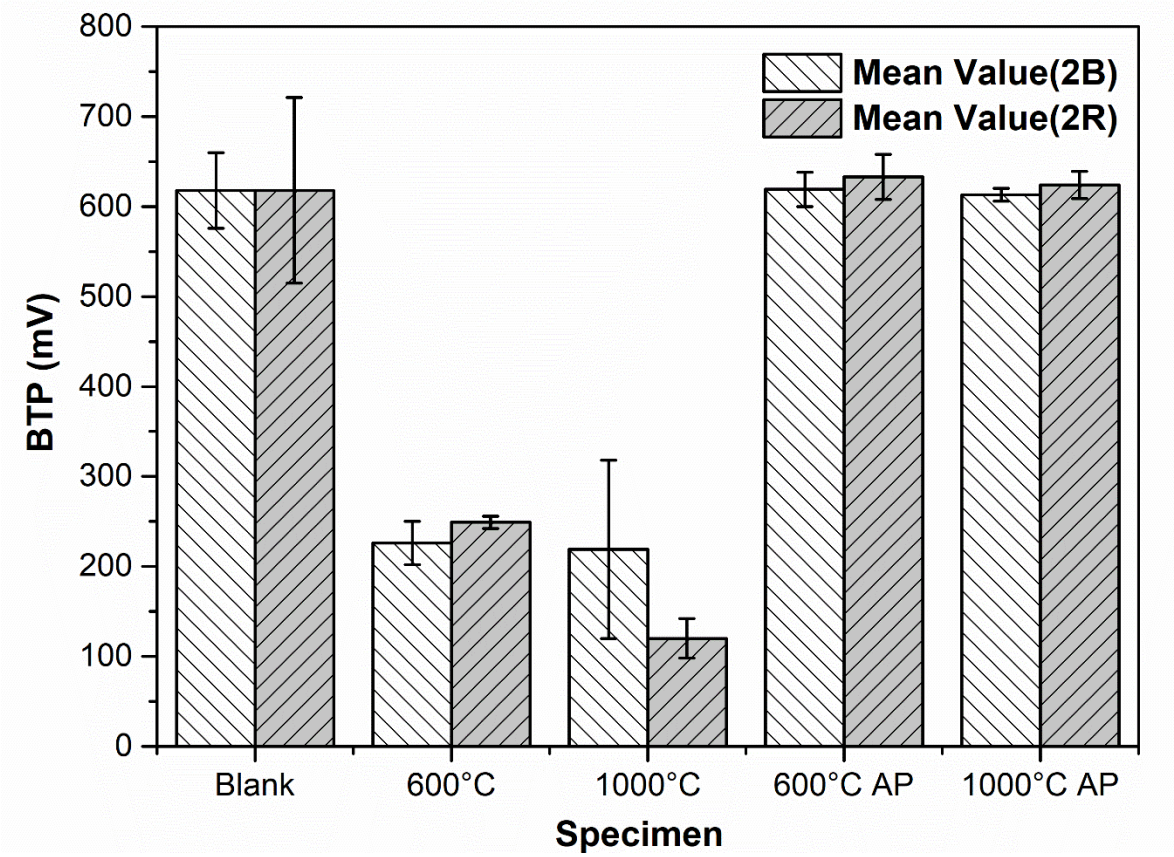

Figure 43 BTP of all the samples: Blank, tinted 10 min at 600 and 1000°C in air and after pickling (AP) / mean value and standard deviation of each 5 tested specimens.

From the Figure 43 it can be noticed that both 2B and 2R surface finishes of blank type shows almost same performance but 2R has a higher deviation when compared with 2B, in case of the tinted samples at 600°C 2R has slightly higher potential increase but smaller deviation than 2B and much lower compared to blank specimens. Moving on to the tinted samples at 1000°C 2R shows less potential increase than 2B with a higher deviation. After pickling the samples tinted at 600°C the BTP could totally be recovered same as blank samples. For the pickled samples after tinting at 600°C and 1000°C the BTP could almost be recovered same as the case of blank see Figure 43.

The highest BTP was found with the after pickled samples and blank samples of both 2B and 2R, followed by samples tinted at 600°C and the lowest BTP for samples tinted at 1000°C. A similar situation was for pickling after 600°C and 1000°C tinting, gaining a BTP same as blank samples, see Figure 43. The standard deviation of the results was found again higher for samples of 2R than for 2B. The former shows more positive BTP than the latter at blank and tinted at

600°C conditions. For samples tinted at 1000°C the BTP values are much varied, whereas 2R shows a higher standard deviation, as noted before. As found for the OCP the pickling method could attain the corrosion resistance of blank material back, see Figure 43.

5.2.6 Passivity range / BTP minus OCP

The difference between the BTP and OCP is determined individually for both 2B and 2R and is equivalent to the so-called passive range, where no significant rise in the current during polarization is measured. The passive range in mean values and standard deviation for both different surface finishes and all five conditions (blank, tinted at 600°C, tinted at 1000°C, after pickling of 600°C and after pickling of 1000°C samples) are shown in Figure 44.

The passive range for 2B is 488 ±39 mV for blank, 391 ±34 mV and 358 ±121 mV for tinted specimens at 600°C and 1000°C. 491±31 and 493±18 for after pickling samples of 600°C and 1000°C.

The passive range for 2R is 484 ±79 mV for blank, 327 ±42 mV and 188 ±13 mV for tinted specimens at 600°C and 1000°C. 502±16 and 499±22 for after pickling samples of 600°C and 1000°C.

The passive ranges for the blank specimens of 2R and 2B showed similar mean values, whereat 2R shows higher standard deviation. Specimens tinted at 1000°C, exhibited for 2R approx. just the half of the passive range from 2R, but 2B shows high standard deviation. For the specimens tinted at 600°C the 2B specimens show somewhat higher passive range than 2R. After pickling the passive range of the tinted specimens could be recovered totally, see Figure 44.

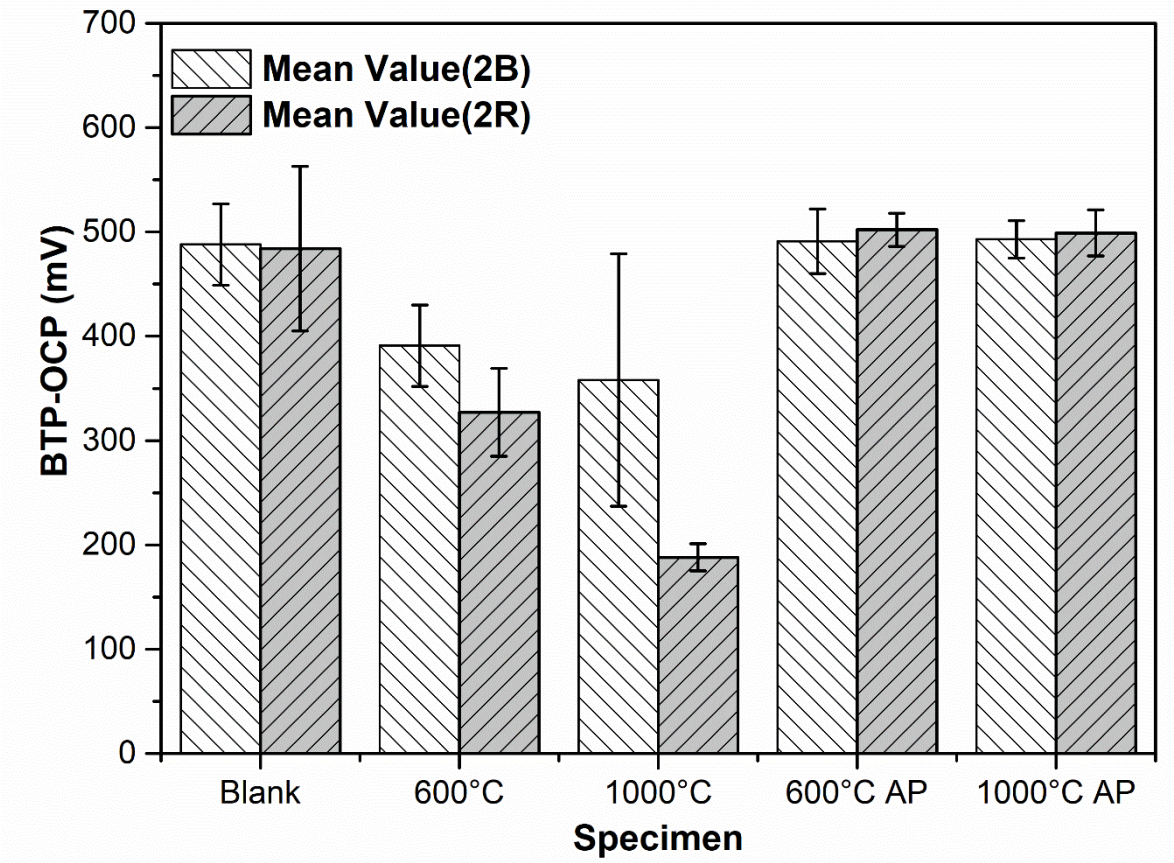

Figure 44 Passive range BTP-OCP of all the samples: Blank, tinted 10 min at 600 and 1000°C in air and after pickling (AP) / mean value and standard deviation of each 5 tested specimens.

5.2.7 Pits Measurement in metallographic cross section

To identify and quantify the corrosion attack, light optical microscopy (LOM) of selected specimen was conducted (refer to appendix A Figure 50 Figure 51). The average value for the number of pits, their depth and width was evaluated in cross sections separately for the blank and for the tinted samples (600°C and 1000°C) as well as for the pickled samples after tinting.

The LOM examination of the blank specimens showed pitting corrosion on all of the specimens. In detail, small pits were found on the surface of the corroded sample of 2B blank after testing. In comparison, the blank specimen 2R showed pits with a higher diameter (width) and the amount of pits are comparable.

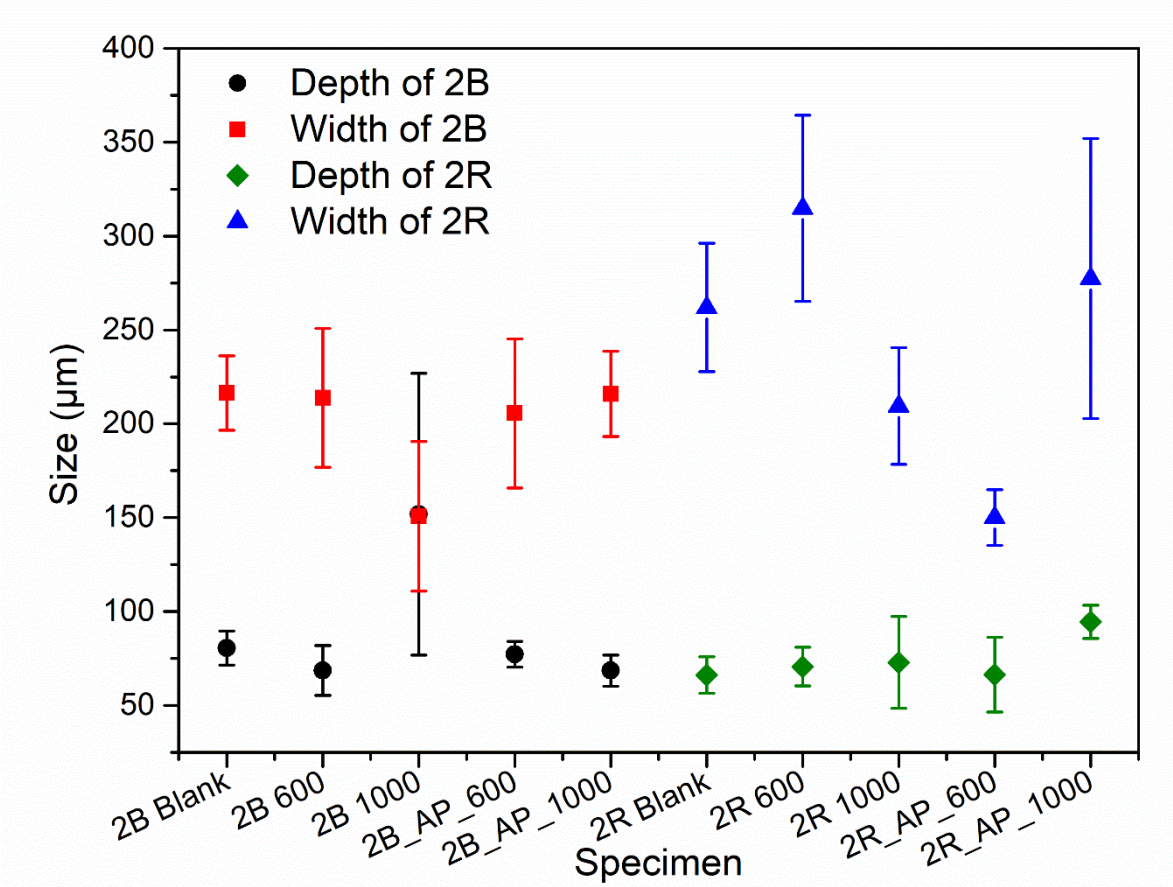

Figure 45 Pits dimensions measurement in metallographic cross sections of the samples used.

Further LOM investigations of the pits showed for 2B an average depth of 80±9 and a width of 216±19 µm. For samples of 2R a depth of 66±9 and a width of 261±34 µm were found. These set of values are also shown in the diagram in Figure 45. The standard deviation was higher for samples of 2R, than for samples of 2B. This is due to the fact, that some pits on the surface of 2R are wider, whereas others are rather narrow. In 2B blank the diameters seem to vary less.

On specimens tinted at 600°C LOM investigations revealed for 2B, a similar amount of small pits like for 2R. Whereas the severity of the pitting attack seems to be higher at 2R specimens, appearing by deeper and wider pits. Derived from further LOM investigations of specimens tinted at 600°C 2B showed 8 and 2R 9 pits. Measurements of the width and the depth showed for 2B tinted at 600°C a depth of 68±8 and a width of 213±36 as well as for 2R a depth of 70±10 and a width of 314±49 µm. These numbers, confirm the findings from above, which was also proved by Figure 45. 2B tinted at 600°C shows a similar amount of pits, which are smaller in diameter (width) and lower in depth than pits in 2R tinted at 600°C. The standard deviation of the width and depth for 2R tinted at 600°C is very high, because of the diversity of pits found.

The corrosion attack is the highest on samples tinted at 1000°C. For 2R specimens narrow but deep pits appear after corrosion testing. The surface is corroded uniformly as well, but not as severe, as the 2B specimens. The LOM

investigations showed for the tinted specimens at 1000°C 8 pits for 2B and 14 pits for 2R. The evaluation of the pits, taking into account the width and depth of the pits, during LOM investigations of the tinted samples at 1000°C, showed for 2B a depth of 15±75 µm and a width of 150±39 µm, which is consistent with the findings above. For 2R on the other hand, a depth of 72±24µm and a width of 209±31 µm were found.

Sample type	Number of pits	Sample type	Number of pits
2B blank	10	2R Blank	9
2B 600°C	14	2R 600°C	15
2B 1000°C	10	2R 1000°C	18
2B after pickling 600°C	6	2B after pickling 600°C	5
2B after pickling 1000°C	5	2R after pickling 1000°C	6

Table 3 number of pits evaluated on the LOM analysis

The LOM evaluation for the after pickled specimens of 2R and 2B tinted at 600°C and 1000°C showed similar mean values, whereas 2B shows higher standard deviation than 2R in case of after pickled samples at 600°C. Specimens after pickling of tinted at 1000°C, exhibited for 2R shows a very high deviation when compared with 2B. For 2B after pickling of 600°C tinted surfaces a depth of 77±6 and a width of 205±39 as well as for 2R a depth of 66±20 and a width of 150±14 µm were measured. For 2B after pickling of 1000°C tinted surfaces a depth of 68±8 and a width of 215±22 as well as for 2R a depth of 94±8 and a width of 277±74 µm.

5.2.8 EDS analyses / estimation of tinted oxide layer composition

The EDS (Energy Dispersive Spectroscopy) analysis are carried out to estimate the composition of the tinted oxide layers. Here the lowest applied energy of the incident electron beam in the SEM of 3keV was relevant, as it has the lowest penetration depth of a few microns. For 2B at 600°C / 10 min in air just iron and oxygen could be found (chromium is not present as could be analysed by Raman spectroscopy in the next chapter). For 2R at the same conditions additionally a nickel peak appears, i.e. Fe and Ni oxides exists on the tinted surface. For tinting at 1000°C / 10 min in air the results are reversed. For 2B an additional Ni peak appears and for 2R it disappears. This can probably be traced back to the different surface conditions (2B deformation via skin pass / 2R bright annealed without deformation).

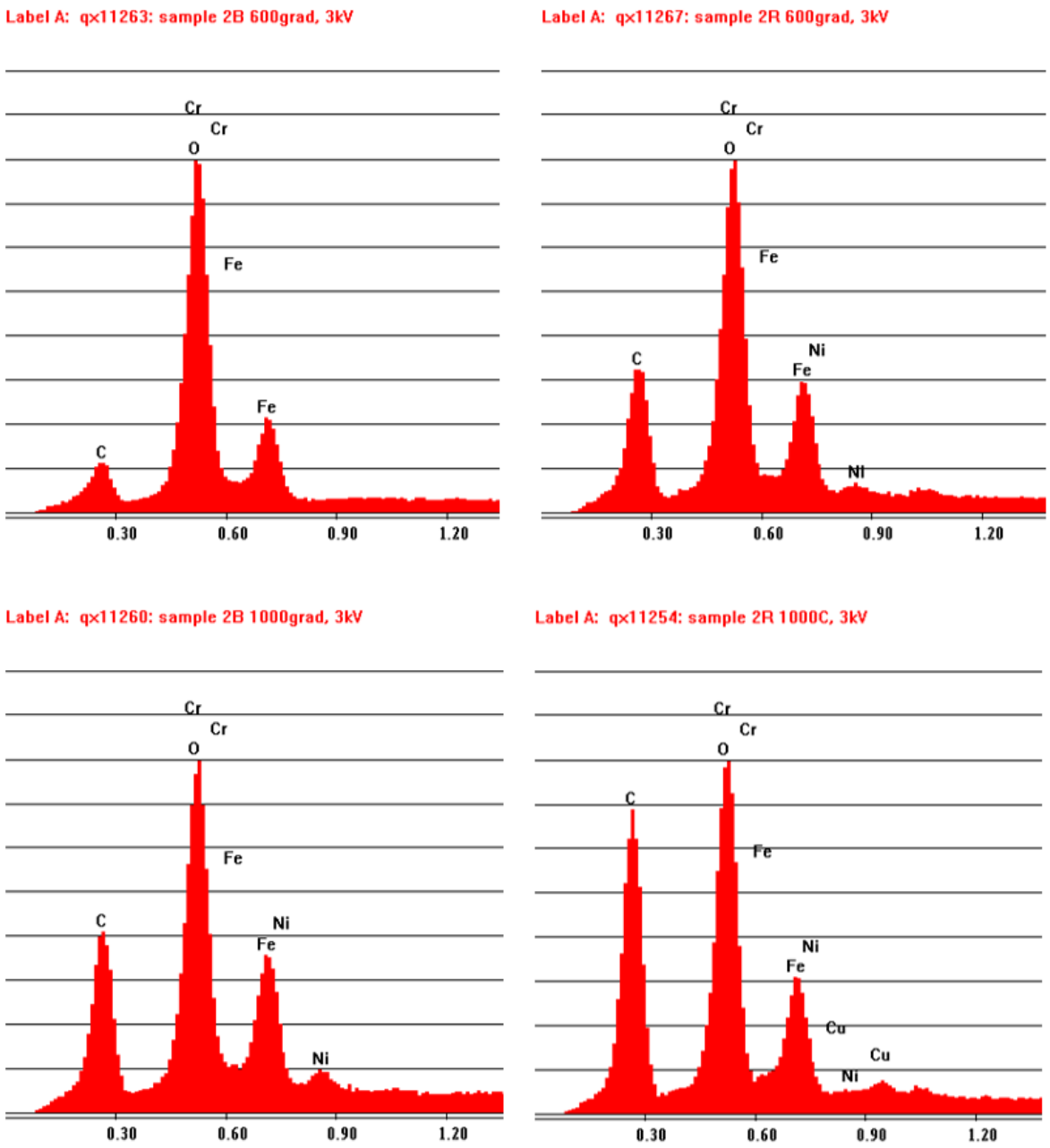

Figure 46 EDS analyses in SEM with 3keV acceleration voltage / left 2B and right 2R at 600 and 1000°C

The different height of the carbon peak is not of relevance as C is considered as contamination in the EDS analyses. For the appearing copper peak at 2B 1000°C, we have no explanation, as its content is not even stated in the chemical analyses, see Figure 46.

The analyses using higher incident beam voltage (9 and 15 keV) does not bring further information's as the penetration depth increase and the surficial resolution decreases.

5.2.9 Raman spectroscopy / tinted oxide layer composition

This analysis shows that for tinted 2B at 600°C / 10 min the surficial oxide layer (10nm) penetration depth) consists just of Hematite Fe2O3 with small areas of Trevorite NiFe2O4, but no chromium (III) oxide Cr2O3 exists. For 2B at 1000°C /

10 min Hematite Fe2O3 and Magnetite Fe3O4 (at the scratches) is present. Tinting at 600°C for 2R leads to Fe2O3 too, with Fe3O4 at scratches - no Cr2O3 appears too. For 2R at 1000°C no analyses are possible with the applied laser (has to be repeated with another laser light), see Figure 47.

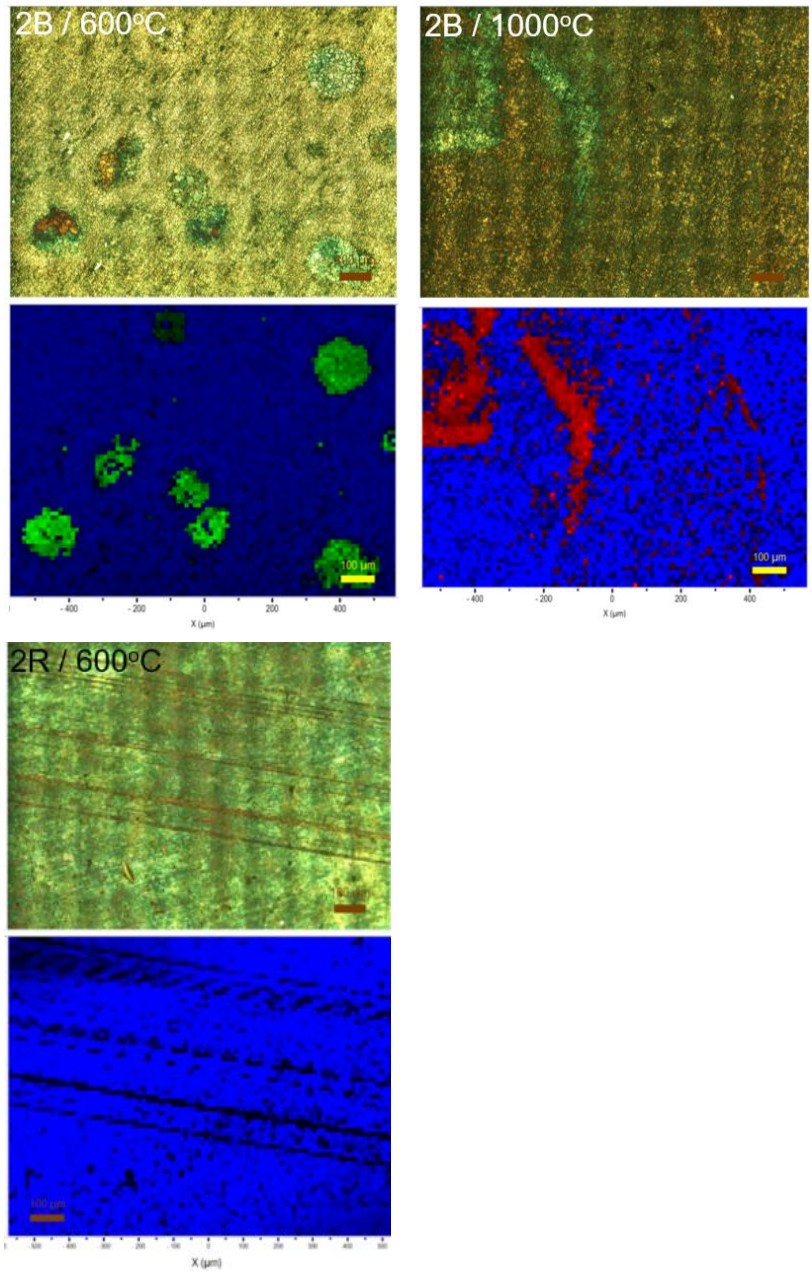

Figure 47 Raman spectroscopy results – (top row) LOM images, (bottom row) Raman images - blue Fe2O3, green NiFe2O4, red Fe3O4.

6. Conclusion

Generally, it is to be noted, that tinting has a clear influence on the corrosion resistance can be determined by the shift of the potentiostatic polarization curves, what can be evaluated by the OCP and the BTP values. No clear conclusion can be drawn from the passivity range (BTP minus OCP), as both the OCP as well as the BTP values are shifted differently due to tinting for the 2B and 2R surfaces.

No clear tendency in metallographic analyses of the pits could be found. It can be stated that for the tinted samples the pits dimensions (average pit volume) and the number of pits vary more than for the blank and tinted plus pickled samples.

7. Summary and discussion

The only clear conclusion able to be drawn is that there is a significant difference in corrosion resistance between the stainless steel AISI 304 (1.4301) of 2B and 2R surface finishes with various different conditions when subjected to higher concentrations of chloride ions.

The influence of tinting at two different peak temperatures (600°C and 1000°C, each for 10min without shielding gas) compared to blank (as received) samples of AISI 304 on the corrosion resistance was investigated. Additionally, these investigations were performed on two different surface conditions, 2B (Skin Passed) and 2R (Bright Annealed). To determine the corrosion resistance, the samples were linear polarized in 5%NaCl electrolyte by means of a potentiostat and the resulting polarization curves evaluated. To confirm the corrosion attack, also metallography on selected samples was performed.

The specimens 2R with bright annealed finish exhibit higher corrosion resistance during polarization than the specimens of 2B with skin passed finish. This means that 2R shows in general a higher Open Circuit Potential (OCP) as well as a higher Break Trough Potential (BTP). Thus the passive range (BTP minus OCP) of 2R is wider too if compared to the one of 2B. This is supposed to be because of the smooth surface with low roughness of 2R (0.03-0.2 µm) hindering the selective attack of chloride ions in forming pits, compared to 2B with a significantly higher surface roughness of 0.1-0.5 µm. It should be noted that the deviations of all measured values (OCP, BTP, BTP-OCP) are high for the 2R specimens. This is probably due to small surface defects, like scratches appearing during handling and transport, the 2R specimens showed.

Later by using the Raman analysis the Hematite and magnetite content in the samples was analyzed. Both surface finishes of 2B and 2R samples showed an uneven oxide layer thickness and oxide layers were difficult to observe.

The artificial produced oxide layers in a furnace without shielding gas, deteriorate the corrosion resistance strongly. Here again the 2R specimens are higher in corrosion resistance, compared to 2B. This was verified by higher (more positive) OCP and higher BTP and a larger passive range for specimens tinted at 600°C. For the specimens tinted at 1000°C the BTP and the passive range for 2R and 2B are very similar, due to the supposed stronger chromium depletion on the surface.

The evaluation of the corrosion attack, which was identified for all specimen as pitting corrosion and crevice corrosion at the edges of the specimens holder (working electrode) 2B specimens showed a low deviation in the mean values of width and depth of the pits for the surface conditions blank and tinted (600°C and 1000°C), after pickling, both 2B and 2R attained almost the same behavior similar to the blank samples but in other words it can be said that 2B has much lower values of depth and width when compared to 2R.. A high

deviation was found for all 2R specimen, whereat the larger pits are probably caused by surface defects (the scratches mentioned above). The comparison of the 2B samples in all five surface conditions (blank, tinted at 600°C and 1000°C, after pickling of tinted samples at 600°C and 1000°C) showed for blank compared with tinted at 600°C a higher depth and width of the pits, whereas for tinted at 1000°C ones the most severe pitting of the samples was analyzed with the highest standard deviation.

For samples of 2B and 2R tinted at 1000°C already uniform surface corrosion occurs additionally to the pitting corrosion. This means that there is a strong depletion of chromium on the surface, leading to a content below the minimum of 12%Cr necessary for a spontaneous surface passivation. It is possible that the depletion is due to the formation of Cr-rich Carbides, like Cr23C6. A sensitization due to the tinting at 600°C and 1000°C for 10 min is unlikely, as this is outside the sensitization time-temperature field, see Figure 46.

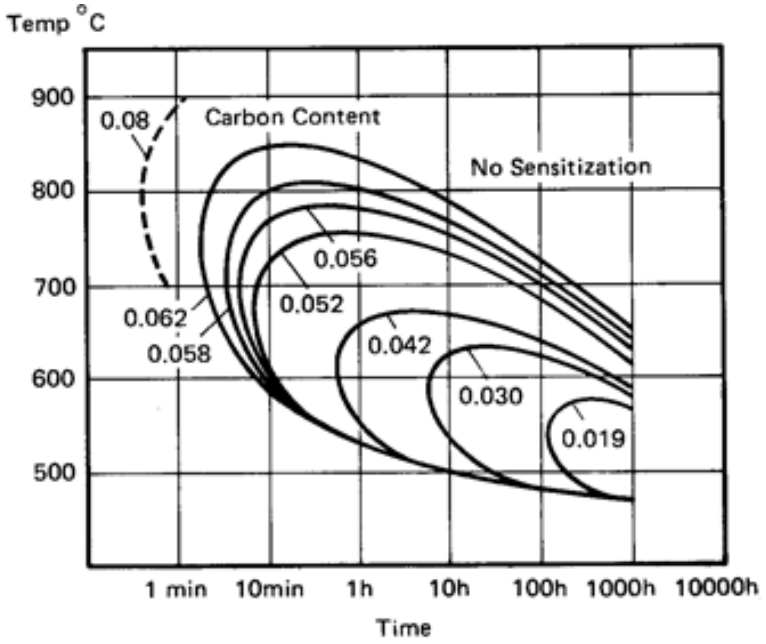

Figure 46 Time-temperature-sensitization curves for Type 304 alloys as a function of C content (www.australwright.com.au/sensitisation-of-austenitic-stainless-steels, AUSTRAL WRIGHT METALS, AUSTRALIA 2000-2015)

It can be concluded, that the 2R bright annealed finish, shows better corrosion resistance compared to the 2B skin passed finish in linear polarization testing and a constant level of pitting in all five tested conditions blank, tinted and after pickled. Attention must be payed to exclude surface defects, especially for 2R. In any case tinting colors have to be removed to save the corrosion resistance of the AISI 304 stainless steel.

8. Outlook

The above potentiostatic corrosion tests should be done with different kinds of stainless steel samples at different sodium chloride concentrations and compare with each other so that one can get a clear idea about the Potentiostatic corrosion tests.

To continue with this project, one should make longer OCP measurements (than 300 seconds) to be able to require a stable value followed by a polarization sweep performed once the system is stabilized. One other alternative is to perform the polarization with a polarization rate on the system a few times before performing the real measurement.

Higher temperatures and shorter tinting times should be investigated, to get closer to the tinting layers appearing during welding. Furthermore, one should produce tinting colors not in air but with different oxygen residues like it happens during purging inside of a tube and arc welding outside (mainly argon or nitrogen with 5%hydrogen gases are used therefore).

The test repetitions were relatively low (5 specimens for one surface condition). As the deviations of the value (OCP and BTP) and especially the pit dimensions and numbers were high. Thus, more repetitions should be performed in future, e.g. 10 per surface condition. Furthermore, it is suggested to perform test using organic acids and substances, as stainless steels are often applied in the food industry. Finally, a series of different surface finishes do exist for stainless steels. It could be of high interest to analyze its corrosion resistance, using the methods applied in the present work.

References

[1] Joseph R. Davis, *Corrosion of Weldments*. United States of America: ASM International, 2006.

[2] J. R. Davis, “Stainless steels, ASM International. Handbook Committee,” 1994, pp. 244–245.

[3] “Handbook series N° 9002,” in *welding of stainless steels and other joining methods*, USA: AISI Institute, 1979, p. 47.

[4] Linda Garverick, *Corrosion in the Petrochemical Industry*, Illustrate. ASM International, 1994.

[5] P. K. S. Erhard Klar, *Powder Metallurgy Stainless Steels: Processing, Microstructures, and Properties*. ASM International, 2007.

[6] D. J. Kearns JR, Scully JR, Roberge PR, Reichert DL, *Electrochemical Noise Measurement for Corrosion Applications*. ASTM International, 1996.

[7] D. S. A. Bruce D. Craig, *Handbook of Corrosion Data*. ASM International, 1994.

[8] Michael F. McGuire, *Stainless Steels for Design Engineers*. ASM International, 2008.

[9] T. L. S. Malcolm Blair, *Steel Castings Handbook*, 6th ed. ASM International, 1995.

[10] Vladimir B. Ginzburg, *Flat-Rolled Steel Processes: Advanced Technologies*. CRC Press, 2009, 2009.

[11] D. KOSHAL, *Manufacturing Engineer’s Reference Book*, 1st editio. 2014.

[12] P. E. Philip A. Schweitzer, *Fundamentals of Metallic Corrosion: Atmospheric and Media Corrosion of Metals*, Second edi. 2006.

[13] G. Krauss, *Stainless Steels, 2nd ed. ASM International, , ISBN-13: 978-1-62708-083-5.*, Second edi. ASM International, 2015.

[14] P. Authors: Marshall, *Austenitic Stainless Steels Microstructure and mechanical properties*, 1st editio. Springer Netherlands, 1984.

[15] Mattias Calmunger, *On High-Temperature Behaviours of Heat Resistant Austenitic Alloys*. LiU-Tryck, Linköping, Sweden, 2015.

[16] P. E. John C. Tverberg, “The Role of Alloying Elements on the Fabricability of Austenitic Stainless Steel,” *Met. Mater. Consult. Eng.*, pp. 4–7.

[17] Hans-Bertram Fischer, *Bemessungshilfen zu nichtrostenden Stählen im Bauwesen*. Euro Inox, 2006.

[18] M.V. Suresh Kumar & P. Anil Kumar, *ENGINEERING CHEMISTRY-I*. Vikas Publishing, 2014.

[19] R. K. G. Sohan L. Chawla, *Materials Selection for Corrosion Control*. ASM

International, 1993.

[20] H. T. Reza Javaherdashti,Chikezie Nwaoha, *Corrosion and Materials in the Oil and Gas Industries*. CRC Press, 26.04.2013, 2013.

[21] P. E. Douglas K. Louie, *Handbook of Sulphuric Acid Manufacturing*, 2nd Editio. 2008.

[22] John M. Beswick, *Bearing Steel Technology*, 7th ed. ASTM International, 2007, 2007.

[23] Ferdinant Henrich, *Chemie und Chemische Technologie Radioaktiver Stoffe*. Springer-Verlag, 2013, 2013.

[24] Myer Kutz, *Mechanical Engineers' Handbook, Volume 1: Materials and Engineering Mechanics*. John Wiley & Sons, 2015, 2015.

[25] Harold M. Cobb, *The History of Stainless Steel*. ASM International, 2010.

[26] A. K. E. George F Schrader, *Manufacturing Processes and Materials*, Fourth edi. Society of Manufacturing Engineers, 2000.

[27] A. S. M. V. G. Behal, *Stainless Steel Castings*. .

[28] "www.aperam.com/uploads/stainlesseurope/ManufacturingProcess/MS_ ManufacturingProcess_Stage1_EN_new.pdf accesed on 27.06.2017." [Online]. Available: 21.%09www.aperam.com/uploads/stainlesseurope/ManufacturingProcess /MS_ManufacturingProcess_Stage1_EN_new.pdf.

[29] William L. Roberts, *Hot Rolling of Steel*. 1983.

[30] "www.aperam.com/uploads/stainlesseurope/ManufacturingProcess/MS_ Manufacturing%20Process_Stage2_EN_new.pdf, accessed on 27.06.2017." [Online]. Available: 23.%09www.aperam.com/uploads/stainlesseurope/ManufacturingProcess /MS_Manufacturing Process_Stage2_EN_new.pdf.

[31] John K. Mahaney, *Advances in the Production and Use of Steel with Improved*. ASTM International, 1998.

[32] "www.aperam.com/uploads/stainlesseurope/ManufacturingProcess/MS_ Manufacturing%20Process_Stage3_EN_new.pdf, accessed on 27.06.2017." [Online]. Available: www.aperam.com/uploads/stainlesseurope/ManufacturingProcess/MS_M anufacturing Process_Stage3_EN_new.pdf,.

[33] Joseph R. Davis, *Stainless Steels*. ASM International, 1995.

[34] "aperam manufacturing process – stage 4 Cold rolling and final annealing (May 2009) www.aperam.com/http://www.aperam.com/about-2/aperam/what-is-stainless-steel/manufacturing-process." [Online]. Available: aperam manufacturing process – stage 4 Cold rolling and final

annealing (May 2009) www.aperam.com/http://www.aperam.com/about-2/aperam/what-is-stainless-steel/manufacturing-process.

[35] Caleb Hornbostel, *Construction Materials: Types, Uses and Applications*, 2nd editio. Wiley-Interscience, 1991.

[36] “Surface finishes of stainless steel 304,” 2017. [Online]. Available: https://www.alibaba.com/product-detail/No-1-2b-Sheet-And-2B_60228317871.html.

[37] “aperam manufacturing process – stage 4 Cold rolling and final annealing (May 2009) www.aperam.com/http://www.aperam.com/about-2/aperam/what-is-stainless-steel/manufacturing-process (seen 21.6.2017).” .

[38] “https://www.researchgate.net/figure/254250249_fig1_Figure-1-Types-of-anodic-dissolution-curves-for-corrosion-processes-Curve-a-Normal accesed on 23.06.2107.” .

[39] Nancy Missert, *Critical Factors in Localized Corrosion 5*. The Electrochemical Society, 2007, 2007.

[40] Luciano Lazzari, *Engineering Tools for Corrosion: Design and Diagnosis*. Woodhead Publishing, 2017, 2017.

[41] Nestor Perez, *Electrochemistry and Corrosion Science*. springer 2016, 2016.

[42] R. Winston Revie, *Corrosion and Corrosion Control*, 4th ed. John Wiley & Sons, 2008, 2008.

[43] S. K. R. U.K. Chatterjee, S.K. Bose, *Environmental Degradation of Metals*. CRC Press, 2001, 2001.

[44] Helmut Kaesche, *Die Korrosion der Metalle*, 3rd ed. Springer-Verlag, 2011, 2011.

[45] E. H. Ragnar Holm, *Electric Contacts Handbook*, 3rd ed. Springer-Verlag, 2013, 2013.

[46] V. M. Philippe Marcus, *Passivation of Metals and Semiconductors, and Properties of Thin Oxide Layers*, 1st editio. Elsevier B.V., 2005.

[47] R. B. P. David A.Hansen, *Materials Selection for Hydrocarbon and Chemical Plants*. marcel dekker, 1996.

[48] W. P. Brian Evans, *A Level Product Design*. Nelson Thornes, 2004, 2008.

[49] George F. Vander Voort, *Applied metallography*. Van Nostrand Reinhold, 1986.

[50] Ian Inman, *Compacted Oxide Layer Formation Under Conditions of Limited Debris Retention at the Wear Interface During High Temperature Sliding Wear of Superalloys*. Universal-Publishers, 2006, 2006.

[51] Helmi A. Youssef, *Machining of Stainless Steels and Super Alloys:*

Traditional and Nontraditional Techniques. John Wiley & Sons, 19.01.2016, 2016.

[52] Masahiro Seo, *Passivity and Localized Corrosion*. the electrochemical society,INC, 1999.

[53] R. H. Daniel Herring, *Heat Treating*. ASM International, 2005, 2005.

[54] M C Chaturvedi, *Welding and Joining of Aerospace Materials*. Elsevier, 2011, 2011.

[55] George F. Vander Voort, *Metallography: Principles and Practice*. 1999.

[56] Finke K. M, "Einfluss thermisch erzeugter Deckschichten auf die Korrosionsbeständigkeit geschweißter CrNi-Stähle," Dissertation TU Braunschweig, 1999.

[57] Madeleine Durand-Charre, *Damascus and pattern-welded steels - Forging blades since the iron age*. EDP Sciences, 1989.

[58] Saleem Hashmi, *Comprehensive Materials Finishing*. Elsevier B.V., 2016.

[59] David John Young, *High Temperature Oxidation and Corrosion of Metals*. Elsevier, 2016, 2016.

[60] H.S. Khatak and B. Raj, *Corrosion of Austenitic Stainless Steels*. Woodhead Publishing Series, 2002.

[61] V. S. R. K. Elayaperumal, *Corrosion Failures: Theory, Case Studies, and Solutions*. 2015.

[62] National Research Council Canada, *International congress on metallic corrosion*. 1984.

[63] William M. Huitt, *Bioprocessing Piping and Equipment Design: A Companion Guide for the ASME BPE Standard*. John wiley & sons,Inc, 2017.

[64] Rudy Mohler, *Practical Welding Technology*. Industrial Press Inc., 1983, 1983.

[65] Prakriti Kumar Ghosh, *Pulse Current Gas Metal Arc Welding: Characteristics, Control and Applications*. Springer, 2017, 2017.

[66] Ramesh Singh, *Applied Welding Engineering: Processes, Codes, and Standards*, First edit. Butterworth-Heinemann, 2012.

[67] J. R. Davis, *Corrosion: Understanding the Basics*. ASM International, 2000.

[68] R. F. Steigerwald, *Intergranular Corrosion of Stainless Alloys*. ASTM International, 1978, 1978.

[69] R. G. George Antaki, *Nuclear Power Plant Safety and Mechanical Integrity*. Butterworth-Heinemann, 2014, 2014.

[70] Sankara Papavinasam, *Corrosion Control in the Oil and Gas Industry*. 2013.

[71] Sudhangshu Bose, *High Temperature Coatings*, 1st editio. Butterworth-Heinemann, 2007.

[72] C. P. Dillon, *Materials Performance*. 1994.

[73] Tony J.A. Richardson, *Shreir's Corrosion*. Elsevier, 2009, 2009.

[74] Zaki Ahmad, *Principles of Corrosion Engineering and Corrosion Control*, 1st Editio. Butterworth-Heinemann, 2006.

[75] "aperam pitting corrosion." [Online]. Available: http://www.aperam.com/uploads/stainlesseurope/Brochures/Leaflet corrosion_Eng_374Ko.pdf ,seen on 30.06.2017 at 6.45pm.

[76] Robert Baboian, *Galvanic and Pitting Corrosion-Field and Laboratory Studies*. ASTM International, 1976.

[77] Philippe Marcus Vincent Maurice, *Passivation of Metals and Semiconductors, and Properties of Thin Oxide Layers*. 2006.

[78] D. A. Shifler, *Corrosion in Marine and Saltwater Environments II*. the electrochemical society,INC, 2005.

[79] "aperam corrosion." [Online]. Available: http://www.aperam.com/uploads/stainlesseurope/Brochures/Leaflet corrosion_Eng_374Ko.pdf ,seen on 30.06.2017 at 6.45pm.

[80] Developed by Subcommittee, "ASTM G150 - 13 Standard Test Method for Electrochemical Critical Pitting Temperature Testing of Stainless Steels," 2013.

[81] M. E. Edward Ghali, V. S. Sastri, *Corrosion Prevention and Protection: Practical Solutions*. Wiley, 2007.

[82] United States. Department of Energy, *Effect of Chloride Concentration and PH on Pitting Corrosion of Waste Package Container Materials*. United States. Department of Energy, 1996.

[83] M. E. G.-A. John O'M. Bockris, Amulya K.N. Reddy, *Modern Electrochemistry 2A: Fundamentals of Electrodics*. 2005.

[84] Philippe Marcus, *Corrosion Mechanisms in Theory and Practice, Third Edition*, Third. CRC Press, 2017.

[85] Michel Froment, *Passivity of Metals and Semiconductors*. Elsevier B.V., 1983.

[86] Florian Mansfeld, Bertocci, T.S. Lee, *Electrochemical Corrosion Testing*. ASTM International, 1981.

[87] J. W. Oldfield & W. H. Sutton, "Crevice Corrosion of Stainless Steels: I. A Mathematical Model," pp. 13–22, 2013.

[88] "Standard Practice for Cleaning, Descaling, and Passivation of Stainless Steel Parts, Equipment, and Systems," ASTM A380 / A380M-13, 2013.

[89] “Nabertherm Furnance,” 2017. [Online]. Available: www.nabertherm.com.

[90] R. Singh, *Weld Cracking in Ferrous Alloys A volume in Woodhead Publishing Series in Welding and Other Joining Technologies*. 2009.

[91] B. S. C. Stephen D. Cramer, *Corrosion: Fundamentals, Testing and Protection*. the University of California, 2003.

[92] S. K. Akihiro Abe, Karel Dusˇek, *Filler-Reinforced Elastomers / Scanning Force Microscopy*. Springer, 2004, 2004.

[93] F. S. Allen J. Bard, György Inzelt, *Electrochemical Dictionary*. Springer Science & Business Media, 2012, 2012.

[94] B. D. Craig, *Handbook of Corrosion Data (Materials Data Series)*, 2nd editio. ASM International, 1995.

[95] “Potentiostat.” [Online]. Available: http://www.ecochemie.nl/Products/Echem/NSeriesFolder/PGSTAT128N.

[96] A. S. A. G5, “Standard Reference Test Method for Making Potentiodynamic Anodic Polarization Measurements,” ASTM G5-14, 2014.

[97] Active Standard ASTM G59, “Standard Test Method for Conducting Potentiodynamic Polarization Resistance Measurements,” ASTM G59-97, 2014.

[98] Active Standard ASTM G61, “Standard Test Method for Conducting Cyclic Potentiodynamic Polarization Measurements for Localized Corrosion Susceptibility of Iron-, Nickel-, or Cobalt-Based Alloys,” ASTM G61-86, 2014.

[99] “Metrohm.” [Online]. Available: https://www.metrohm.com/en/products/electrochemistry/autolab-supplementary-products/%7B293E5A46-EFB8-4849-AA4D-4CA3B00B1E56%7D seen on 23.06.2017.

[100] “Metrohm.” [Online]. Available: https://www.metrohm.com/en/products-overview/%7B6330FC85-E253-429C-81A3-3BC9F64B5746%7D, Seen on 5/7/2017.

[101] D. E. B. Carl A. Burtis, Edward R. Ashwood, *Textbook of Clinical Chemistry and Molecular Diagnostics*. Elsevier Health Sciences, 2012.

[102] A. G.-R. DC Bell, *Energy Dispersive X-ray Analysis in the Electron Microscope*. Garland Science, 2013.

[103] J. R. Autoren: Goldstein, J., Newbury, D.E., Joy, D.C., Lyman, C.E., Echlin, P., Lifshin, E., Sawyer, L., Michael, *Scanning Electron Microscopy and X-ray Microanalysis*. 2003.

[104] Brian Greene, *Der Stoff, aus dem der Kosmos ist*. Goldmann, 2008.

[105] Michio Kaku, *Die Physik des Bewusstseins*. Rowohlt Verlag GmbH, 2014.

[106] “RamanEffect.”[Online].Available:

http://www.nanophoton.net/raman/raman-spectroscopy.html.

Appendix A Materials and potentiostatic tests

1) Samples after water jet cutting

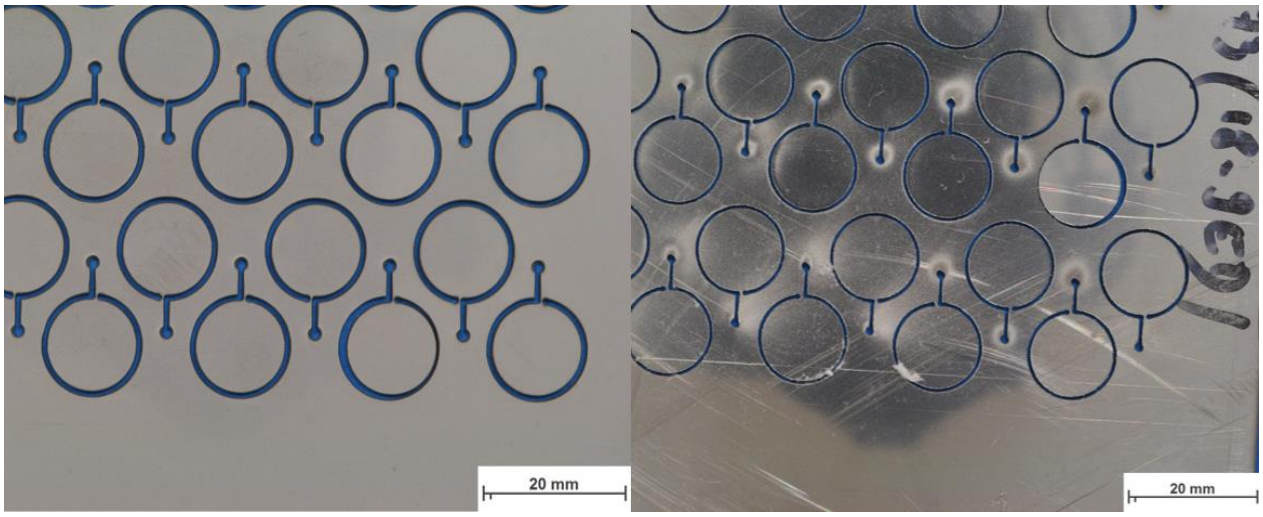

Figure 47 samples after water jet cutting 2B on left side and 2R on the right side.

2) pH and Temperature table

a) for 2B

Sample no.	Material Type	Tinted/blank	If Tinted	pH		Temperature [°C]	
			Temp+time	before	After	before	after
1	2B	Blank	_____	7.022	9.173	25	25
2	2B	Blank	_____	6.083	9.233	25	25
3	2B	Blank	_____	6.516	8.819	25	25
4	2B	Blank	_____	7.254	9.828	25	25
5	2B	Blank	_____	6.359	9.62	25	25
11	2B	Tinted	1000,10 Min	6.717	10.028	25	25
12	2B	Tinted	1000,10 Min	6.107	9.461	25	25
13	2B	Tinted	1000,10 Min	6.621	9.299	25	25
14	2B	Tinted	1000,10 Min	6.501	9.473	25	25
15	2B	Tinted	1000,10 Min	6.554	9.764	25	25
6	2B	Tinted	600,10 Min	6.395	9.994	25	25
7	2B	Tinted	600,10 Min	6.396	9.713	25	25
8	2B	Tinted	600,10 Min	6.439	9.906	25	25
9	2B	Tinted	600,10 Min	7.231	9.858	25	25
10	2B	Tinted	600,10 Min	6.462	9.972	25	25
16	2B	tinted+AP	600,10 Min	6.604	9.357	25	25
17	2B	tinted+AP	600,10 Min	5.978	9.635	25	25
18	2B	tinted+AP	600,10 Min	6.056	8.639	25	25
19	2B	tinted+AP	600,10 Min	6.255	9.476	25	25
20	2B	tinted+AP	600,10 Min	6.799	9.315	25	25
21	2B	tinted+AP	1000,10min	6.567	8.764	25	25
22	2B	tinted+AP	1000,10min	6.569	9.495	25	25
23	2B	tinted+AP	1000,10min	6.653	9.498	25	25
24	2B	tinted+AP	1000,10min	6.022	9.402	25	25
25	2B	tinted+AP	1000,10min	6.425	8.863	25	25
				6.5034	9.4634		
				0.336144	0.392571		

Table 4 2B pH and Temperature values

b) 2R

Sample no.	Material Type	Tinted/blank	If Tinted	pH	Temperature [°C]	

			Temp+time	before	After	before	after
5	2R	Blank	_____	6.578	10.037	25	25
6	2R	Blank	_____	6.172	10.128	25	25
7	2R	Blank	_____	6.374	9.407	25	25
8	2R	Blank	_____	6.276	9.488	25	25
9	2R	Blank	_____	6.547	9.749	25	25
14	2R	Tinted	1000,10 Min	6.191	9.564	25	25
13	2R	Tinted	1000,10 Min	6.395	10.107	25	25
12	2R	Tinted	1000,10 Min	6.144	9.953	25	25
11	2R	Tinted	1000,10 Min	6.559	9.8	25	25
10	2R	Tinted	1000,10 Min	6.088	10.045	25	25
16	2R	Tinted	600,10Min	6.602	9.836	25	25
17	2R	Tinted	600,10Min	6.294	10.121	25	25
18	2R	Tinted	600,10Min	6.152	9.867	25	25
19	2R	Tinted	600,10Min	6.017	9.916	25	25
20	2R	Tinted	600,10Min	6.301	10.136	25	25
21	2R	Tinted+AP	600,10Min	6.675	9.672	25	25
22	2R	Tinted+AP	600,10Min	6.801	9.411	25	25
23	2R	Tinted+AP	600,10Min	6.937	9.154	25	25
24	2R	Tinted+AP	600,10Min	7.187	9.644	25	25
25	2R	Tinted+AP	600,10Min	6.514	9.75	25	25
26	2R	Tinted+AP	1000,10 Min	6.214	9.327	25	25
27	2R	Tinted+AP	1000,10 Min	7.519	9.338	25	25
28	2R	Tinted+AP	1000,10 Min	6.423	9.854	25	25
29	2R	Tinted+AP	1000,10 Min	6.507	8.518	25	25
30	2R	Tinted+AP	1000,10 Min	6.672	9.916	25	25
				6.48556	9.70952		
				0.351787	0.375886		

Table 5 2R pH and Temperature values

3) i-E curves that are taken from the potetntiostatic tests

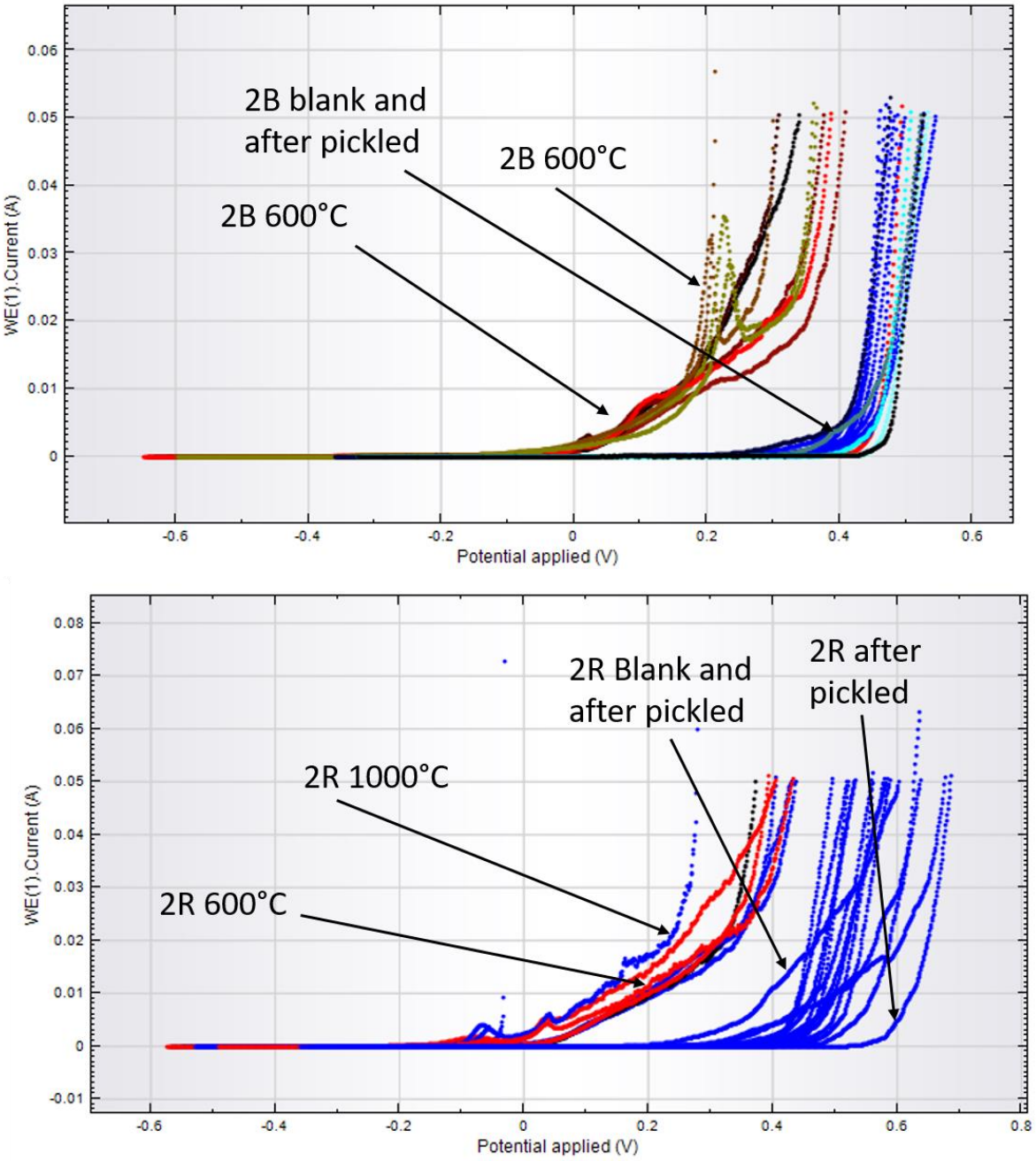

Figure 48 Linear polarization curves (I vs E) from the potentiostatic tests.

4) Current density vs SHE calculated curves from the potentiostat data (curves obtained from origin)

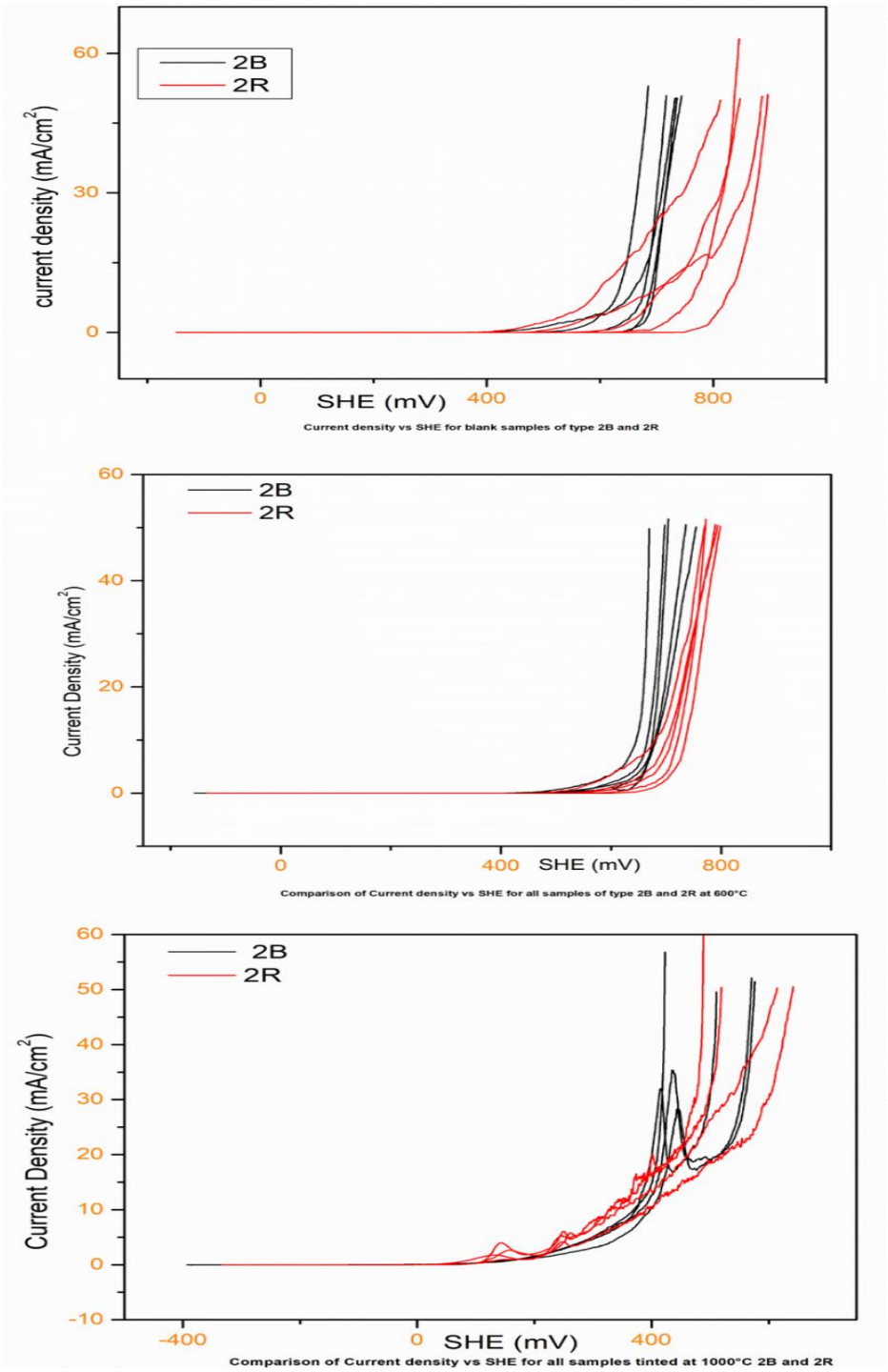

Figure 49 Linear polarization curves - comparison of deviations of 2B and 2R with the same set of samples

5) Pits measurement of 2B and 2R at 600°C and 1000°C
   a) From the surface and cross section

Figure 50 2B and 2R at 600°C (on left side) at 1000°C (on right side)

   b) Different pits that were found in cross section evaluation of 2B and 2R at 1000°C and 600°C

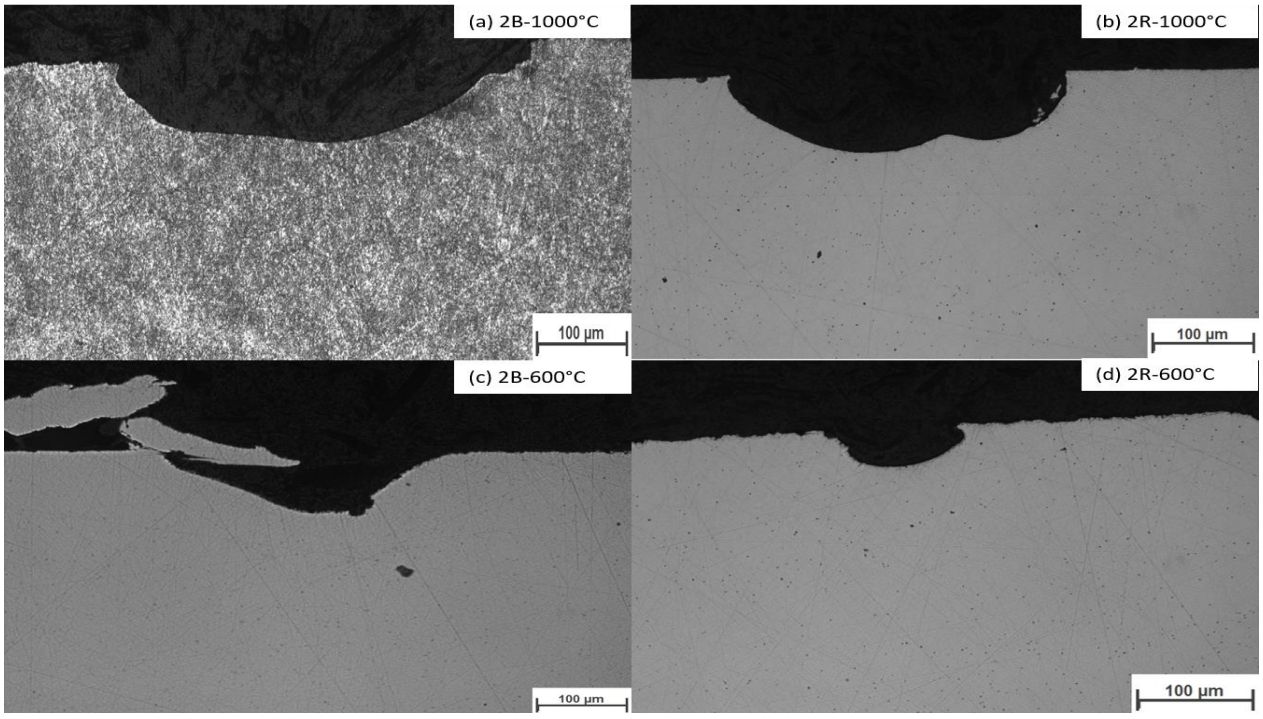

Figure 51 comparison of pits with the cross section of 2B and 2R at 600°C and 1000°C.

Appendix B EDX and Raman analysis

1) EDX for 2B and 2R blank at 3kV

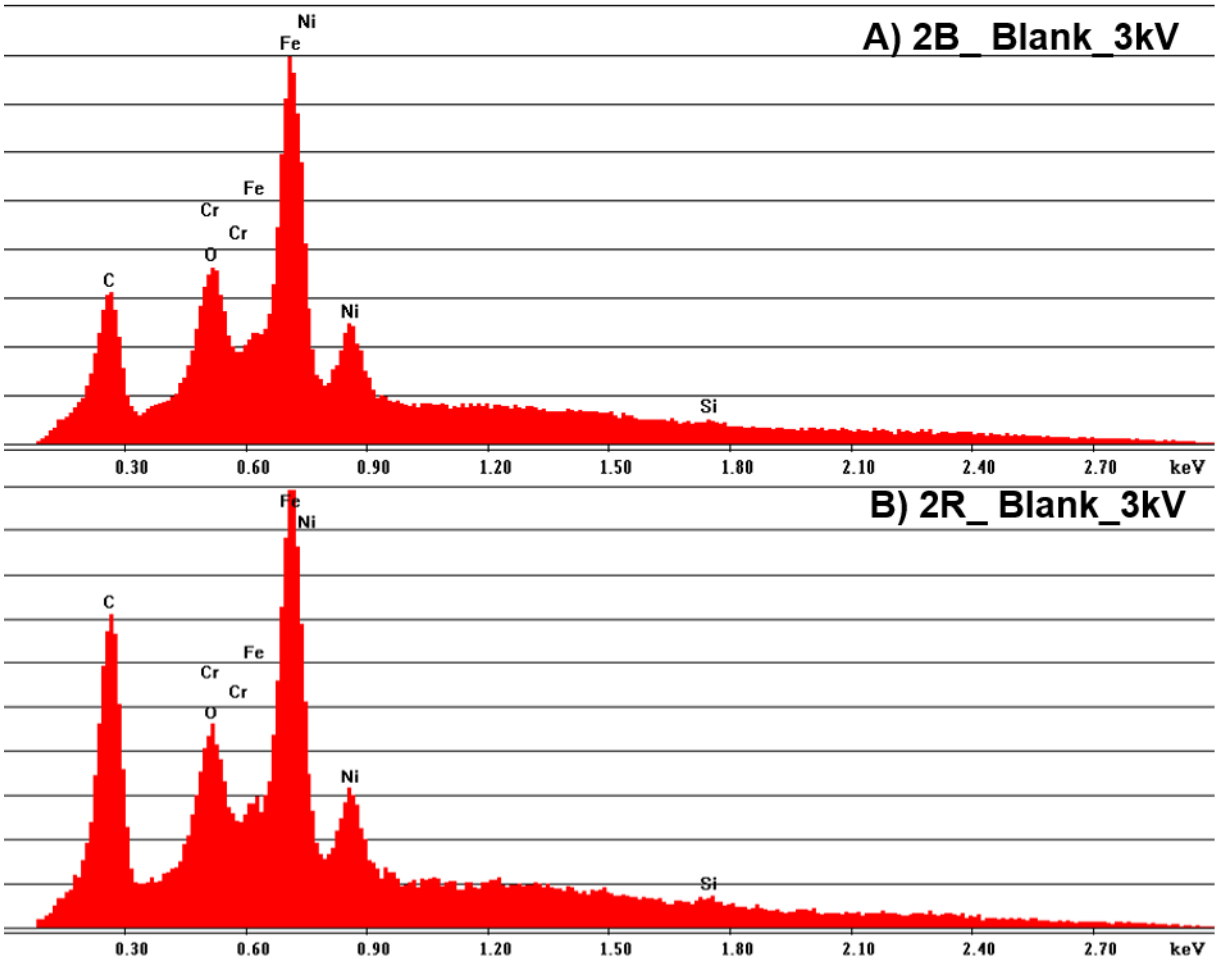

Figure 52 EDX for 2B and 2R blank at 3kV

2) EDX for 2B and 2R tinted (600°C) at 3kV

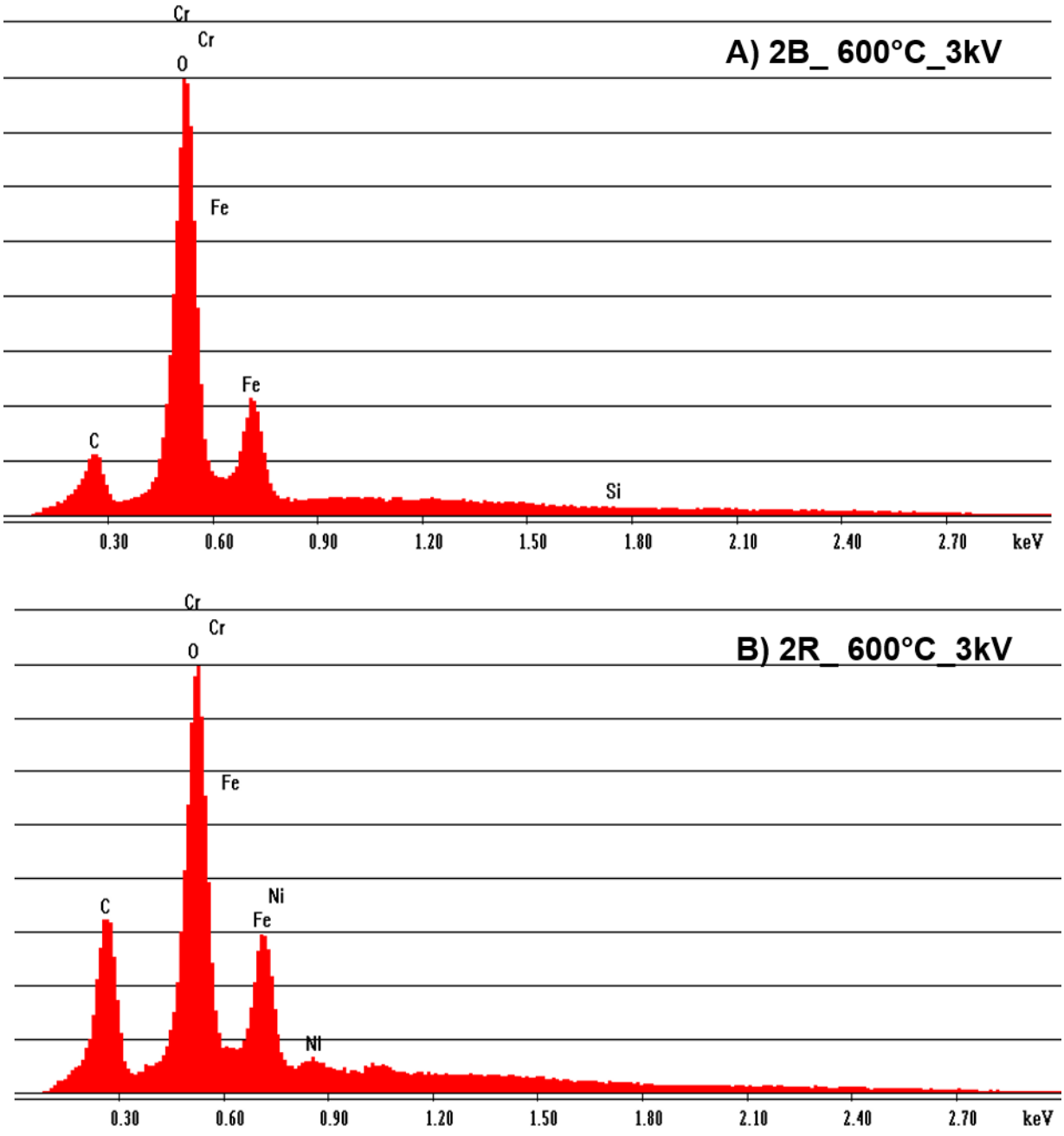

Figure 53 EDX for 2B and 2R tinted (600°C) at 3kV

3) EDX for 2B and 2R tinted (1000°C) at 15kV

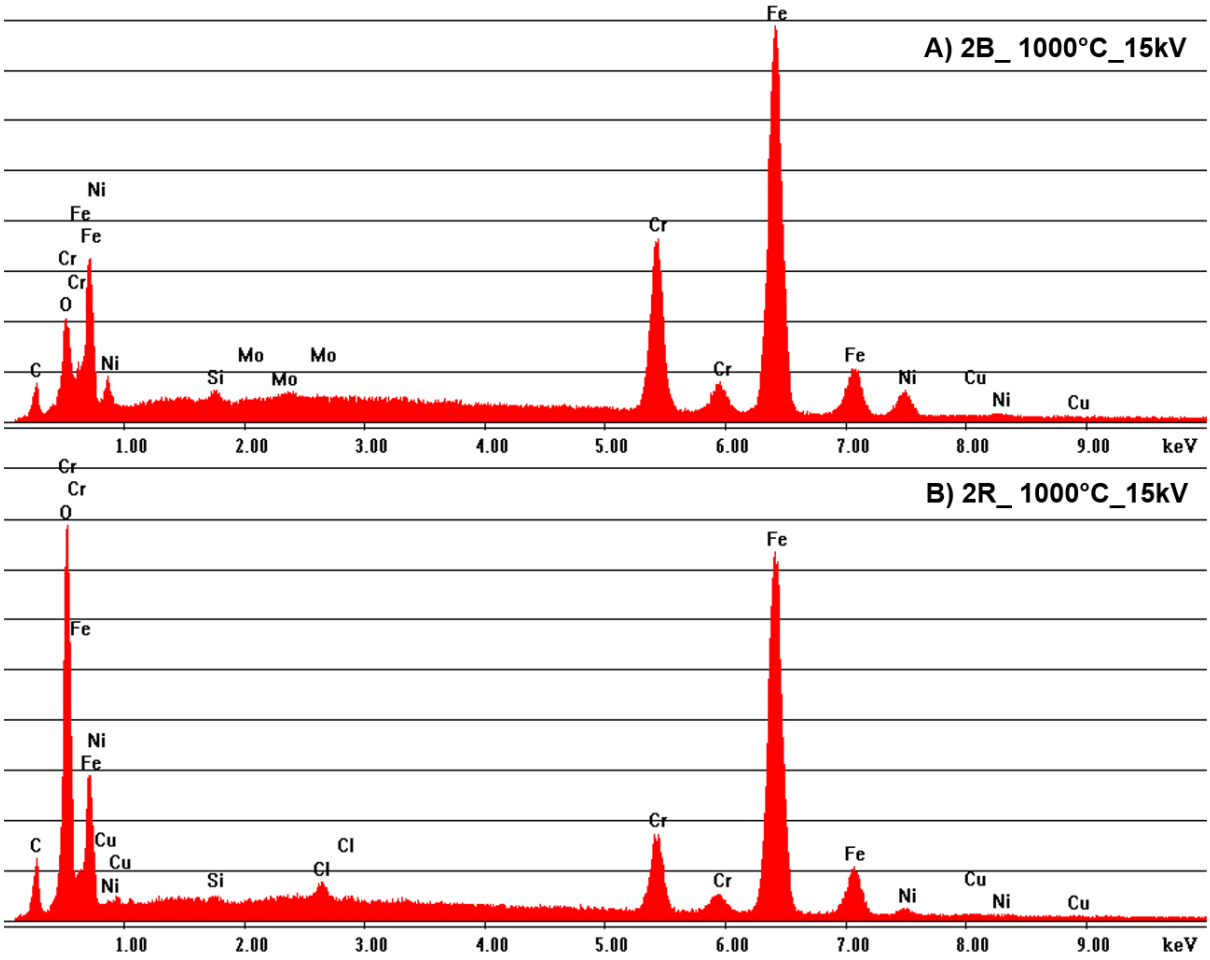

Figure 54 EDX for 2B and 2R tinted (1000°C) at 15kV

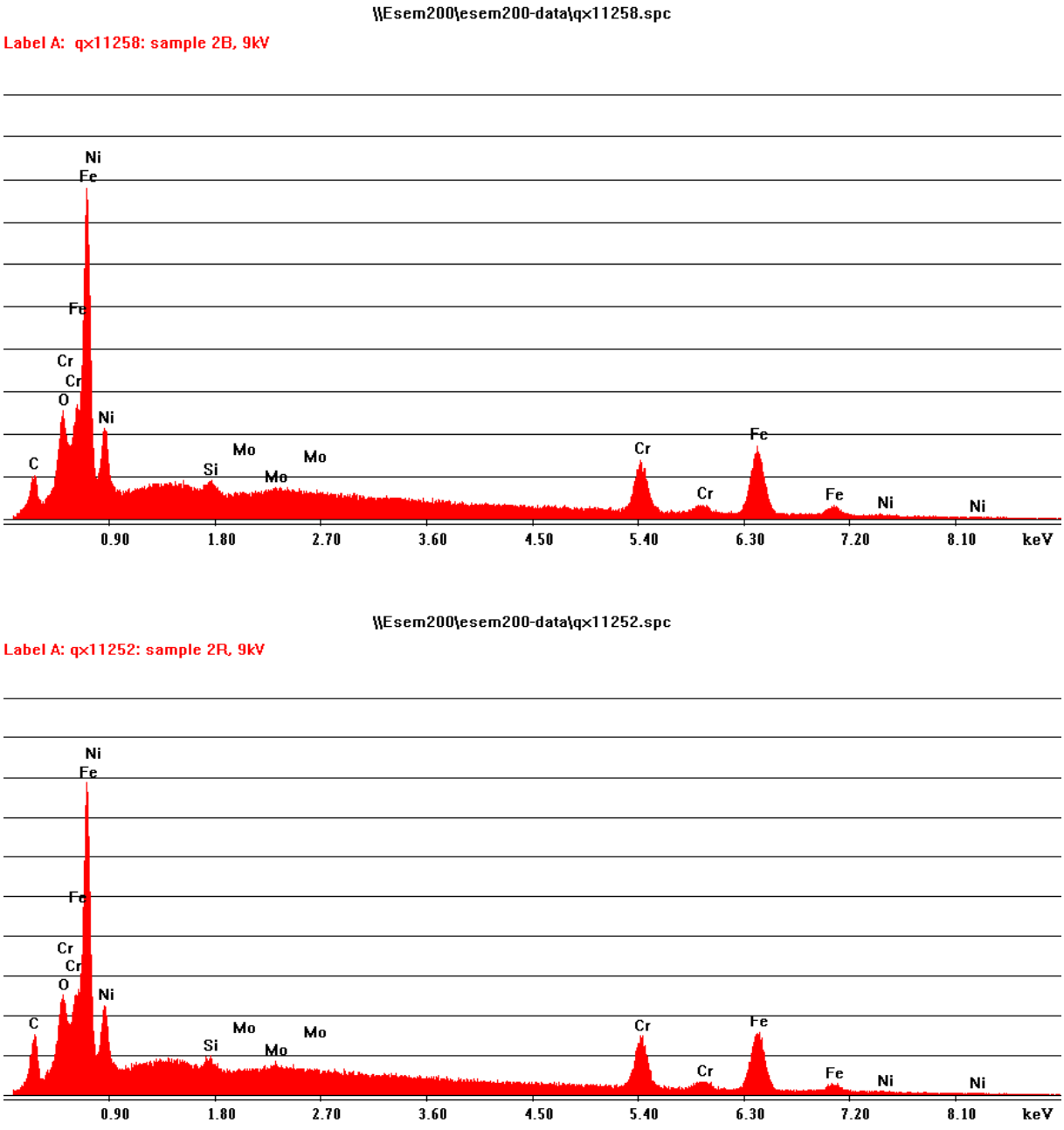

Figure 55 *EDX for 2B and 2R blank at 9kV*

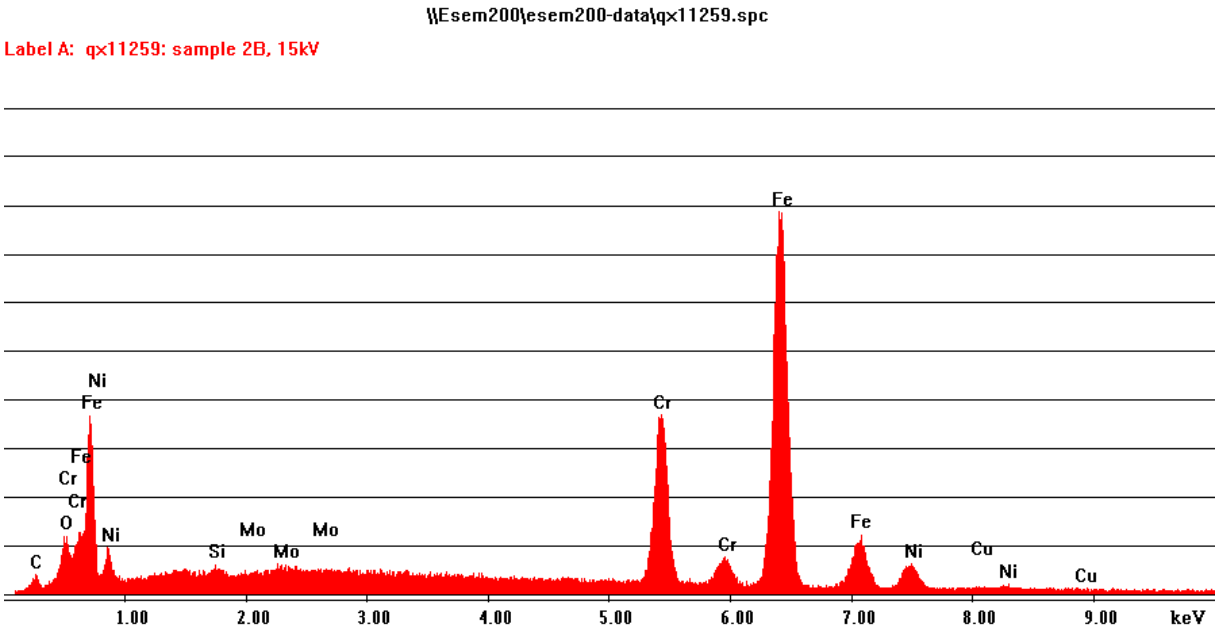

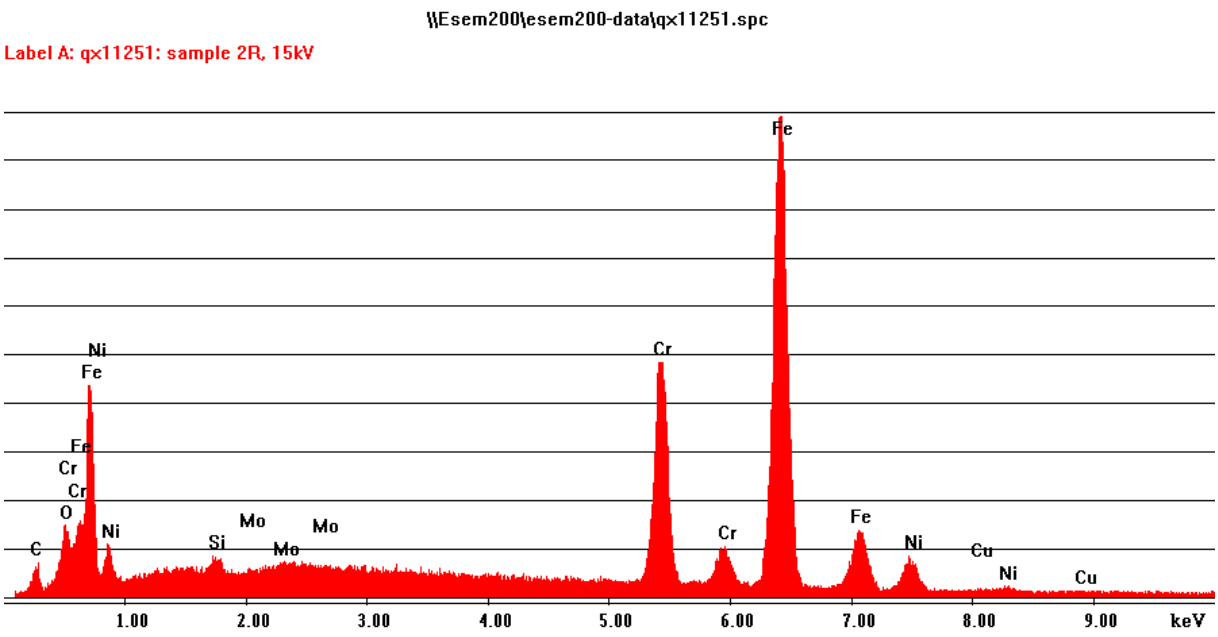

Figure 56 EDX for 2B and 2R blank at 15kV

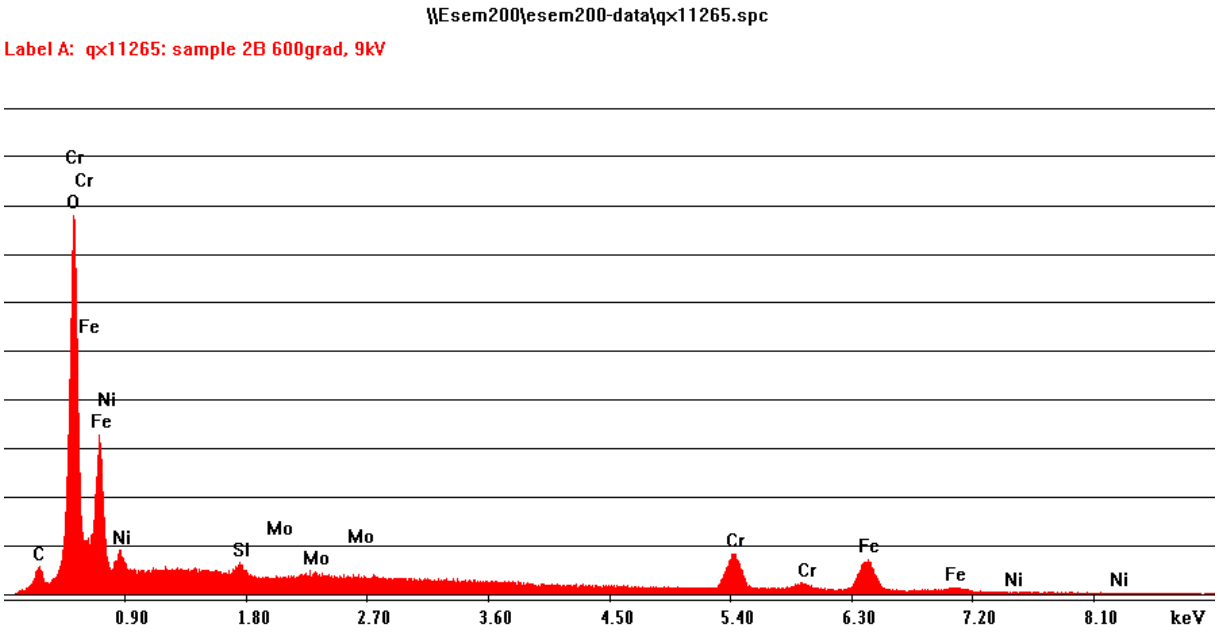

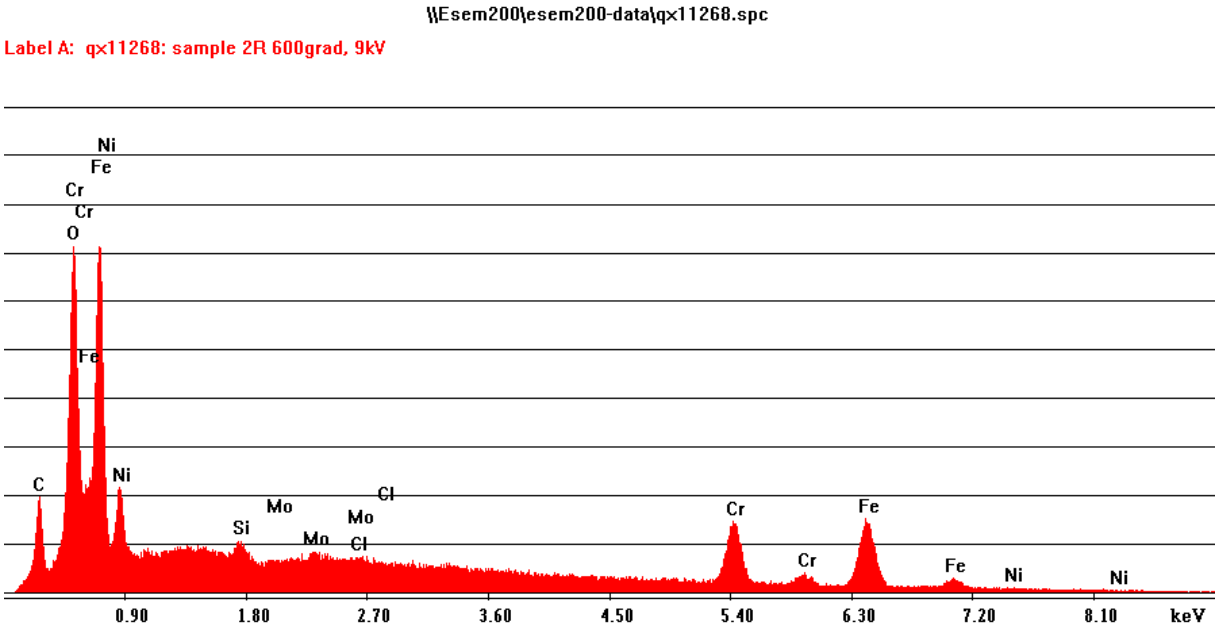

Figure 57 EDX for 2B and 2R 600°C at 9kV

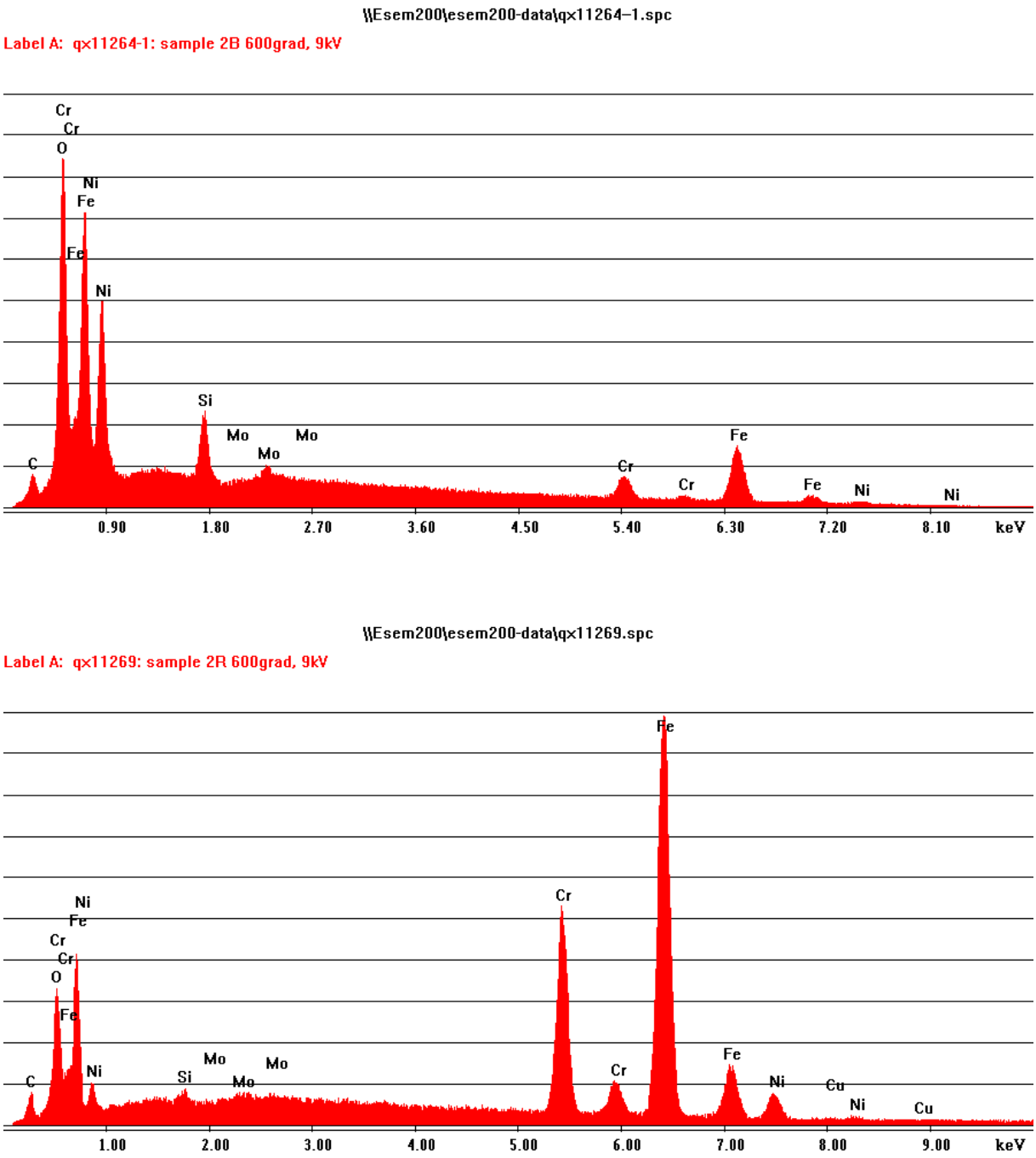

Figure 58 EDX for 2B and 2R 600 °C at 9kV

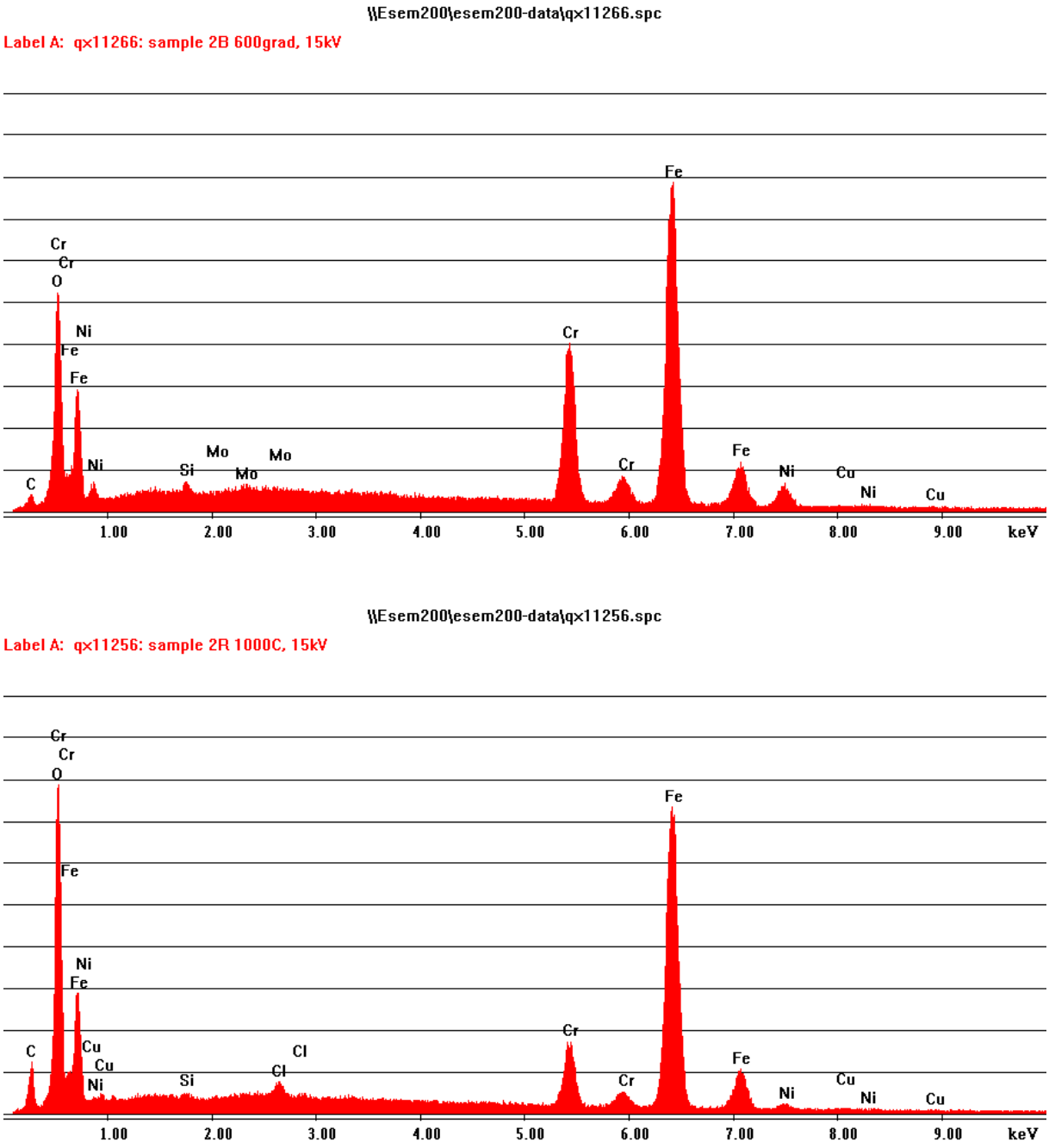

Figure 59 EDX for 2B and 2R 1000°C at 15kV

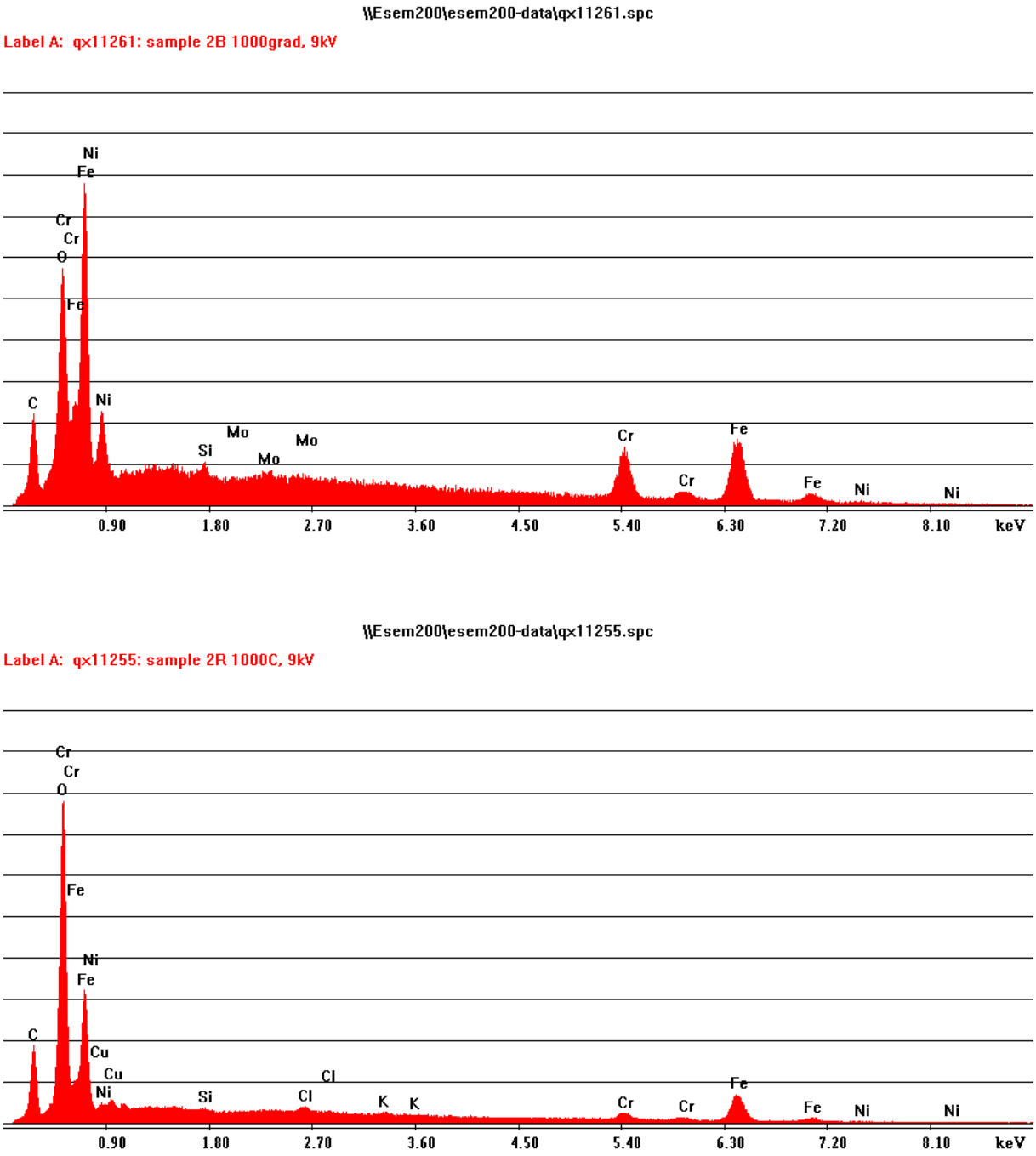

Figure 60 EDX for 2B and 2R 1000°C at 9kV

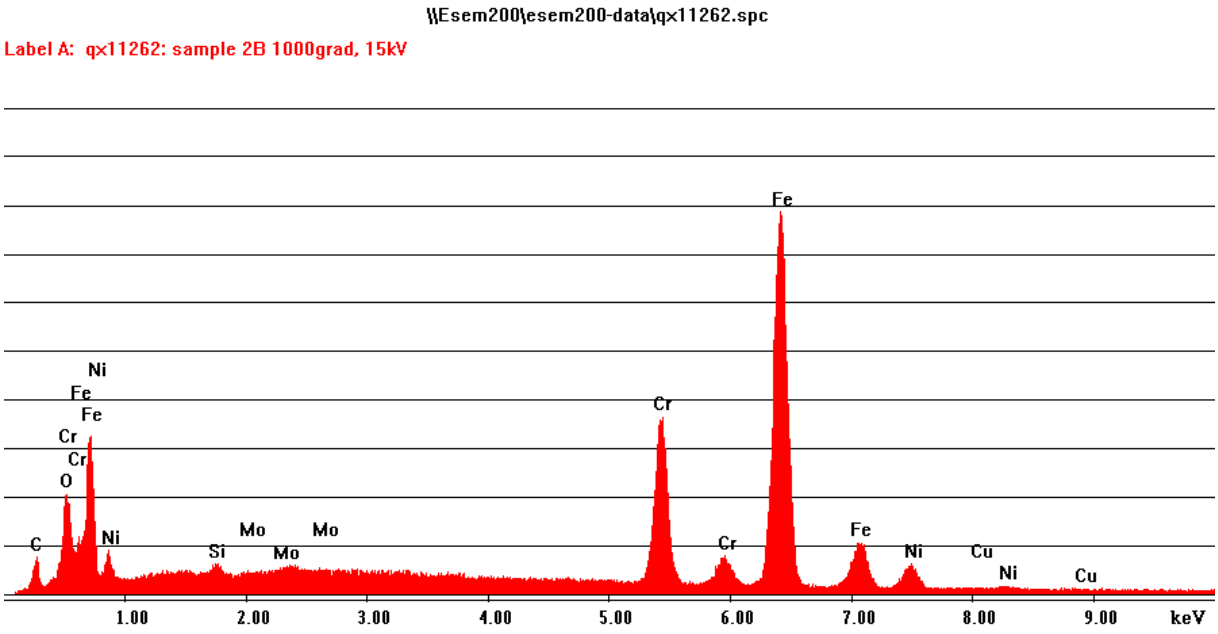

Figure 61 EDX for 2B 1000°C at 15kV

4) Raman analysis
   a) Color analysis of hemitite magnetite and trevorite

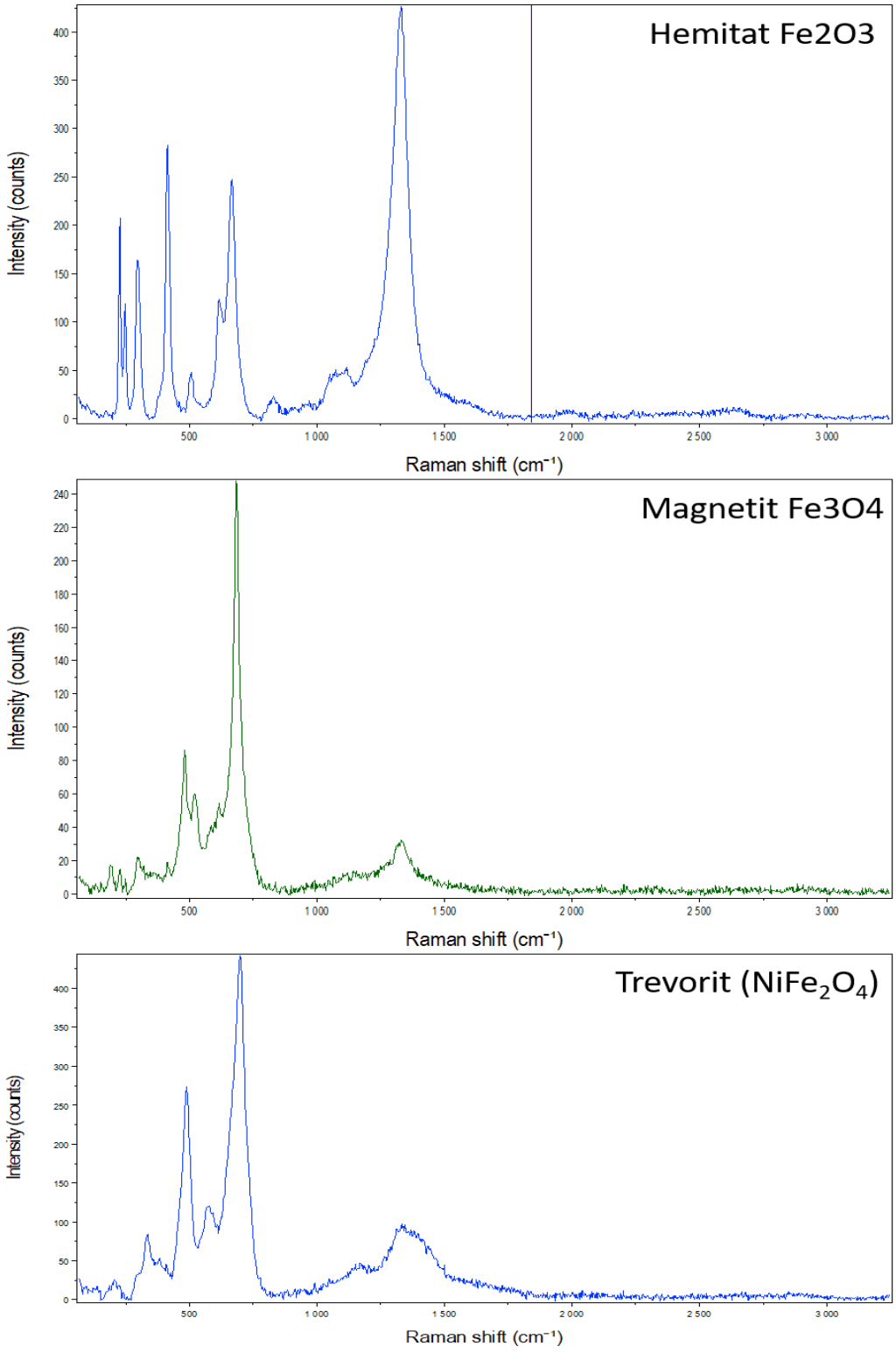

Figure 62 Hemitite Magnetite and Trevorit colors in Raman analysis